(2)

FINAL REPORT

Optoelectronic Integrated Circuits Fabricated Using Atomic Layer Epitaxy

submitted in partial fulfillment of
ARO Contract # DAAL03-89-K-0072

Prepared by:

Professor P. Daniel Dapkus
Departments of Electrical Engineering
and Materials Science Engineering
University of Southern California
Los Angeles, CA 90089-0271

Prepared for :

The Army Research Office
Research Triangle, NC

December, 1993

REPORT DOCUMENTATION PAGE

Form Approved
OMB No. 0704-0188

1. AGENCY USE ONLY (Leave blank)	2. REPORT DATE	3. REPORT TYPE AND DATES COVERED
	DECEMBER, 1993	FINAL REPORT - 03/01/89 to 09/30/92

4. TITLE AND SUBTITLE
Optoelectronic Integrated Circuits Fabricated Using Atomic Layer Epitaxy

5. FUNDING NUMBERS
DAAL03-89-K-0072

6. AUTHOR(S)
Professor P. Daniel Dapkus

7. PERFORMING ORGANIZATION NAME(S) AND ADDRESS(ES)
Departments of Electrical Engineering and Materials Science
University of Southern California
Los Angeles, CA 90089-0271

8. PERFORMING ORGANIZATION REPORT NUMBER

9. SPONSORING/MONITORING AGENCY NAME(S) AND ADDRESS(ES)
Contracting Officer
US Army Research Office
P.O. Box 12211
Research Triangle, NC 27709-2211

10. SPONSORING/MONITORING AGENCY REPORT NUMBER
ARO 26898.1-EL-SDI

11. SUPPLEMENTARY NOTES

12a. DISTRIBUTION/AVAILABILITY STATEMENT
Approved for Public Release: Distribution Unlimited

12b. DISTRIBUTION CODE

13. ABSTRACT (Maximum 200 words)

The interest in monolithic integration of optoelectronic devices based on III-V semiconductors has presented a great challenge to crystal growth and device processing. Laser assisted atomic layer epitaxy (LALE) is attracting increased attention as a candidate to meet the challenge because it offers localized deposition at a control of layer thickness, doping profile, and interface roughness on an atomic scale.

This work starts with a detailed study of the gas phase thermal decomposition of trimethylgallium (TMGa) and its relevance to atomic layer epitaxy (ALE) using molecular beam sampling mass spectrometry.

The growth of GaAs by LALE is then first studied using triethylgallium (TMGa) and arsine (AsH_3) as precursors. The influence of growth chemistry on the carbon contamination in the epilayers is further studied by using combinations of TMGa and tertiarybutylarsine (TBAs) and triethylgallium (TEGa) and AsH_3. The device application of the growth technique is demonstrated for the first time through laser diodes with the GaAs QW grown by LALE

14. SUBJECT TERMS
Laser assisted atomic layer epitaxy (LALE)

15. NUMBER OF PAGES
197

16. PRICE CODE

17. SECURITY CLASSIFICATION OF REPORT	18. SECURITY CLASSIFICATION OF THIS PAGE	19. SECURITY CLASSIFICATION OF ABSTRACT	20. LIMITATION OF ABSTRACT
Unclassified	Unclassified	Unclassified	UL

INTRODUCTION

This report describes work performed on the contract # DAAL03-89-K-0072 "Optoelectronic integrated circuits fabricated using atomic layer epitaxy," during the period of time March 1, 1989 to September 30, 1992. The objective of this program was to explore the suitability of atomic layer epitaxy and laser assisted atomic layer epitaxy for the selected area growth and fabrication of electronic and optoelectronic devices with the eventual goal of demonstrating integration of these devices.

The report as presented here was submitted as the doctoral dissertation of Dr. Qisheng Chen who was the key performer on the program. All of the work presented in this report except the material presented in chapter 2 was supported in whole or in part by the subject program. The materials contained herein have been reported to ARO and to SDIO/IST, the funding source, at various annual reviews of the program.

Significant progress toward the end goals have been made during the course of this program. This has resulted in a number of achievements that are particularly noteworthy:

1.) The first demonstration of a semiconductor laser with the active region selectively grown by laser assisted ALE.

2.) The first demonstration of a laser integrated with a passive waveguide by laser assisted ALE.

3.) The first growth of device quality materials by an optimized laser assisted ALE process.

4.) The first selective growth of complex patterns by laser pattern projection.

5.) Demonstration of the smallest patterns grown by laser ALE.

6.) Exploration and demonstration of alternate arsenic sources for laser ALE to reduce the carbon incorporation.

7.) Demonstration of low carrier concentration GaAs grown by laser ALE using triethylgallium.

These accomplishments show that high quality materials can be grown by LALE at temperatures as low as 300°C and that complex device patterns can in principal be formed optically with coherent light.

FUTURE WORK

In spite of the accomplishments achieved during the course of this program, many questions remain concerning the suitability and flexibility of LALE as an integration process. Among these are:

1. What is the ultimate resolution of LALE for integration of micron or sub micron sized devices? At present the smallest device pattern that has been generated is 20μm. The current limitation is fixed by the reactor design and by the optics used.

2. How does the coherence of the laser source limit the resolution of the LALE process? Can interference effects be overcome?

3.Can a practical reactor be designed that will permit optical imaging with the required resolution and still allow moderate throughput?

4. Can high quality ternary or quaternary alloys be grown by LALE so that entire device structures can be fashioned by the process? At present only binary active regions have been demonstrated to have high quality.

These topics are currently under study in a follow on program funded by ARO and BMDO.

TABLE OF CONTENTS

LIST OF FIGURES

LIST OF TABLES

ABSTRACT

The interest in monolithic integration of optoelectronic devices based on III-V semiconductors has presented a great challenge to crystal growth and device processing. Laser assisted atomic layer epitaxy (LALE) is attracting increased attention as a candidate to meet the challenge because it offers localized deposition at a control of layer thickness, doping profile, and interface roughness on an atomic scale.

This work starts with a detailed study of the gas phase thermal decomposition of trimethylgallium (TMGa) and its relevance to atomic layer epitaxy (ALE) using molecular beam sampling mass spectrometry. TMGa is found to decomposed appreciably above ~430 °C. The presence of H_2 reduces the apparent activation energy of the decomposition. The rate limiting step for the decomposition is the breakage of the first Ga-C bond with an activation energy of 64.6 kcal/mol. The activation energies for the reactions in rupturing the second and third Ga-C bonds are estimated to be 52.6 kcal/mol and 54.1 kcal/mol.

The growth of GaAs by LALE is then first studied using triethylgallium (TMGa) and arsine (AsH_3) as precursors. Thin and small area of deposits were characterized by photoluminescence (PL), capacitance-voltage (C-V), and secondary ion mas spectrometry (SIMS). A correlation between the growth parameters and the material quality leads to an optimization of the latter and to the first demonstration of device quality GaAs grown by LALE. The influence of growth chemistry on the carbon

contamination in the epilayers is further studied by using combinations of TMGa and tertiarybutylarsine (TBAs) and triethylgallium (TEGa) and AsH_3. Carbon levels are found greatly reduced. The device application of the growth technique is demonstrated for the first time through laser diodes with the GaAs QW grown by LALE. Threshold current density as low as 515 A/cm^2 is obtained.

CHAPTER ONE

INTRODUCTION

1.1 The Advantages of Selective Area Growth in Optoelectronic Integration

The advantages of using photons instead of electrons in information transmission and processing have been perceived for many years. Chief among them are the extremely high bit rate-distance products, meaning that data can be carried through at a high rate over a long distance, e.g., 10 Gbit/s for 151 km,[1] and immunity from electromagnetic interference. The progress in single wavelength semiconductor lasers, low loss and low cost optical fibers, and components such as optical switches, modulators, and high efficiency and low noise photodetectors has made the fiber interconnected commercial communication system a reality. One of the goals of the research and development in this field is geared towards monolithic or hybrid integration of lasers, waveguides, modulators, detectors, and the closely related electronics circuit, the so called optoelectronic integrated circuit (OEIC[2]), to achieve a designated functionality at high reliability. A key to the economic attainment of such a goal is the availability of a crystal growth technique that allows the deposition of high quality semiconductor materials in a highly controllable manner in terms of layer thickness, doping, composition, and their uniformity and interface smoothness.

Employing various active and passive devices as its building blocks, a practical OEIC requires different vertical layer structures in the areas where different devices are located to insure an optimized operation of the individual devices. One of the examples is to integrate four lasers, waveguides, and an optical amplifier to fabricate a wavelength division multiplexed transmitter, as is shown schematically in Fig.1.1. In this design, the outputs of four individually modulated and tunable multiple quantum well distributed Bragg reflector (MQW-DBR) lasers are combined through a passive wave guide combiner to an on-chip MQW optical amplifier. Although the lasers and the amplifier can share the same MQW stack design, the DBR corrugation is only applicable to the lasers. As is shown in Fig.1.2, the vertical structure of the lasers differs from that of the passive

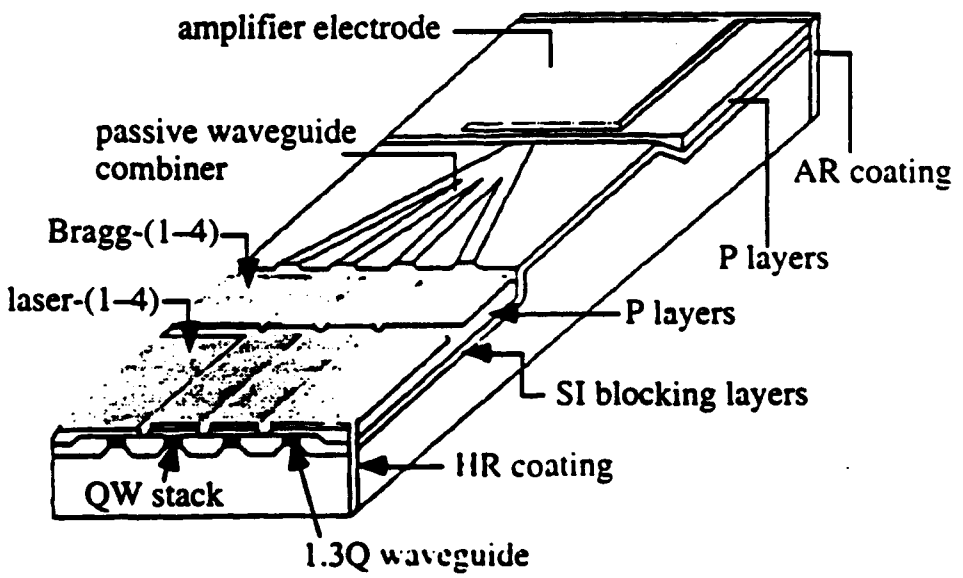

Fig.1.1 An example of experimental wavelength division multiplexing OEIC, from Koch and Koren[3]

waveguides. Different material parameter requirements in the active and the passive regions also complicate the OEIC design and fabrication. In general, a compromise has to be made between the optimized performance

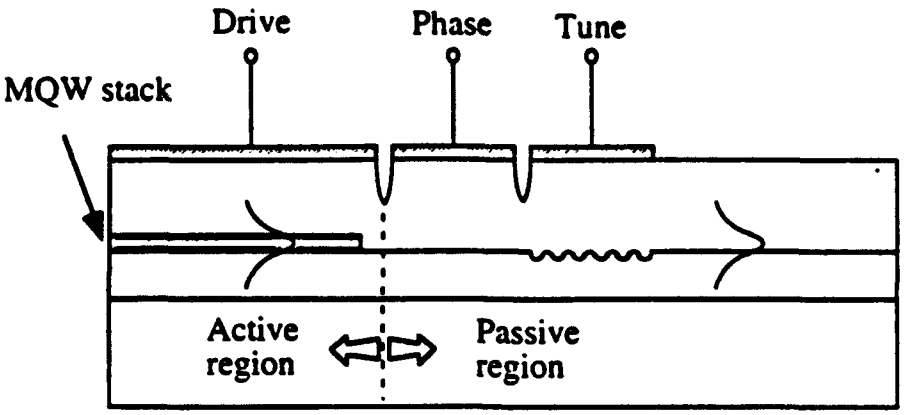

(a) Butt-joint

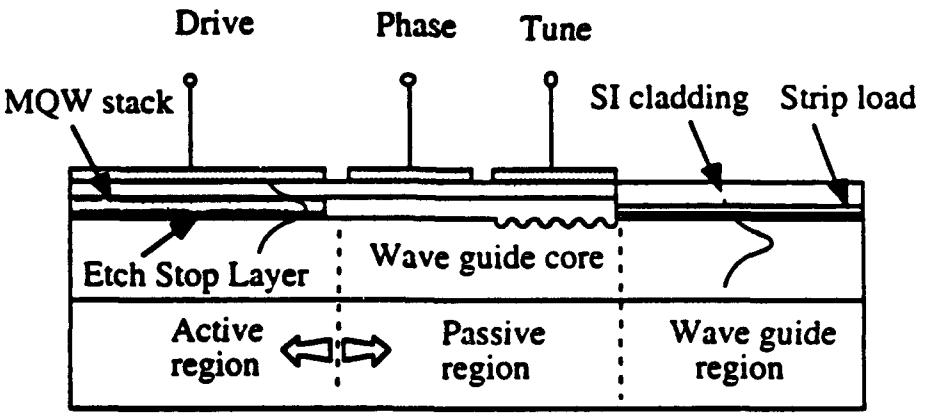

(b) Optical tunneling

Fig.1.2 Two schemes of active-to-passive transitions. Note the vertical layer structures are very different in the active and passive regions.

of the individual devices and the feasibility of the fabrication process. Despite this complexity, various functional monolithic OEICs have been demonstrated.[3] The entire processing typically involves multiple step selective etch and re-growth. The precise location of the etch front is only possible with the use of etch-stop layers which are parasitic in nature and would otherwise be avoided. In addition, exposing the active region to atmosphere before re-growth is frequently problematic since it results in the poor re-growth interface being in the direct vicinity of the active region. The yield can be expected low. It is evident that a selective area growth technique that permits localized deposition of a semiconductor material without interfering with the continuity of the deposition of the entire structure is highly desirable. Such an in-situ approach not only minimizes the exposure of critical interfaces to the atmosphere giving superior optical and electrical quality. It also affords a degree of freedom in device design and fabrication to achieve optimal performance of individual devices as well as the resulting OEICs with a cost effective yield. Among the selective area growth techniques that have been explored, growth through the windows opened on a mask of insulators (SiO_2 or Si_3N_4) bears the same degree of complexity as the etch and re-growth approach because the re-growth process is still needed. The abnormal growth at the edge of the mask excludes its usefulness in OEIC fabrication process. The etch and re-growth approach has had limited success and is currently most frequently used simply because the conventional growth techniques such as metalorganic chemical vapor deposition (MOCVD) and molecular beam epitaxy (MBE) are now mature enough to produce uniform multilayered semiconductor structures of high quality.

A seemingly straight forward way to realize selective area deposition of compound semiconductors is to utilize a beam of microscopic particles (photons, electrons, ions etc.) to stimulate the growth process. This is especially possible in the case of CVD where chemical reactions are involved in order to release the relevant element from their precursors. Indeed, there have been reports on successful selective area growth of GaAs by laser-assisted MOCVD [4]-[6] and laser-assisted MOMBE. [7][8] The potential of laser-assisted MOCVD for device application has been demonstrated through the fabrication of p-i-n photodiodes,[9] metal-semiconductor-field-effect transistors,[10] and multiple wavelength light-emitting diodes.[6] A general feature in the laser-assisted MOCVD is that the process is surface reaction kinetics controlled. Therefore, the growth rate is a sensitive function of temperature and the power density of the laser beam, as is manifested by a Gaussian cross-section profile of the deposit replicating the intensity profile of the beam. A precise control of thicknesses is thus difficult.

The work described here exploits an alternative approach to selective area deposition, namely laser-assisted atomic layer epitaxy (LALE). This technique combines the benefit from laser-assisted growth for selective area deposition and ALE for thickness control down to atomic dimension. In the next section, selective area growth of GaAs by LALE will be introduced in relation to conventional MOCVD and ALE.

1.2 An Introduction to MOCVD, ALE, and LALE

MOCVD (sometimes also termed as metalorganic vapor phase epitaxy (MOVPE), organometallic chemical vapor deposition (OMCVD), and organometallic chemical vapor epitaxy (OMVPE)) growth of compound semiconductor was introduced more than two decades ago by Manasevit.[11] The interest in this growth technique rose rapidly only after it was shown to deposit III-V semiconductor layers with device quality.[12] To date, MOCVD has been applied to the growth of almost all kinds of compound semiconductors as can be seen in Table 1.1, where various types of semiconductor materials that have been grown by MOCVD are listed. It is now a preferred technical tool for production and research as well.

Table 1.1 Examples of semiconductors grown by MOCVD.

Group	Examples
III-V	GaAs, GaP, GaN, GaSb, AlSb, InAs, InP,AlN
	GaAlAs, InGaAs, GaAsSb, GaAsP, InAsP, InAsSb,InGaP,AlAsP, GaAlSb, InAlAs, InAlP
	AlGaAsSb, AlGaAsP, InGaSbP, InGaAsP, AlGaInP, InGaAsSb, InAsSbP
II-VI	CdTe, CdSe, CdS, HgTe, ZnO, ZnS, ZnSe, ZnTe
	CdSeS, CdHgTe, ZnSSe
IV-VI	PbS, PbSe, PbTe, SnS, SnSe, SnTe,
	PbSnTe,

Shown in Fig.1.3 is a schematic of an MOCVD growth system capable of growing AlGaAs/GaAs materials of both p and n types of dopings. A carrier gas, usually H_2, flows through the bubblers containing metalorganic compounds, trimethylgallium (TMGa) or trimethylaluminum (TMAl) in this example. These group III precursors are transported in the carrier gas, mixed with the group V hydride (AsH_3) in the manifold, and are injected into the reactor vessel. Situated in the vessel is a substrate on a graphite susceptor which is RF induction heated to ~750 °C. The reaction between TMGa, TMAl, and AsH_3 produces a GaAs or AlGaAs epitaxial film on the substrate. The reaction is generically written as

$$(1\text{-}x)R_3Ga + xR_3Al + AsH_3 \rightarrow Al_xGa_{1-x}As + 3RH \qquad (1.1)$$

A group II metalorganic compound (diethylzinc DMZn) or a group IV hydride (Si_2H_6) can be used to dope the growing layer to p or n type.

The use of metalorganics in crystal growth takes advantages of the following facts: 1) Most metalorganics are in a liquid or a solid state having a reasonably high vapor pressure and therefore can be transported easily with a carrier gas. This has the benefit of simplified equipment setup, operation, and maintenance. 2) They dissociate at moderate temperature in an irreversible manner. The irreversible nature of the reaction requires only the substrate be heated (so called cold wall, single temperature zone reactor). Alloy composition is basically adjustable by the independent adjustment of the input ratios of the precursors. The states of being far from equilibrium is suitable for hetero-epitaxy on insulators where the nucleation

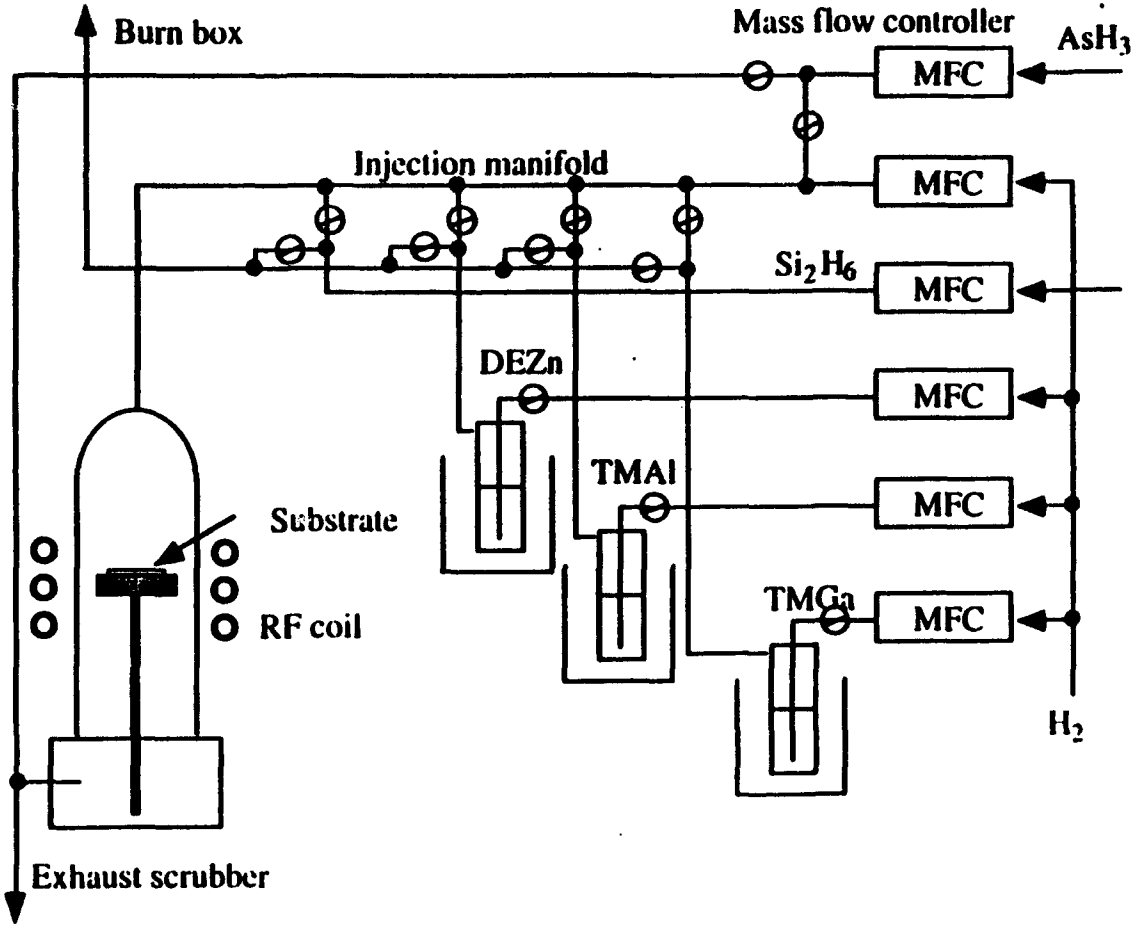

Fig.1.3 Schematics of an MOCVD system

requires a high degree of supersaturation. 3) The absence of an etchant reaction by-product eliminates auto-doping and assures abrupt composition and doping transitions in a multilayered structure.

MOCVD growth of GaAs using TMGa and AsH_3 is generally carried out at temperatures above the temperature where gas phase decomposition of TMGa occurs appreciably, > 550 °C. In this temperature range up to ~850 °C, depending on the reactor geometry and other operating conditions, the growth rate varies slightly with temperature, signifying a mass transport limited growth. At even higher temperature, the growth rate decreases with increasing temperature due probably to the loss of reactants upstream as a result of premature decomposition. In a lower temperature range, the growth rate increases rapidly with he increasing temperature. The growth in this temperature regime is believed to be limited by the surface reaction kinetics. A schematic temperature dependence of GaAs MOCVD growth rate is displayed in Fig.1.4.[13][14]

MOCVD growth is normally performed at a group V to group III ratio great that unity, V/III » 1. Under such a condition, the growth rate is only a function of TMGa partial pressure (or flux in moles/unit time). As is shown in Fig.1.5,[14] the growth rate depends linearly on the partial pressure of TMGa (P_{TMGa}) in the mass transport limited regime while tends to saturate in the kinetic limited regime. Some benefit of growing in the surface reaction kinetics limited temperature regime are exploited with a technique called atomic layer epitaxy (ALE).

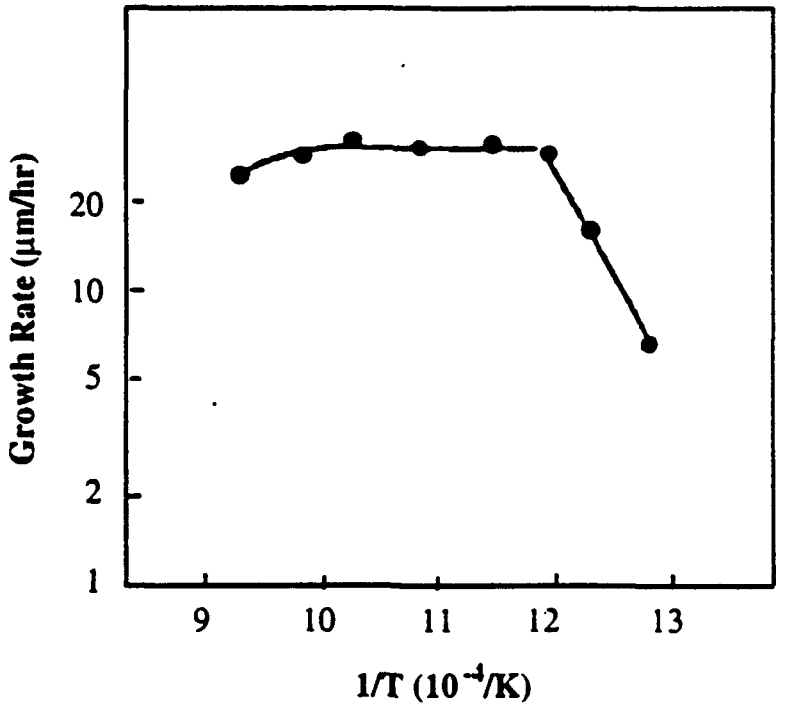

Fig.1.4 Temperature dependence of MOCVD growth rate, from Ref.[14].

A major difference between conventional MOCVD and ALE is that in ALE, the group III and group V precursors are introduced to the substrate surface one at a time. A complete separation of TMGa and AsH_3 is desirable as appreciable MOCVD growth still results at 450 °C (~7 Å/s in Fig.1.4). This is accomplished by purging with H_2 gas in atmospheric and low pressure reactors or by allowing time for pumping in high vacuum system in between the III and V injections. As is depicted in Fig.1.6, at a temperature that the gas phase decomposition of TMGa is not appreciable, the exposure of the substrate to TMGa molecules results in an "atomic" layer of Ga-containing species. TMGa molecules and/or their subsequent intermediates will not adsorb further on this Ga-species covered surface or they will have a very weak bonding to such a surface that they desorb

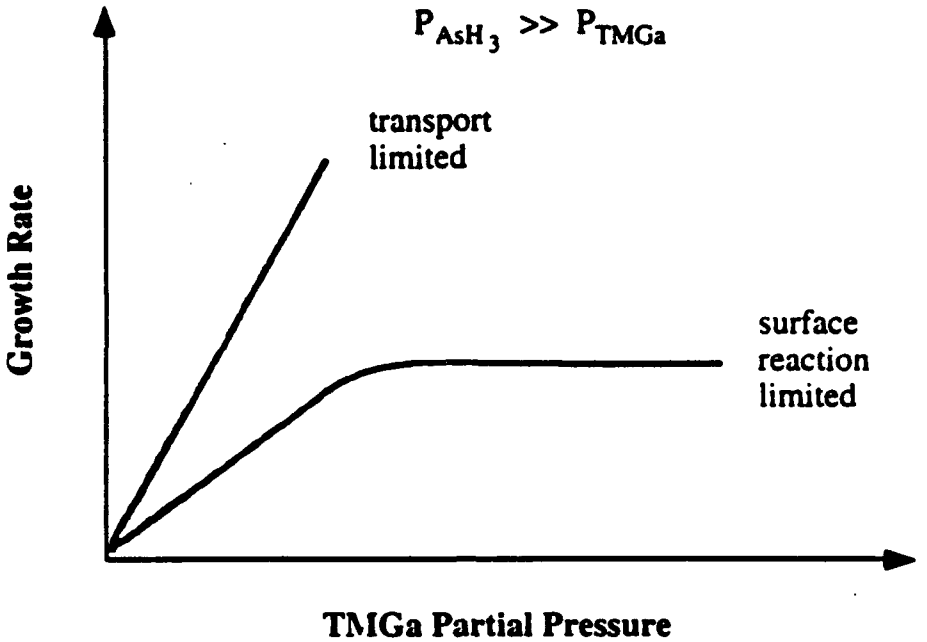

Fig.1.5 TMGa partial pressure dependence of MOCVD growth rate.

rapidly during the purge period. Upon exposure to AsH_3, the surface Ga specie reacts with AsH_3 or its intermediates to form a monomolecular layer of GaAs (2,827 Å in the [100] direction).

One obvious advantage of ALE over MOCVD is its precision in layer thickness control that is principally in an atomic dimension. Larger area, uniform, deposition free from hydrodynamic restriction is anticipated. The idea of ALE can be utilized in analogy to obtain atomically abrupt doping profile. There is, however, a penalty associated with growth in an alternating exposure mode and at reduced temperatures in that the average growth rate is relatively low, typically ≤ 0.25 μm/hr. Some innovative designs in reactor systems have appeared to address the issue of speeding up the process of alternating exposure of the substrate to the precursors without suffering from intermixing and gas phase breakdown of the

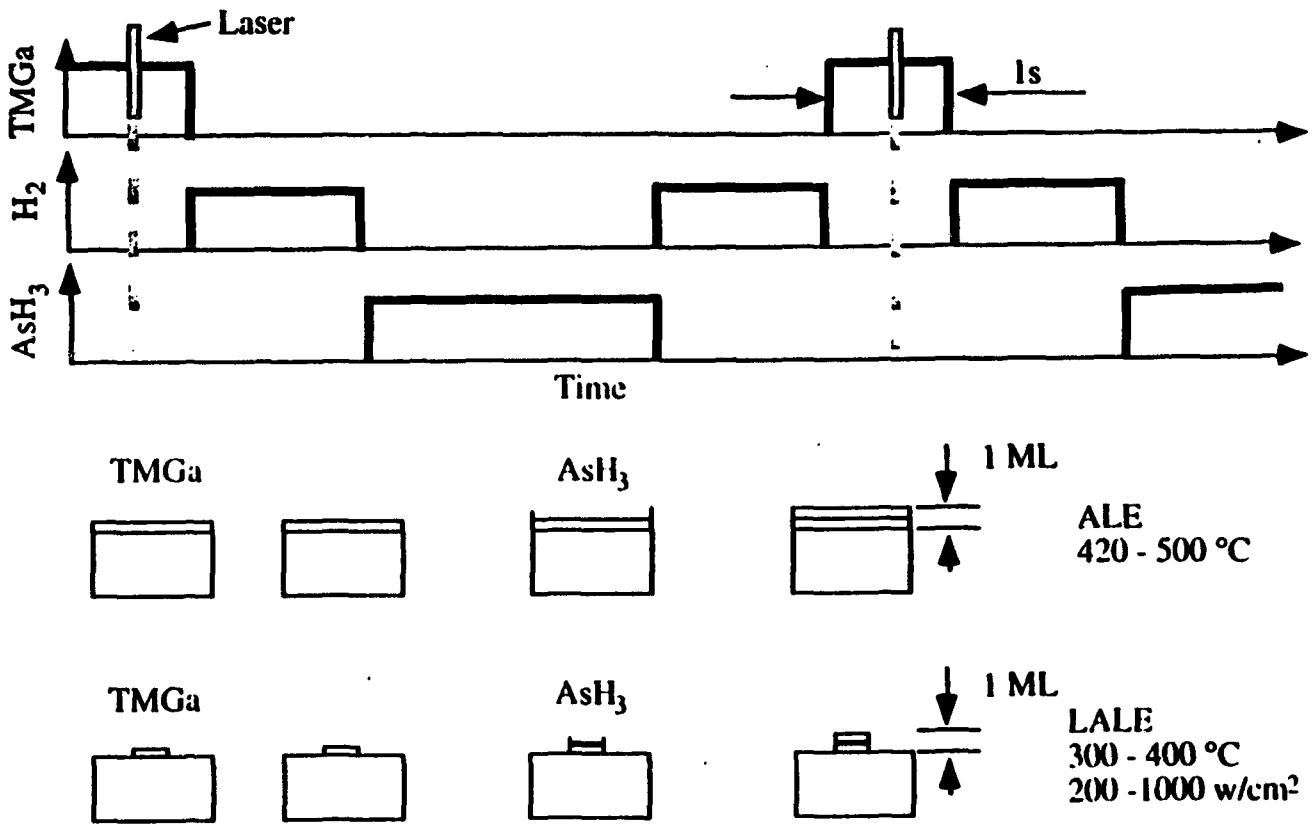

Fig.1.6 Schematics of ALE and LALE processes.

relevant species, a review of which will be given in the next section. Thus the temperature of ALE growth may be increased without losing the self limiting feature and the growth rate increased accordingly. Another solution to the low growth rate in ALE is to apply large area beam stimulation, such as a laser beam, to shorten the time required for a complete dissociative adsorption of the relevant molecules. This actually represent one aspect of laser-assisted ALE where growth rate and material property are the primary concern instead of the area selective deposition.

Laser assisted ALE (LALE) is closely related to ALE in the sense that the exposure of the substrate to TMGa and AsH_3 must be temporally separated to obtain monolayer self limiting growth. In LALE, however, the temperature is further reduced (~380 °C for LALE using TMGa) to suppress the thermally driven dissociative adsorption of Ga-containing species. As is also shown schematically in Fig.1.6, the application of the laser beam is normally synchronized with the TMGa exposure. After AsH_3 exposure, a monolayer of GaAs is deposited in the area illuminated by the laser beam. Similar to ALE, precise control in layer thickness is guaranteed due to the monolayer self limiting nature of the process. It must be pointed out that the saturation of the growth rate with respect to the TMGa partial pressure in the kinetics limited regime in MOCVD mentioned earlier (Fig.1.5) is not to be confused with the monolayer self limiting growth in the ALE and LALE. In the former case, the duration of injection has to be so adjusted to obtain monolayer of deposition.

It will become clear later that the combined use of laser illumination and of even lower temperature in LALE not only widens the operation window for self limiting growth but also affords the use of chemically less stable metalorganics, such as TEGa, to obtain monolayer self limiting growth. Both p and n type doping in LALE of GaAs has been demonstrated in this work. LALE, when combined with conventional MOCVD, is truly a powerful tool for in-situ processing. In the next section, a review of the current development of ALE and LALE will be given in order to identify the remaining problems in LALE. Finding solutions to some of these problems forms the main topic of the current work.

1.3 A Review of ALE and LALE of III-V Compounds Using Metalorganics

ALE was originally developed by Suntola[15],[16] to meet the needs of depositing ZnS and dielectric thin films for larger area electroluminescent displays. The main concern was then the stoichiometry and uniformity of the poly-crystal materials on glass substrates. Since then, the ALE idea has been applied to the growth of various single crystalline III-V semiconductors in the existing reactor systems using different forms of precursors.[17]-[25] LALE has also been carried out to grow GaAs,[26]-[29] AlAs,[30] AlGaAs,[30] and GaP.[31] In this section, the results of ALE and LALE growth of GaAs are reviewed in a unified manner. The areas of importance where further work is needed are thus highlighted, which serves as a guidance for the direction of this work.

1.3.1 Monolayer Self Limiting Growth

ALE is distinguished from conventional MOCVD by the self-limiting monolayer/cycle growth that is achieved. This phenomenon can be observed independent of the TMGa source mole fraction in a suitable temperature range for a given amount of exposure time, as is shown in Fig.1.7.[31] With adequate AsH_3 exposure, the growth rate is TMGa-supply-limited below a certain value and saturates at one monolayer per cycle above that value. The closeness of the growth rate to one monolayer/cycle upon further increasing the TMGa mole fraction illustrate the robustness of the self limiting feature. For ALE growth using TMGa

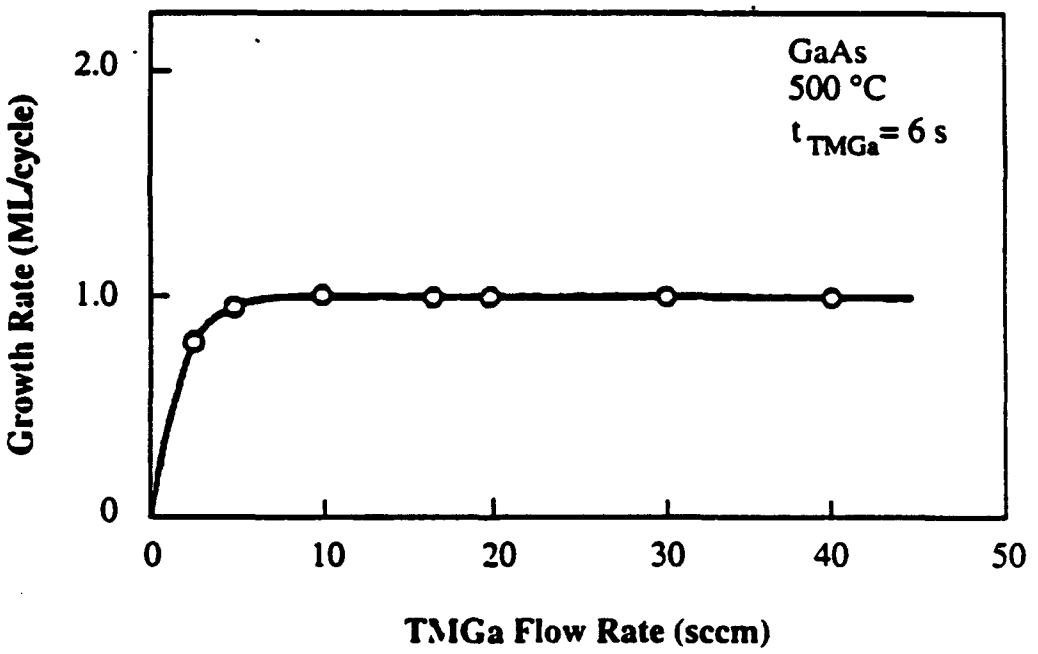

Fig.1.7 TMGa flow rate dependence of ALE showing perfect self liming at one monolayer/cycle, from Ozeki *et al.*.[31]

and AsH_3 in most existing reactor systems, the TMGa flux (used here as the moles of TMGa injected per cycle) window for monolayer self limiting growth will be more that an order of magnitude, frequently limited by the available flow settings in the reactor. The extreme cases are, on the one hand, ALE in vacuum or at low pressure eliminates the gas phase decomposition of TMGa and produces a near-perfect self limiting growth habit. On the other hand, a slight increase of growth rate from a monolayer/cycle is observed for ALE in an atmospheric pressure reactor, especially for ALE attempted at high temperature (e.g. above 500 °C). At high temperature, the deviation from monolayer growth is accompanied by a narrowing in the TMGa flux window for ALE operation.[32] This is frequently attributed to the contribution to Ga deposition from the gas phase decomposition, which is not a self limiting process.[33]

If a self limiting mechanism is operative, a minimal test of a true ALE is the observation of the regime where the growth rate is one monolayer /cycle independent of TMGa mole fraction for a given exposure mode and substrate temperature. This is distinguishable from the mode of operation where the TMGa flux is so adjusted that the growth rate is 1 ML/cycle. The tight control on TMGa flow offers no advantage over conventional continuous growth techniques except that the surface mobility of the adsorbed species may be enhanced under alternate exposure. A careful review of a few earliest ALE references bears out the conclusion that not all of them pass the test. In the foregoing, we have presented the ALE self limiting growth characteristics in terms of the growth rate per cycle versus TMGa mole fraction. In the literature, ALE growth data were

also presented with respect to the moles of TMGa injected per cycle or to the duration of the TMGa exposure time under a constant TMGa mole fraction. The former tends to ignore or disguise the differences that may arise from the different ways that the same amount of material can be delivered into the reactor, unless all the data points are obtained under the same specified TMGa exposure time. In the latter case, an increasing TMGa exposure time not only increases the counts of collisions of the substrate by the TMGa molecules but also prolongs the allowable time for reactions to proceed. The self limiting growth, if observable, in this case will have a stronger sense than the minimal test we proposed earlier.

So far, only ALE growth with TMGa displayed reasonably good self limiting growth behavior. There was one report on the observation of monolayer growth using TEGa and AsH_3 in the vacuum under 0.1 w/cm^2 Hg lamp irradiation.[34] Further ALE experiments carried out in a pulsed-jet, low pressure reactor using TEGa[35][36] and ethyldimethylgallium (EDMGa)[37] resulted in no self limiting growth. Monolayer self limiting LALE, on the other hand, has been achieved using both TMGa[27][28][38] and TEGa,[38] as is shown in Fig.1.8. This behavior is so far similar to that of the thermal ALE. LALE differs from ALE by having an additional control parameter, i.e. the laser power density. Shown in Fig.1.9 is the laser intensity dependence of LALE growth rate per cycle. It can be seen that there exists a rather wide laser intensity window for achieving monolayer self limiting growth. In most of the LALE experiments reported, the 514.5 nm or a shorter wavelength line from an Ar^+ laser was used. The laser beam was either chopped and then delivered synchronously or directly scanned

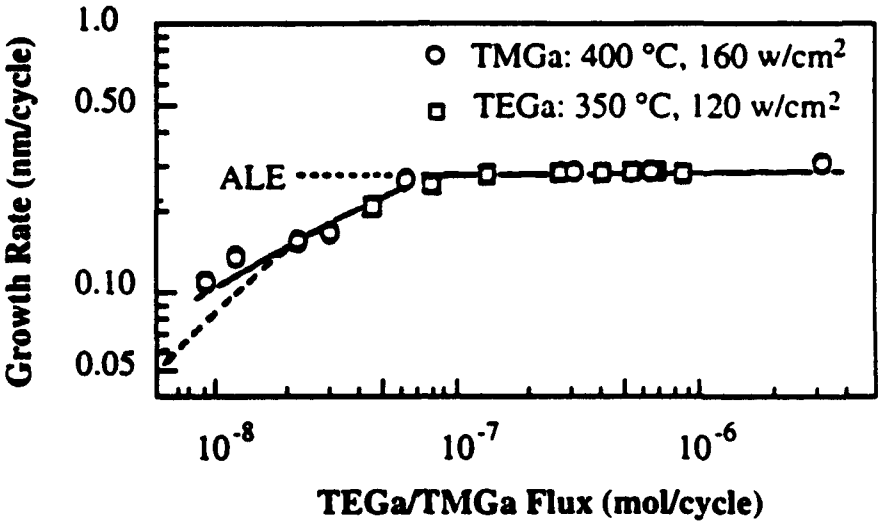

Fig.1.8 Growth rates as a function of group III flux in LALE using TMGa and TEGa, from Aoyagi *et al.*.[38]

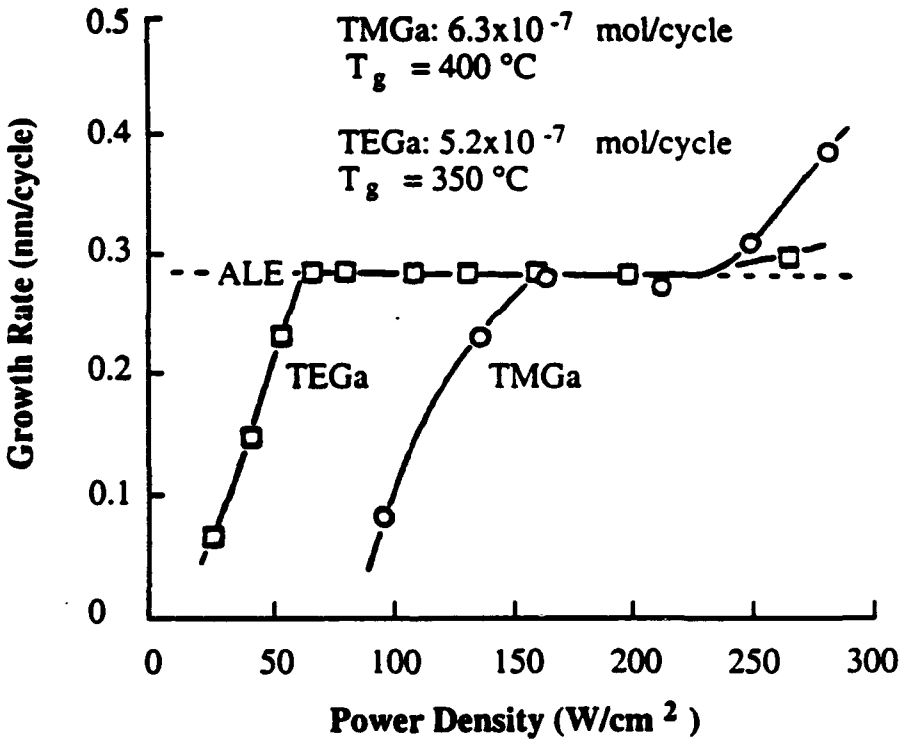

Fig.1.9 Laser power intensity dependence of LALE growth rates, from Aoyagi *et al.*.[38]

across the substrate during the group III exposure. Illumination during the AsH_3 exposure alone was found having no enhancement to LALE growth. A wavelength dependence of LALE growth was demonstrated by the monotonous increase in the growth rate per cycle with increasing laser intensity of an YAG laser operating at 1.064 μm wavelength.[28][39]

ALE growth studies conducted at various temperatures offer an opportunity to probe the surface kinetics pertaining to ALE and MOCVD, as well. The temperature dependence from a few reported works is summarized in Fig.1.10, disregarding the fact that there may be differences in temperature calibrations and other operating conditions that may shift the

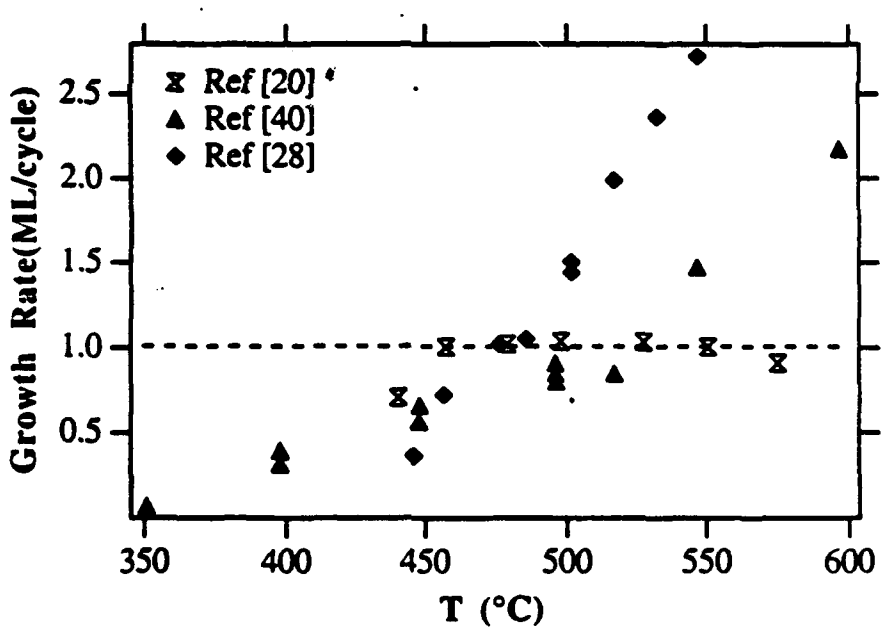

Fig.1.10 ALE growth rate as a function of temperature obtained in different systems.

apparent temperature regimes along the temperature scale. In low temperature regime, the ALE growth is a strong function of temperature. There appears a difference in the observation of a temperature processing window for ALE. Experiments performed in both vacuum[40] and at atmospheric pressure[28] found very narrow or virtually no plateau in this plot while that performed in a pulsed jet reactor gave a temperature window as wide as ~100 °C.[20][41] This discrepancy extends into the high temperature regime where the growth rate was seen to either increase or decrease. Since both the ALE in vacuum and at atmospheric pressure behaved similarly, premature TMGa gas phase decomposition alone will not explain the phenomenon. The decrease of ALE growth rate with temperature in the high temperature regime was stipulated[20] as the desorption of Ga-containing species but a conclusive evidence is still lacking. By fitting the growth data to a simple model at different temperature, Ozeki *et al.* was able to find a kinetic parameter of $k_{dc} \approx 5 \times 10^{11} \exp(-42000/RT)$ for the decomposition of TMGa on GaAs surface.[20]

From these temperature dependence studies one can see that for a true area selective LALE growth, it is desirable to grow at temperature approximately 100 °C lower than that used in ALE. The effect of laser illumination in this temperature range was found to widen the ALE processing window by ~50 °C towards lower temperature.[28][38] This difference in temperature dependence between ALE and LALE indicates that LALE does not proceed solely by laser induced local heating.

1.3.2 Self Limiting Mechanisms

The mechanism of self limiting in ALE using metalorganics has been the subject of extensive studies not only because the result can provide knowledge necessary for optimizing the ALE process but also because it offers a different point of view on the surface kinetics for conventional MOCVD, especially at low pressure and reduced temperature. Various models are proposed to explain ALE self limiting growth phenomenon. Surface sensitive tools and techniques are utilized to identify the species responsible for self limiting growth and to quantify their evolution along course of the process, such as X-ray photoelectron spectroscopy (XPS), reflection high energy electron diffraction (RHEED), reflectance difference spectroscopy (RDS), temperature programmed desorption (TPD), and time-resolved molecular beam mass spectrometry. Of more visibility are the three proposed mechanisms as depicted schematically in Fig.1.11. The selective adsorption mechanism (SA) or similar proposals assumes that the impinging TMGa molecules only chemisorb on As sites but not on Ga sites therefore the adsorption ceases at full monolayer coverage of Ga. This assumption is not always stated explicitly but is implicitly included in kinetic models as the term of $(1-\theta_{Ga})$, where the θ_{Ga} is the surface coverage by nonvolatile Ga species. The SA model has been used by many[20][28][42][43] to explain the ALE self limiting growth behavior to certain degree of success, especially for perfect saturation case. This model will not predict the failure of ALE for prolonged exposure and/or at high temperature without invoking the gas phase decomposition of the source molecules. As there is experimental evidence that failure of ALE can also occur in vacuum,[40] this picture of perfect self limiting is still

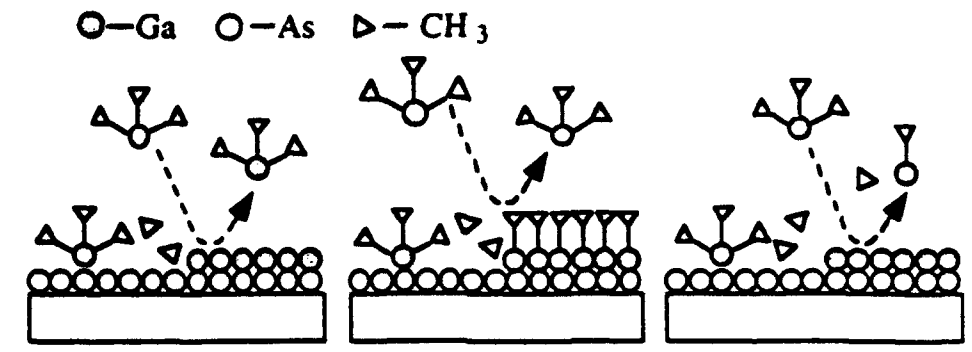

(a) Selective Adsorption (b) Site-Blocking (c) Flux Balance

Fig.1.11 Proposed ALE self limiting mechanisms of GaAs using TMGa.

controversial. The adsorbate inhibition (AI, also referred to as site-blocking) model depicts the self limiting in ALE as arising from the existence of a full layer of methyl radicals, resulting from TMGa dissociative adsorption, which prohibit further dissociative chemisorption of TMGa. The key experiment facts believed to support this model are the observation of CH_3 desorption during TPD experiments and the irreversible decomposition of TMGa on the Ga-rich (1x6) or "(4x6)" surfaces.[44]-[48] One problem with the AI mechanism is that the measured methyl residence time is too short for methyl radicals still available to inhibit further adsorption at high temperature (T> 500 °C). Another point of view of the ALE mechanism is to propose[47][49] that even though TMGa decomposes on the Ga-rich surfaces, the net Ga coverage of one monolayer could be obtained because of the in-coming Ga-containing flux (TMGa) is counter balanced by the desorbing flux of a volatile Ga specie, specifically CH_3Ga. This is referred to as the flux balance mechanism (FB). The key

observations are the decreasing CH_3 signal accompanied by an increasing CH_3Ga signal during repeated dosing of an originally C(2x8) As-rich (100) GaAs surface in a molecular beam mass spectrometric experiment.[49] It is well known and also will become clear in the next chapter that the detection of short lived intermediates using conventional impact ionization mass spectrometer is complicated by the chemistry in the ionization chamber. There was no indisputable positive identification of CH_3Ga specie in the desorption products and the evidence of substantial quantity of CH_3Ga that is essentially equal to the TMGa flux in the later stage of dosing if the FB model were a true representation of the situation.

As the chemistry of ALE is complex and is likely to vary at different stages of the process, these mechanisms alone will not be a valid representation of the ALE self limiting process. It necessitates the use of a blend of these mechanisms, as was done by Maa and Dapkus.[48] Based on their XPS, RDS, and RHEED observations of ALE process in ultrahigh vacuum, they suggested that several mechanisms contributed to the self limiting growth in ALE using TMGa. Surface As sites were the only active site for TMGa dissociative adsorption. Excess exposure to TMGa caused these molecules to react at As sites exposed by the Ga-Ga dimer vacancies on the initially reconstructed surface. The CH_3 radicals formed from the dissociation of TMGa attach themselves to the near-by Ga sites causing the original Ga-Ga dimers to dissociate. These CH_3 not only block effective further dissociative adsorption of TMGa but also co-desorb with the excess Ga during subsequent reconstruction upon termination of TMGa supply. While these mechanisms are all plausible and self consistent with the

specific set of observations, a complete mechanism that can explain qualitatively and predict quantitatively all observed ALE self limiting phenomena is still not developed. It is also clear from this review discussion that the attainment or failure of ALE growth of GaAs using TMGa and AsH_3 depends critically on the surface and gas phase chemical properties of TMGa. We have addressed this problem partially in this work by carrying out a gas phase thermal decomposition study of TMGa, the results of which will be presented in the next chapter.

The mechanism of self limiting in LALE is complicated by the fact that one needs not only to explain the self limiting phenomena but also to clarify the role of the laser illumination in localized enhancement of deposition. A somewhat complete analysis available for comment is the one proposed by Doi *et al.*[51] In this analysis, the self limiting was described as a result of the different decomposition rates of the metal alkyls at As and Ga sites, which becomes similar to the SA mechanism of ALE discussed earlier in the limit of $\tau_{As}/\tau_{Ga} \rightarrow 0$, where the τ_{As} and τ_{Ga} were the decomposition time constants for TMGa at As and Ga sites, respectively. The effect of laser illumination was assumed to reduce the activation energies for both decomposition of TMGa at As and Ga sites with different power dependence. The reduction in the activation energies followed an empirical expression as

$$E_a = A - BP \qquad (1\text{-}2),$$

where the parameters A and B were to be obtained from a fit to the growth data and P was the laser intensity. No physical pictures of this decrease in activation energies due to laser illumination were discussed. Such phenomenological description, though it agrees well with their own LALE growth data through extensive use of non-physical fitting parameters, offers limited understanding to the LALE process. Furthermore, the different behaviors displayed by TEGa in ALE and LALE is yet another puzzle. If explained properly, this may lead to a clue for the self limiting mechanism in LALE. Nevertheless, much more work is needed before an acceptable mechanism for LALE is established.

1.3.3 GaAs material properties by ALE and LALE

GaAs material grown by ALE using TMGa and AsH_3 has been characterized by capacitance-voltage (CV), secondary ion mass spectrometry (SIMS), Hall , and photoluminescent (PL) measurements. The layers obtained under typical ALE conditions where perfect self limiting is observable exhibit unintentional hole concentration of 10^{16} ~$5x10^{18}$ cm^{-3}. These acceptors have been identified as carbon by SIMS measurement.[52] Carbon incorporation is found to depend strongly on ALE operation conditions, as is shown in Fig.1.12.[52] This suggests that the carbon contamination could be reduced further by reducing TMGa exposure while increasing AsH_3 exposure. ALE GaAs with n type impurity as low as $2x10^{14}$ cm^{-3} and electron mobility of 65000 cm^2/vs at 77 K was also reported,[20] though the credibility of the data is still in question because of the thin layer (0.5 μm) used in the Hall measurement. It is interesting to note that the electrical properties of GaAs by ALE in vacuum reported so

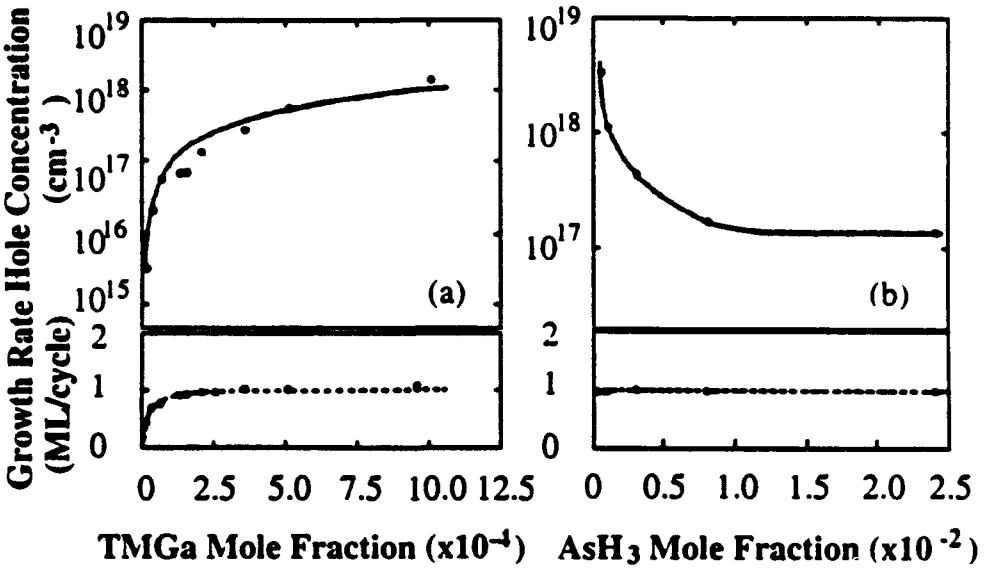

Fig.1.12 The influence of (a) TMGa flux and (b) AsH_3 flux on carbon incorporation in GaAs grown by ALE, from Mochizuki *et al.*[52]

far are inferior with hole concentrations ranging from 10^{18} cm^{-3} to 10^{20} cm^{-3} and mobilities of ~100 cm^2/vs (the measurement temperature was unfortunately neglected).[17] This occurs despite the fact that one expects a wider ALE operation window through the elimination of gas phase decomposition of TMGa.

Under favorable conditions, the films grown by ALE using TMGa and AsH_3 displayed excitonic features[20] in low temperature (4.2K) PL spectra. The quantum wells (QW's) with the well material grown by ALE and the AlGaAs barriers by conventional MOCVD showed sharp QW peaks with full width at half minimum (FWHM) as narrow as 6.3 mev at 8 K.[19] These reported data indicate good optical quality of GaAs by ALE.

As the intensity required for truly area selective LALE of GaAs is typically above ~200 w/cm^2 even for long illumination time (2.5s),[27] the area of LALE deposit is usually small. The techniques that can be applied to the characterization of materials grown by LALE is limited by the small areas available for electrical contacts and other diagnostic probing. Prior to this work, no electrical measurements were reported to be performed on GaAs grown by LALE operating within the true area selective and the self limiting process windows. Optical measurements, on the other hand, offers an easy access to probe the small LALE deposits. The 77 K PL spectrum reported by Karam *et al.*[27] showed a sharp peak of FWHM ~10 mev for LALE GaAs grown at bias temperature of 300 °C, indicating reasonably good quality. Raman spectroscopy was used by Miyoshi *et al.*[53] to assess the crystallinity of GaAs grown by LALE using TEGa and AsH_3. Only a pure LO-phonon mode was observed in the LALE GaAs at 295.2 cm^{-1}. The spectral shape of the LALE GaAs was similar to that of the bulk substrate. The spectra did not reveal any difference between the measurements at different location of the illuminated area. These results indicate that the crystalline quality of the LALE GaAs is as good as that of the substrate. The fact that an LO phonon-plasma coupled mode was not observable was used to estimate the carrier concentration to be less than $5x10^{17}$ cm^{-3}.In this dissertation, we will extend these areas of investigation to quantify the LALE growth process and to improve the quality of GaAs grown by this technique.

1.4 Organization of the Thesis

In the proceeding sections, we have seen that LALE is an attractive alternative technique for in-situ OEIC fabrication. As the technique is still in its infancy, earlier work had primarily focused on the growth phenomena of LALE. There was no systematic correlation between the growth parameters and material quality. Consequently, there was no evidence of device quality materials obtained by LALE. The choice of a precursor appeared to be random, based only on commercial availability and convenience because the effect of reaction chemistry on material quality was still not understood. In the remainder of this thesis, we shall address certain aspects of these issues based on our experimental results.

As the attainment or failure of ALE self limiting growth depend critically on the stability of TMGa in the gas phase, a study of TMGa gas phase decomposition is carried out and the results and their implications to ALE and LALE are discussed in CHAPTER TWO. In CHAPTER THREE, LALE using TMGa and AsH_3 is taken as a model combination for a systematic investigation of the effects of growth parameters on the GaAs material quality. The outcome is the knowledge of optimization of LALE growth for low carbon impurity contamination and the demonstration of device quality GaAs by LALE. The use of other precursors in ALE and LALE to obtain low carbon impurity GaAs are also explored and the results are given in CHAPTER FOUR and CHAPTER FIVE, respectively. In CHAPTER SIX, an attempt is made to explain the growth phenomena pertaining to the situation where the additional energy for growth is

supplied in the form of a laser (may also apply to electron) beam. From a quantitative modeling of ALE process and the temperature rise due to laser illumination, the thermal effect during LALE is assessed. In CHAPTER SEVEN, we demonstrate for the first time some successful applications of LALE to the fabrication of photonic devices. Finally, in Chapter Eight, the important conclusions that can be drawn from this work are summarized. Suggestions on the directions of further work are given including the preliminary result of direct alloy growth of InGaAs by LALE, which we hope to serve as stimulus for further work.

References for Chapter One

[1] S.Norimatsu and K.Iwashita, "10 Gbit/s Optical PSK Homodyne Transmission Experiment Using External Cavity DFB LDs," Electron. Lett., Vol.26(10), 648(1990).

[2] For an introductory account of this subjected the readers are referred to a book by R.G.Hunsperger, "Integrated Optics: Theory and Technology," 2nd ed., Springer-Verlag, 1985.

[3] T.L.Koch and U.Koren, "InP-Based Photonic Integrated Circuits," IEE Proceedings-J, Vol.138(2), 139(1991).

[4] Y.Aoyagi, S.Masuda, and S.Namba, "Laser Enhanced Metalorganic Chemical Vapor Deposition Crystal Growth in GaAs," Appl. Phys. Lett., Vol.47(2), 95(1985).

[5] S.M.Bedair, J.K.Whisnant, N.H.Karam, M.A.Tischler, and T.Katsuyama, "Laser Selective Deposition of GaAs on Si," Appl. Phys. Lett. Vol.48(2), 174(1986).

[6] J.E.Epler, H.F.Chung, D.W.Treat, and T.L.Paoli, "AlGaAs Multiple-Wavelength Light-Emitting Bar Grown by Laser-Assisted Metalorganic Chemical Vapor Deposition," Appl. Phys. Lett., Vol.52(18), 1499(1988).

[7] H.Sugiura, R.Iga, T.Yamada, and M.Yamaguchi, "Ar Ion Laser-Assisted Metalorganic Molecular Beam Epitaxy of GaAs," Appl. Phys. Lett., Vol.54(4), 335(1989).

[8] V.M.Donnelly, C.W.Tu, J.C.Beggy, V.R.McCrary, M.G.Lamont, T.D.Harris, F.A.Baiocchi, and R.C.Farrow, "Laser-Assisted Metalorganic Molecular Beam Epitaxy of GaAs," Appl. Phys. Lett., Vol.52(13), 1065(1988).

[9] H.Liu, J.C.Roberts, J.Ramdani, S.M.Bedair, J.Farari, J.P.Vilcot, and D.Decoster, "Fabrication of GaAs Photodiode Using Laser Selective Area Epitaxy," Appl. Phys. Lett., Vol.58(4), 388(1991).

[10] H.Liu, J.C.Roberts, J.Ramdani, and S.M.Bedair, "Laser Selective Area Epitaxy of GaAs Metal-Semiconductor-Field-Effect Transistor", Appl. Phys. Lett, Vol.58(15), 1659(1991).

[11] H.M.Manasevit, "Single-Crystal Gallium Arsenide on Insulating Substrates," Appl. Phys. Lett., Vol.11, 156(1968) and H.M.Manasevit and

W.I.Simpson, "The Use of Metal-Organics in the Preparation of semiconductor Materials: I. Epitaxial Gallium-V Compounds," J. Electrochem. Soc., Vol.116(12), 1725(1969).

[12] S.Ito, T.Shinohara, and Y.Seki, "Properties of Epitaxial Gallium Arsenide from Trimethylgallium and Arsine," J. Electrochem. Soc., Vol.120(10), 1419(1973).

[13] D.H.Reep and S.K.Gandhi, "Deposition of GaAs Epitaxial Layers by Organometallic CVD: Temperature and Orientation Dependence," J. Electrochem. Soc., Vol.130(3), 675(1983).

[14] H.Heinecke, E.Veuhoff, N.Putz, M.Heyen, and P.Balk, "Kinetics of GaAs Growth by Low Pressure MOCVD," J. Electron. Mat., Vol.13(5), 815(1984).

[15] T.Suntola and J.Antson, U.S. Patent No. 4058430 (1977).

[16] T.Suntola, A.Pakkala, and S.Lindfors, U.S. Patent No.4413022(1983).

[17] J.Nishizawa, H.Abe, and T.Kurabayashi, "Molecular Layer Epitaxy," J. Electrochem. Soc., Vol.132(5), 1197(1985).

[18] M.A.Tischler and S.M.Bedair, "Self-Limiting Mechanism in the Atomic Layer Epitaxy of GaAs," Appl. Phys. Lett., Vol.48(24), 1961(1986).

[19] S.P.DenBaars, C.A.Beyler, A.Hariz, and P.D.Dapkus, "GaAs/AlGaAs Quantum Well Lasers with Active Region Grown by Atomic Layer Epitaxy," Appl. Phys. Lett., Vol.51(19), 1530(1987).

[20] M.Ozeki, K.Mochizuki, N.Ohtsuka, and K.Kodama, "New Approach to the Atomic Layer Epitaxy of GaAs Using a Fast Gas Stream," Appl. Phys. Lett., Vol.53(16), 1509(1988).

[21] A.Usui and A.Sunakawa, "GaAs Atomic Layer Epitaxy by Hydride VPE," Jpn. J. Appl. Phys., Vol.25, L212(1986).

[22] H.Ohno, S.Ohtsuka, A.Ohuchi, T.Mutsubara, and H.Hasegawa, "Growth of GaAs, InAs, and GaAs/InAs Superlattice Structures at Low Substrate Temperature by MOVPE," J. Cryst. Growth, Vol93, 342(1988).

[23] W.G.Jeong, E.P.Menu, and P.D.Dapkus, "Steric Hindrance Effects in Atomic Layer Epitaxy of InAs," Appl. Phys.Lett., Vol.55(3), 244(1989).

[24] A.Koukitu, H.Nakai, A.Saegusa, T.Suzuki, O.Nomura, and H.Seki, "Solid Composition of $In_{1-x}Ga_xAs$ Grown by the Halogen Transport Atomic Layer Epitaxy," Jpn. J. Appl. Phys., Vol.27, L744(1988).

[25] Y.Sakuma, M.Ozeki, K.Kodama, and N.Ohtsuka, "Role of Interface Strain in Atomic Layer Epitaxy Growth Kinetics of $In_xGa_{1-x}As$," J. Cryst. Growth, Vol.114, 31(1991).

[26] A.Doi, Y.Aoyagi, and S.Namba, "Stepwise Monolayer Growth of GaAs by Switched Laser Metalorganic Vapor Phase Epitaxy," Appl. Phys. Lett., Vol.49(13), 785(1986).

[27] N.H.Karam, H.Liu, I.Yoshida, and S.M.Bedair, "Direct Writing of GaAs Monolayer by Laser-Assisted Atomic Layer Epitaxy," Appl. Phys. Lett., Vol.52(14), 1144(1988).

[28] S.P.DenBaars and P.D.Dapkus, "Atomic Layer Epitaxy of Compound Semiconductors with Metalorganic Precursors," J. Cryst. Growth, Vol.95, 195(1989).

[29] S.Iwai, T.Meguro, A.Doi, Y.Aoyagi, and S.Namba, "Monolayer Growth and Direct Writing of GaAs by Pulsed Laser Metalorganic Vapor Phase Epitaxy," Thin Solid Films, Vol.163, 405(1988).

[30] T.Meguro, S.Iwai, Y.Aoyagi, K.Ozaki, Y.Yamamoto, T.Suzuki, Y.Okano, and A.Hirata, "Atomic Layer Epitaxy of AlAs and AlGaAs," J. Cryst. Growth, Vol.99, 540(1990).

[31] M.Ozeki, K.Kodama, Y.Sakuma, N.Ohtsuka, and T.Takanohashi, "GaAs/GaP Strained-Layer Superlattices Grown by Atomic Layer Epitaxy," J. Vac. Sci. Technol. B8(4), 741(1990).

[32] P.C.Colter, S.A.Hussien, A.Dip, M.U.Erdogan, W.M.Duncan, and S.M.Bedair, "Atomic Layer Epitaxy of Device Quality GaAs with 0.6 μm/h Growth Rate," Appl. Phys. Lett, Vol.59(12), 1440(1991).

[33] P.D.Dapkus, B.Y.Maa, Q.Chen, W.G.Jeong, and S.P.DenBaars, "Atmospheric Pressure Atomic Layer Epitaxy: Mechanisms and Applications," J. Cryst. Growth, Vol.107, 73(1991).

[34] J.Nishizawa, H.Abe, and T.Kurabayashi, "Doping in Molecular Layer Epitaxy," J. Electrochem. Soc., Vol.136(2), 478(1989).

[35] M.Ozeki, K.Mochizuki, N.Ohtsuka, and K.Kodama, "Growth of GaAs and AlAs Thin Films by A New Atomic Layer Epitaxy Technique," Thin Solid Films, Vol.174, 63(1989).

[36] Y.Sakuma, K.Kodama, and M.Ozeki, "Atomic Layer Epitaxy of GaP and Elucidation for Self-Limiting Mechanism," Appl. Phys. Lett., Vol.56(9), 827(1990).

[37] Y.Sakuma, M.Ozeki, N.Ohtsuka, and K.Kodama, "Comparative Study of Self-Limiting Growth of GaAs Using Different Ga-Alkyl Compounds: $(CH_3)_3Ga$, $C_2H_5(CH_3)_2Ga$, and $(C_2H_5)_3Ga$," J. Appl. Phys., Vol.68(11), 5660(1990).

[38] Y.Aoyagi, A.Doi, and S.Iwai, and S.Namba, "Atomic-Layer Growth of GaAs by Modulated-Continuous-Wave Laser Metalorganic Vapor-Phase Epitaxy," J. Vac. Sci. Technol., B5(5), 1460(1987).

[39] T.Meguro, T.Suzuki, K.Ozaki, Y.Okano, A.Hirata, Y.Yamamoto, "Surface Process in Laser-Atomic Layer Epitaxy (Laser-ALE) of GaAs," J. Cryst. Growth, Vol93, 190(1988).

[40] J.Nishizawa, T.Kurabayashi, H.Abe, and A.Nozoe, "Mechanism of Surface Reaction in GaAs Layer Growth," Surface Sci., Vol.185, 249(1987).

[41] M.Ozeki, N.Ohtsuka, Y.Sakuma, and K.Kodama, "Pulsed Jet Epitaxy of III-V Compounds," J. Cryst. Growth, Vol.107, 102(1991).

[42] H.Ishii, H.Ohno, K.Matsuzaki, and H.Hasegawa, "Effect of Exposure to Group III Alkyls on Compound Semiconductor Surfaces Observed by X-ray Photoelectron Spectroscopy," J. Cryst. Growth, Vol.95, 132(1982).

[43] K.Kodama, M.Ozeki, K.Mochizuki, and N.Ohtsuka, "In Situ X-ray Photoelectron Spectroscopic Study of GaAs Grown by Atomic Layer Epitaxy," Appl. Phys. Lett., Vol.54, 656(1989).

[44] J.R.Creighton and B.A.Banse, in "Atomic Layer Growth and Processing," Eds., T.F.Kuech, P.D.Dapkus, and Y.Aoyagi, Mat. Res. Soc. Symp. Proc., Vol222, 15(1991).

[45] J.R.Creighton, "Chemisorption and Decomposition of Trimethylgallium on GaAs (100)," Surface Sci., Vol.234, 287(1990).

[46] J.R.Creighton, K.R.Lykke, V.A.Shamamian, and B.D.Kay, "Decomposition of Trimethylgallium on the Gallium-rich GaAs (100) Surface: Implications for Atomic Layer Epitaxy," Appl. Phys. Lett., Vol.57(3), 279(1990).

[47] M.L.Yu, U.Memmert, N.I.Buchan, and T.F.Kuech, in "Chemical Perspectives of Microelectronic Materials II," Eds., L.V.Interante, K.F.Jensen, L.H.Dubois, and M.E.Gross, Mat. Res. Soc. Symp. Proc., Vol.204, 37(1991).

[48] V.M.Donnelly, J.A.McCaulley, and R.J.Shul, in "Chemical Perspectives of Microelectronic Materials II," Eds., L.V.Interante, K.F.Jensen, L.H.Dubois, and M.E.Gross, Mat. Res. Soc. Symp. Proc., Vol.204, 15(1991).

[49] M.L.Yu, N.I.Buchan, R.Souda, and T.F.Kuech, in "Atomic Layer Growth and Processing," Eds., T.F.Kuech, P.D.Dapkus, and Y.Aoyagi, Mat. Res. Soc. Symp. Proc., Vol222, 3(1991).

[50] B.Y.Maa and P.D.Dapkus, in "Atomic Layer Growth and Processing," Eds., T.F.Kuech, P.D.Dapkus, and Y.Aoyagi, Mat. Res. Soc. Symp. Proc., Vol222, 25(1991).

[51] A.Doi, S.Iwai, T.Meguro, and S.Namba, "A Growth Analysis for Metalorganic Vapor Phase Epitaxy of GaAs," Jpn. J. Appl. Phys., Vol.27(5), 795(1988).

[52] K.Mochizuki, M.Ozeki, K.Kodama, and N.Ohtsuka, "Carbon Incorporation in GaAs Layer Grown by Atomic Layer Epitaxy," J. Cryst. Growth, Vol.93, 557(1988).

[53] T.Miyoshi, S.Iwai, Y.Iimura, Y.Aoyagi, and S.Namba, "Characterization of GaAs and AlGaAs Layers Grown by Laser Atomic Layer Epitaxy," Jpn. J. Appl. Phys, Vol.29(8), 1435(1990).

CHAPTER TWO

THE STUDY OF THERMAL DECOMPOSITION OF TRIMETHYLGALLIUM AND ITS RELEVANCE TO MOCVD, ALE, AND LALE

Despite the success in growing high quality III-V semiconductor materials by metalorganic chemical vapor epitaxy (MOCVD), the under standing of the process is still speculative in nature. Attempts to quantitatively predict MOCVD growth behavior through equilibrium[1],[2] and kinetic[3] analyses rely on the estimation of large number of estimated thermodynamic and kinetic parameters. Recent interest in atomic layer epitaxy (ALE) and laser-assisted ALE (LALE) of GaAs using trimethylgallium (TMGa) and AsH_3 increased the need for accurate information concerning the gas phase stability of TMGa and its surface reactivity. The work presented in this chapter deals with thermal decomposition of TMGa in a flow system monitored by molecular beam sampling mass spectrometry.

2.1 Basic Properties of TMGa

2.1.1 Thermodynamics

A property that describes the thermodynamic stability of TMGa is the standard enthalpy of formation, $\Delta H°_f$. The value recommended for TMGa in liquid form is $\Delta H°_f(TMGa(l)) = -79.8 \pm 6.3$ kJ/mol.[4] The value in the gas phase can be determined to be $\Delta H°_f(TMGa(g)) = -46.8 \pm 6.7$ kJ/mol

by using a value of ΔH_{vap}(TMGa) = 32.6 kJ/mol for the enthalpy of vaporization. The calculations from different sources of thermodynamic data agree well with each other, e.g. the values given by Pilcher and Skinner[5] are $\Delta H°_f$(TMGa(l)) = -74.7±6.2 kJ/mol and $\Delta H°_f$(TMGa(g)) = -46.1 kJ/mol. A more recent compilation by Tirtowidjojo and Pollard[1] gives $\Delta H°_f$(TMGa(g)) = -43.5 kJ/mol.

From the enthalpies of formation for TMGa(g), CH_3(g), and Ga(g),the mean Ga-methyl bond in TMGa can be calculated, D= 245 kJ/mol. Since the enthalpies of formation for $Ga(CH_3)_2$ (DMGa) and $GaCH_3$ (MMGa) are unknown, the individual bond strength is not accessible from thermodynamic calculations.

2.1.2 Kinetics

The kinetics process of interest are the decomposition of TMGa through reactions

$$TMGa \rightarrow DMGa + CH_3 \qquad (2\text{-}1a),$$

$$DMGa \rightarrow MMGa + CH_3 \qquad (2\text{-}1b),$$

$$MMGa \rightarrow Ga + CH_3 \qquad (2\text{-}1c).$$

The rate parameters most often given are those for reactions (2-1a) and (2-1b) reported by Jacko and Price,[6] i.e. $\log k_{1a}(s^{-1}) = 15.54 - 248.7\times10^3/(2.303RT)$ and $\log k_{1b}(s^{-1}) = 7.94 - 148\times10^3/(2.303RT)$, where

the activation energies are in units of kJ/mol. These activation energies for such simple first order unimolecular reactions correspond closely to the bond dissociation energies for the fission of first and second Ga-methyl bonds, respectively. Using the total bond dissociation energy quoted in the last subsection, 3xD, the bond dissociation energy for the third Ga-methyl bond is estimated to be 339 kJ/mol.

2.1.3 Spectroscopy

Spectroscopic data and their assignment are useful in species identification. The known vibrational responses of TMGa in the infrared (IR) range[4] are the Ga-Me (Me=methyl) symmetric stretching mode at 521 cm^{-1} and the asymmetric stretching mode 570 cm^{-1} numbers. Other significant vibrations and the corresponding assignments are the GaC_3 deformation at 163 cm^{-1} and the Ga-Me rocking modes at 612, 727, and 769 cm^{-1}. Unfortunately, the vibrational data of the intermediates, DMGa and MMGa, are not available. The frequencies of the IR active modes in these intermediates may be close to those of the corresponding modes in the parent molecules, judging from the Ga-Me stretching modes, in $(CH_3)_2GaCl$, at 540 (cm^{-1}) for symmetric and 600 (cm^{-1}) for asymmetric modes.[4]

In the ultraviolet range, TMGa in the vapor phase exhibits a broad band absorption with one maximum at $\lambda = 193$ nm. Appreciable absorption extends to ~260 nm.[7]-[9] The peak molar absorption coefficient is e ~$5x10^3$ $(mol/l)^{-1}cm^{-1}$, where $a = 6.023x10^{20}x\log_{10}(e)s$ relates the molar absorption coefficient to absorption cross section s in cm^2., where the e is the base of

the natural logarithm There was no report of observable absorption of light by the TMGa vapor in the visible range under normal intensity.

2.1.4 Structure

Structural information about a molecular species is important when the steric effect for reactions is considered. Vapor phase electron diffraction studies[10] have established that TMGa is monomeric, that it is a near-planar triangle structure with the bond length r(Ga-Me) 1.9672 Å and the C-Ga-C angles of 118.6°. A consistent assignment of IR and Raman spectra also requires the compliance to the selection rules of a planar GaC_3 structure with D_{3h} symmetry.[11]

2.2 Thermal Decomposition of TMGa – A Review

Early work of Jacko and Price[6] on TMGa thermal decomposition in toluene showed that only two thirds of the methyl radicals were released from TMGa up to temperatures as high as 650 °C. In that experiment, the volatile products were separated from the condensable substances and part of the sample was transferred to be analyzed by chromatography. The observation of carbon imbalance was used to describe the decomposition behavior of TMGa as that of a divalent metal alkyl, e.g. dimethylzinc, for the data obtained below 650 °C. The data analyses was based on a more critical assumption stating that, at temperatures above ~550 °C but < 650 °C, the TMGa quickly converted to DMGa ($Ga(CH_3)_2$) during a small fraction of the contact time. Below ~550 °C the decomposition of DMGa was not an important source of methyl radicals. The rate constants for the

breakage of the second and the first Ga-Me bond were then to be extracted independently. The division of the temperature ranges was determined by inferring to the change in the slope of the $\log(k_a/k_r^{1/2})$ versus 1/T plot, where the k_a is the rate constant for the methyl abstraction of a H from the carrier gas (toluene in this case) and the k_r is that of the recombination reactions between the methyl radicals. As other factors such as the concentration and the decomposition behavior of the carrier gas, from which hydrogen is abstracted by CH_3, may affect the $k_a/k_r^{1/2}$, thus, this division of temperature ranges has no solid ground. In addition, the analysis resulted in the assignment of an extremely low pre-exponential factor (8.7×10^7, cf. k_{1b} in section 2.1.2) for a first order unimolecular reaction that awaits further explanation. TMGa thermal decomposition was subsequently studied by infrared spectroscopy(IR),[12]-[15] mass spectroscopy,[16]-[20] and laser induced fluorescence (LIF)[21]. From the decrease in the mole fraction of TMGa as a function of temperature, DenBaars *et al.* were able to determine the activation energy for the rupture of the first Ga-methyl bond to be 58-62 kcal/mol.[14] Other investigations have been qualitative in general. TMGa decomposition is generally found to occur appreciably above about 420 °C. The major volatile low hydrocarbons are CH_4 and C_2H_6. The decomposition is more complete than previously found in the Ref.[6]. By isotope labeling, Larsen *et al.*[20] were able to identify the main source of CH_4 was from the abstraction of atomic H(D) from $H_2(D_2)$ by the methyl radicals liberated during TMGa decomposition. Various mechanisms are proposed for the initial step(s), the detailed path(s), and the role of carrier gases in the decomposition. However, a consistent picture

along with reliable kinetics information of TMGa gas phase thermal decomposition is not available.

2.3 The Molecular Beam Sampling Mass Spectrometry

Among the techniques used in the studies of TMGa gas phase decomposition, mass spectrometry has the advantages of being direct in species identification, highly sensitive, and reasonably accurate in quantitative measurement. There are doubts, however, whether the small volume of sample introduced into the ionization chamber through a conventional sampling assembly, such as a long capillary tube, is still representative of the system under investigation. In this work, we adopted a differentially pumped molecular beam sampling assembly that could extend into the hot zone of the decomposing gas stream. The basic design of the sampling nozzle assembly is shown in Fig.2.1. A huge pressure difference across the nozzle (P_I/P_{II} ~$4x10^4$) of orifice diameter ~150 μm causes directed flow at supersonic velocity. Part of this flow passes through the skimmer (the second orifice of diameter ~300 μm) located at a distance ~5mm down stream, forming a molecular beam in the high vacuum zone (zone III).

A number of features can be cited for this kind of sampling assembly. First, it was established that the beam intensity F, the number of molecules passing through the skimmer orifice per second, is in direct proportion to the molecular density in the source chamber, as is given by[22]

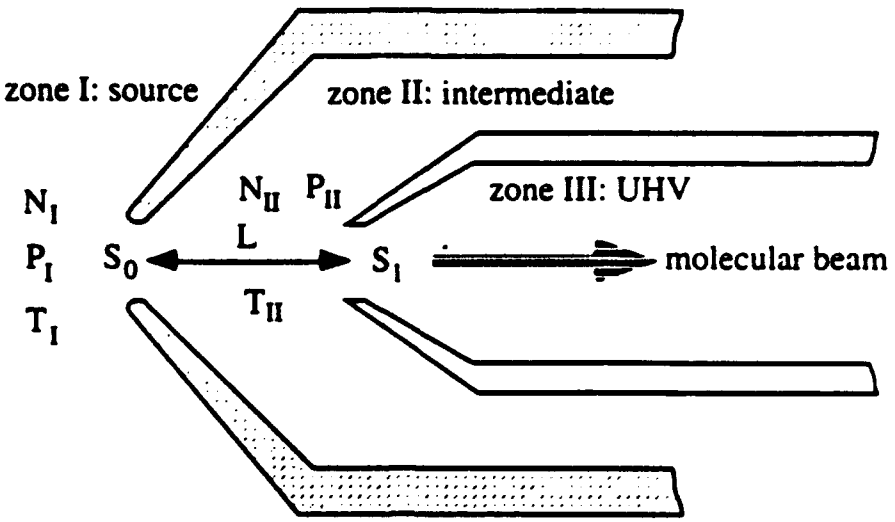

Fig.2.1 Schematic of a differentially pumped molecular beam sampling assembly.

$$F = S_1 N_{II} a_I \frac{M_n}{(1 + \frac{RM_n^2}{2C_v})^{\frac{1}{2}}} \qquad (2\text{-}2),$$

where the S_1 is the area of the skimmer, a_I is the velocity of sound in the source chamber, M_n the Mach number, R the idea gas constant, C_v the isochoric heat capacity, and the N_{II} is the molecular density at the entrance of the skimmer orifice, which is related to the molecular density in the source by

$$N_{II} = N_I \frac{P_{II}}{P_I} \frac{1}{(1 + \frac{RM_n^2}{2C_v})} \qquad (2\text{-}3).$$

This simple linear relationship is desirable for quantitative measurements.

Secondly, for the same pumping capacity that maintains the zone III under ultrahigh vacuum, this sampling technique gives a much stronger beam intensity seen by the ionization chamber of the mass spectrometer than the capillary bleeding technique does. Maintaining a high working vacuum in zone III is important to reduce the background contribution to mass spectroscopic detection of low abundance and evasive species.

Since the gas undergoes adiabatic expansion, part of the molecular energy, translational, rotational etc., is converted into ordered mass motion, which has the effect of quenching. Reduced random translational motion also minimizes collisions between molecules. Through a simple exercise one can estimate that it takes less that few milliseconds for molecules of M=100 to traverse a distance of ~1m at a source temperature of about 400 °C. These factors help to preserve, to a certain extent, some short-lived species. A differentially pumped sampling assembly has been used to monitor reactive intermediates.[23][24] It must be pointed out that the sampling is molecular mass selective and has a complicated temperature dependence. These effects can be canceled out by calibration runs with known standards.

2.4 Experimental Procedure

Fig.2.2 shows the schematic diagram of the experiment setup. The quartz reactor is 5.4 cm I.D. and 100 cm in length while the length of the temperature uniform zone can be varied from 67 cm to 33 cm by using

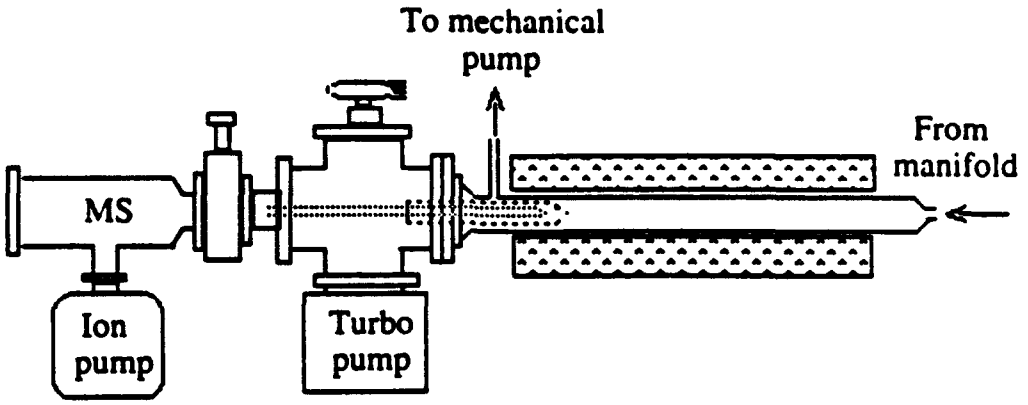

Fig.2.2 Schematic of molecular beam sampling mass spectrometry for TMGa thermal decomposition in a flow system.

different furnaces. The large diameter geometry and central positioning of the sampling assembly assures considerably less contribution from the reactions at the surface. Under typical operation conditions, the average contact time is in the range of a few seconds, as calculated by assuming the idea gas law. The reactor chamber is pumped by a mechanical pump to reduce the pressure drop across the first nozzle for stable molecular beam formation. The volume between the two orifices (zone II) is turbo pumped at a pressure of about 5×10^{-5} Torr under gas load. The nozzles are made of quartz tube corned at one end and with pin hole through the thin wall at the tip. The first nozzle and the skimmer (the second orifice) are critically aligned for concentricity. When the longer furnace is used, the sampling head is immersed in the hot zone. This allows a nearly *in situ* probing of the gas mixture under investigation. On the other hand, the sampling head assembly can also be located outside the hot zone when the shorter furnace is used.

Palladium purified H_2 or scientific grade N_2(MG 5.5) is used as the carrier gas for TMGa. The TMGa bubbler is kept in an ice bath. All gas flows are controlled by mass flow controllers. Total flow is fine adjusted by a metering valve at the inlet of the reactor. The pressure of the reactor is measured by a capacitance barometer. The quadrupole mass spectrometer (model 100-C, UTI) is interfaced to an HP Vectra E5 PC with a SPECTRALINK unit (UTI). The data acquisition is thus made simple, quick, accurate, and reproducible.

Before each run, the reactor tube is cleaned with a mixture of HF and HNO_3 (1:9), thoroughly rinsed with DI water, and blown dry with N_2. The tube was then heated to 200 °C under vacuum for degassing. The molecular beam sampling system is first tested for its behavior of beam intensity with respect to pressure and mole fraction. Trial runs were also done to calibrate the entire system with H_2, CH_4, C_2H_6, N_2, and TMGa in order to obtain a complete knowledge of the temperature dependent mass selectivity of the sampler. Experiments on TMGa thermal decomposition are generally carried out by monitoring multiple peak intensities at constant pressure and fixed TMGa to H_2 ratio with varying temperature or at constant pressure and temperature while varying the TMGa to H_2 ratio. In the former case, kinetic parameters can be extracted and in the latter case, the effect of H_2 on TMGa thermal decomposition is studied. Peak intensities are corrected for the temperature dependent mass selectivity and the thermal expansion of the gas. The corrections are made as if the effluent gas is cooled to room temperature.

2.5 Experimental Results

The molecular beam sampling system showed a linear dependence of the beam intensity on total pressure over the pressure range of operation (0.01—2 Torr.) for a gas mixture of H_2 saturated with TMGa maintained at 0 °C when the m/e=99 ion from TMGa is monitored. A slightly different test is also done for a H_2/N_2 mixture where a variable amount of H_2 is introduced into a N_2 flow but the total pressure remains constant. The detected H_2 signal (m/e=2) changes linearly with the change in the H_2 mole fraction. This linear relationship between the beam intensity and the volume density of molecules, eqn.s(2-2) and (2-3), was derived by Kantrovitz and Grey[22] and refined by Parker *et al.*.[25]

Typical mass spectra for TMGa in N_2 at room temperature(24 °C) and the temperature where considerable decomposition occurs(e.g. 720°C) are shown in Fig.2.3 (a) and (b). One task in using a mass spectrometer to obtain quantitative information is to identify peaks that best represent the molecular species of the sampled gas phase. Even at low ionization voltage (nominal 29 V measured from the terminals in the instrument console) where further reduction of the ionization voltage would result in drastic fall off in the sensitivity for this particular gas analyzer, TMGa produces only a very weak peak at the molecular ion position, i.e. m/e=114 and 116. Consequently the $Ga(CH_3)_2^+$ ions at m/e =99 and 101 are monitored as a measure of the remaining TMGa concentration. To obtain knowledge on the ionization behavior of TMGa, the ion current for several species of

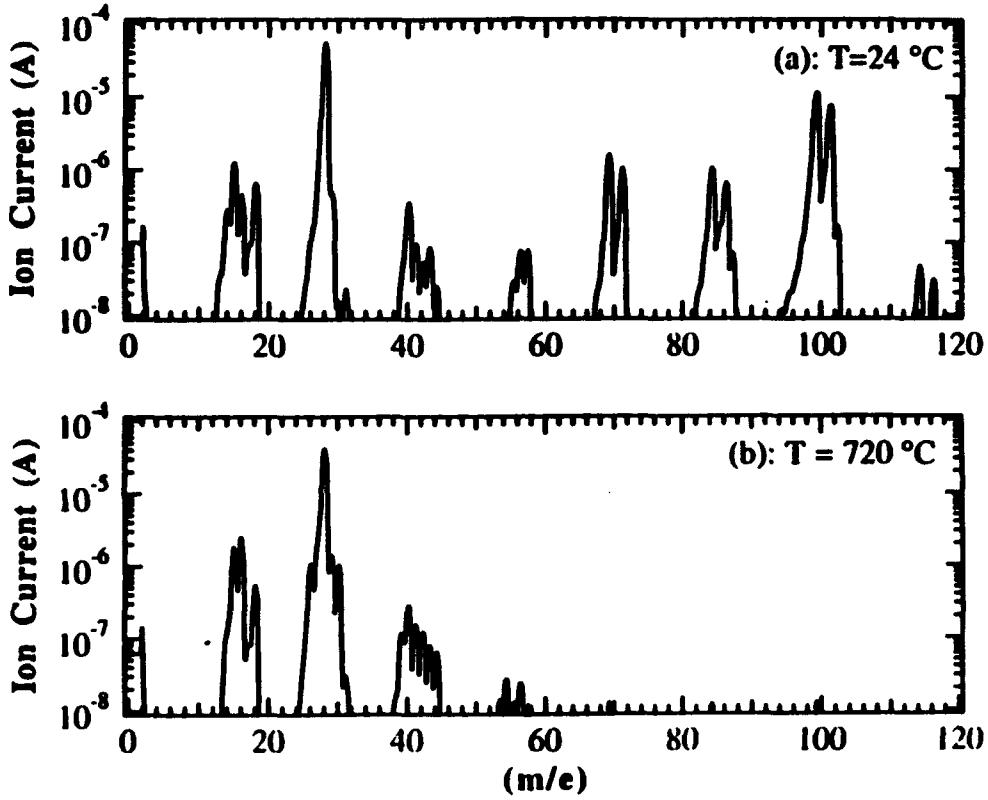

Fig.2.3 Typical mass spectra of TMGa in nitrogen obtained at ionization voltage of 29 v and at temperatures of (a) 24 °C and (b) 720 °C.

interest, CH_3 etc., were first recorded as a function of the ionization voltage for TMGa in N_2 without heating the furnace. This gives the ionization efficiency curves for TMGa and N_2. Similar ionization efficiency curves for CH_4 and C_2H_6 were also obtained. By using a procedure suggested by Warren[26] and McDowell and Warren,[27] these ionization efficiency curves are analyzed to yield the ionization potentials IP(M) for molecular ions and appearance potentials (AP(X^+/M)) for ion species X^+ from a parental molecule M, by referring to the known IP(N_2) = 15.58 ev.[28] The results are listed in Table 2.1. The ionization of TMGa has been studied by Glockling and Strafford.[29] The IPs and APs for species from TMGa agrees well with those of the Ref.[29] except the AP(Ga^+/TMGa). It is likely that the higher working pressure of the ionization chamber in their case ($6x10^{-6}$ mmHg) may have caused the Ga^+ to appear from two electron impact process, i.e. the residence time of certain Ga containing species is long enough to be ionized by subsequent electron impact, which give rise to an AP(Ga^+/TMGa) even lower than the AP($MMGa^+$/TMGa). There has been no report on AP(CH_3^+/TMGa) measurement. The important implication of our measurement of AP(CH_3^+/TMGa) will become clear in the discussion.

The low mass hydrocarbons evolving from the reaction are measured by the changes in the peak intensities at m/e=16 and 30. They are identified as mainly CH_4 and C_2H_6 according to the spectra obtained from 0.409% CH_4 in H_2 and 0.5% C_2H in H_2 standards, Fig.2.4 (a) and (b). The molecular ion of C_2H_6 is monitored instead of the stronger peak at m/e=28 because the ionization pattern of TMGa at m/e=28 would interfere with the

Table 2.1: Ionization and appearance potentials for selected species.

Molecules (M)	Ion Species (X^+)		This Work (ev)	Literature (ev)	Ref.
TMGa	TMGa	IP	9.88	9.87	[29]
	DMGa	AP	10.70	10.16	
	MMGa		13.52	13.65	
	Ga		15.16	13.24	
	CH_3		12.70		
CH_4	CH_4	IP	13.26	12.6	[27]
	CH_3	AP	14.98	14.39	
C_2H_6	C_2H_6	IP	11.63	11.6	[30]
	CH_3	AP	14.03	14.2	
CH_3	CH_3	IP		9.83	[28]
N_2	N_2	IP		15.58	

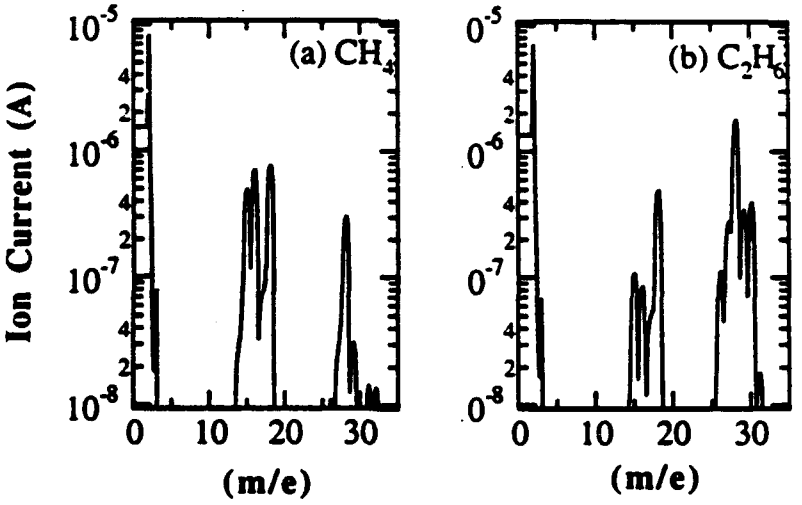

Fig.2.4 (a) The spectrum of 0.409% methane in hydrogen standard and (b) the spectrum of 0.5% ethane in hydrogen standard.

measurement and also because N_2 will be used as carrier gas for some relevant runs. The multiple peak monitoring and auto ranging features of the computer data acquisition are especially useful in this case to pick up a weak peak adjacent to a strong peak. The signal amplitudes for all of the Ga containing ion species decreased with the same dependence as the temperature was increased. This allows us to reasonably speculate that the measured Ga containing species all originate from the remaining parent molecules and that the signals from directly sampled intermediates are lower by at least two orders of magnitudes. In other words, the detection of any Ga containing species as the products of the thermal decomposition is masked by the high background contributed by the TMGa ionization pattern at nominal ionization voltage of 29 V, (cf. Fig.2.3 (a)).

When the peak intensities of undissociated TMGa at different temperatures are plotted, Fig.2.5 results. It is evident that appreciable decomposition does not occur until about 430 °C for TMGa in H_2 and 480 °C for TMGa in N_2. TMGa molecules disappear almost completely from the gas stream above about 610 °C. The data as shown in Fig.2.5 can be analyzed to yield apparent activation energies characteristic of the rate at which molecular TMGa disappears. The results are listed in Table 2.2 for several TMGa to H_2 mole ratios, where a known amount of N_2 is used as part or the whole of the carrier gas.

The involvement of H_2 in the reaction under the conditions used in our experiment can best be seen from the result of the experiment where variable admixture of TMGa/H_2/N_2 is fed into the reactor at T=600 °C and

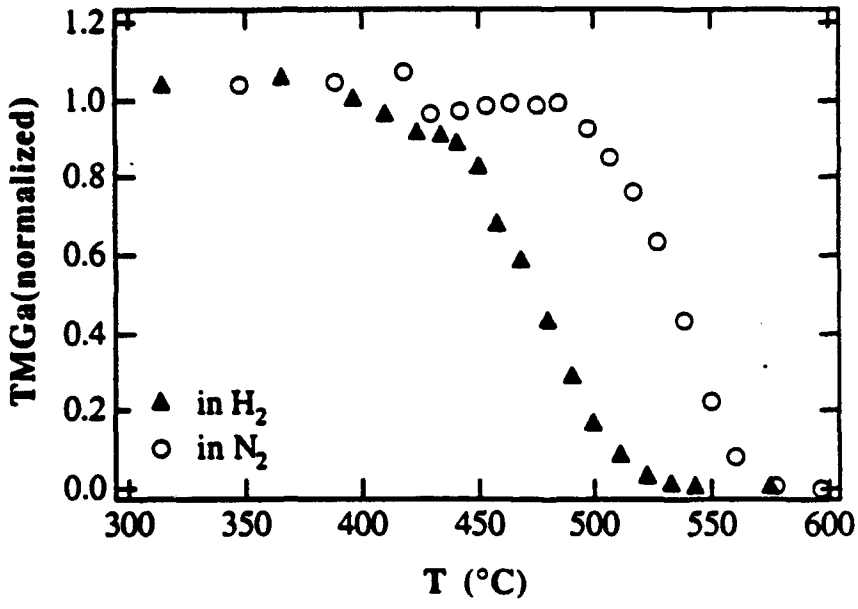

Fig.2.5 Percentage of undissociated TMGa as a function o temperature.

Table 2.2: Apparent First Order Rate Constants

$$(\ln k(s^{-1}) = \ln A - \frac{E_a}{RT}).$$

$\frac{[TMGa]}{[H_2]}$	0.30%	1.71%	8.03%	∞
lnA	31.3	31.7	31.7	37.9
Ea ($\frac{kcal}{mol}$)	50.9	51.5	54.8	64.6

P=2 Torr. The intensity of the remaining TMGa dropped drastically when the dose of H_2 is increased as shown in Fig.2.6. This implies that the introduction of H_2 generates species that will attack molecular TMGa. The

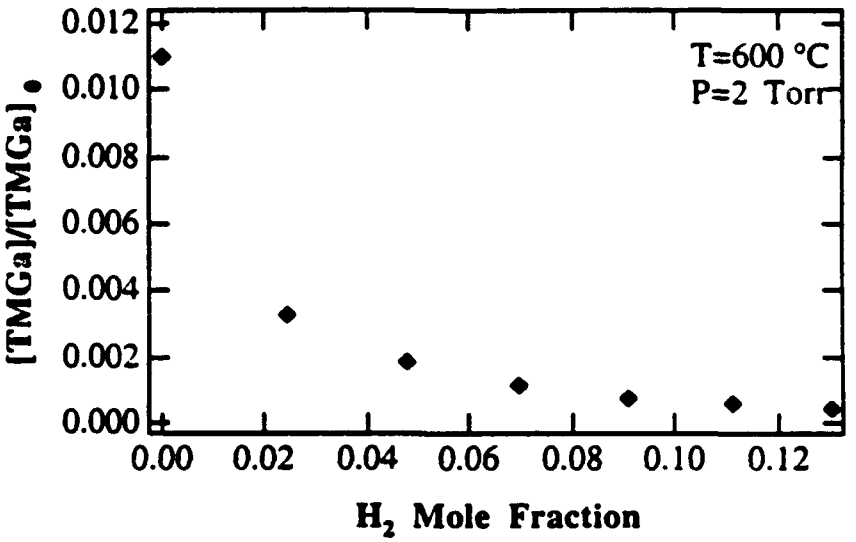

Fig.2.6 Percentage of remaining TMGa as a function of H_2 dosing mole fraction, showing the effect of carrier gas on the completeness of decomposition.

change in the relative amount of H_2 in the input gas mixture also changes the relative amount of CH_4 and C_2H_6 in the products as shown in Fig.2.7(a). The Fig.2.7(b) is from a steady state analysis. The advantage of plotting the abscissa in terms of $[TMGa]_0/([TMGa]_0+[H_2]_0)$ in the Fig.2.7(a) will become apparent during the discussion.

We can define a quantity which is the sum of the moles of CH_4 and two times the moles of C_2H_6 produced from the decomposition of each mole of the input TMGa,

$$PRD(CH_3)= \frac{[CH_4]}{[TMGa]_0} + 2\frac{[C_2H_6]}{[TMGa]_0} \qquad (2\text{-}4).$$

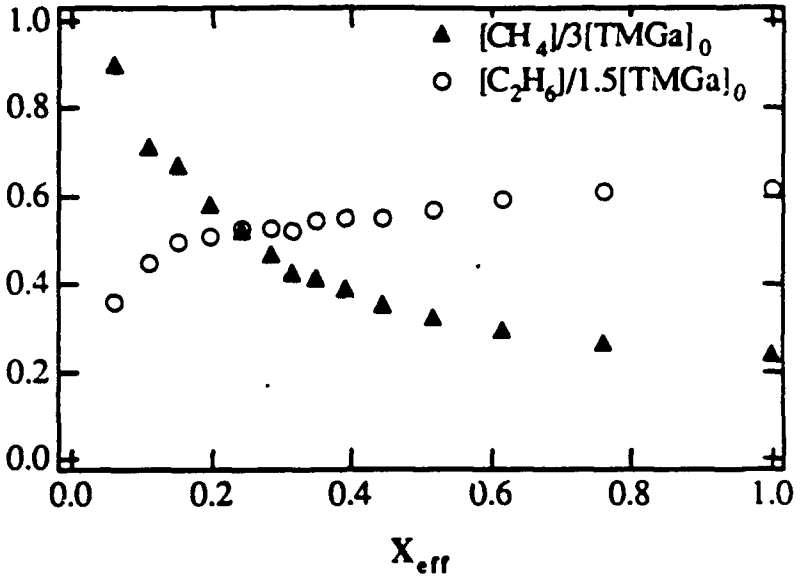

Fig.2.7 (a) Methane and ethane formation versus the effective TMGa mole fraction at 600 °C.

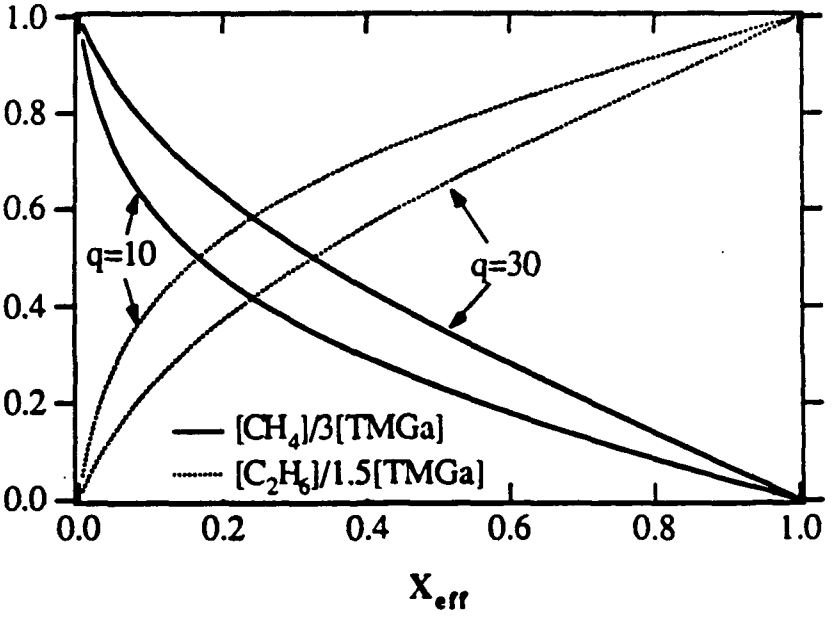

Fig.2.7 (b) Simulated methane and ethane production as a function of effective TMGa mole fraction, where the $q = k_{1a}k_y/k_{abst}^2$.

This quantity is then a measure of the number of moles of methyl radicals released for each mole of TMGa input into the reactor, ignoring much smaller contributions from other low mass hydrocarbons. This is a true measure of the over all decomposition progress, irrespective of the details of how these products are formed. The quantity PRD(CH_3) is plotted in Fig.2.8 as a function of reactor temperature. The smooth increase of low mass hydrocarbon products during TMGa decomposition does not seem to indicate a multiple rate limiting process.

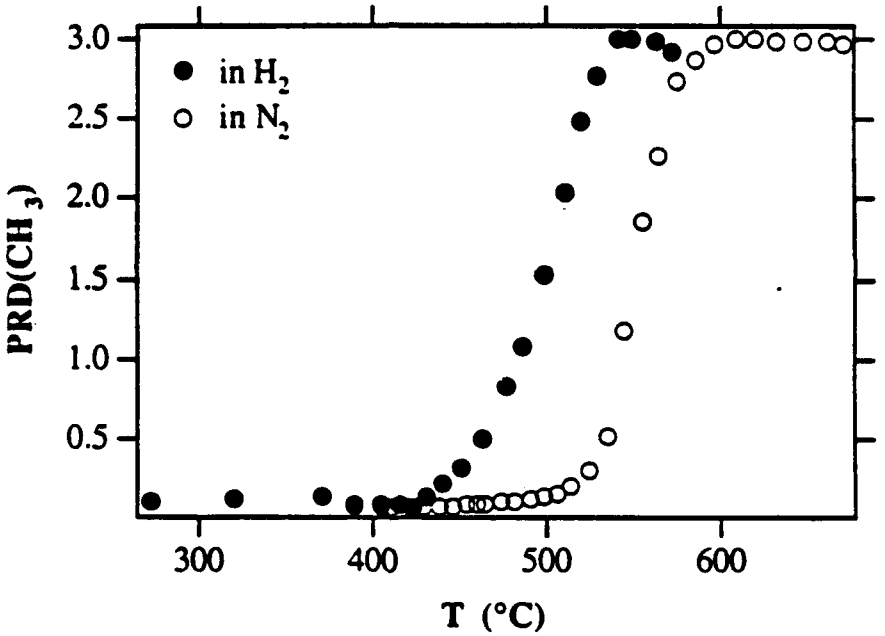

Fig.2.8 The moles of methyl radicals released from each mole of decomposing TMGa.

The completion of the decomposition is also tested by putting a few small pieces of Si wafers and quartz plates in the uniform hot zone of the reactor for several runs. They are taken out for evaluation. Droplets of diameters up to about 6 μm can be seen on the surface after decomposition

in either H_2 or N_2. The overall film on the quartz plates is electrically conducting. The deposit dissolves slowly in HCl with little residue. On the contrary, the deposit on the entrance section of the reactor wall, where the rising shoulder of the temperature profile occurs, leaves more residue even after the etch in 1:9 mixture of HF and HNO_3. This is especially true after decomposition in N_2. These observations suggests that the decomposition is complete with the production of Ga atoms under most conditions used here, that certain reactions involving CH_3 are more pronounced in N_2 ambient (cf. Reaction(2-8) below), and that any polymeric deposit tend to form in or diffuse to the low temperature region.

2.6 Discussion and Further Data Extraction

To explain our data, we propose the following minimal reaction scheme specifically for TMGa decomposition in H_2 with relatively long contact time so that steady state conditions are likely to be established:

$$TMGa \longrightarrow DMGa^* + CH_3^* \qquad (2\text{-}1a),$$

$$DMGa^* \longrightarrow MMGa^* + CH_3^* \qquad (2\text{-}1b),$$

$$MMGa^* \longrightarrow Ga + CH_3^* \qquad (2\text{-}1c),$$

$$H_2 + CH_3^* \longrightarrow CH_4 + H \qquad (2\text{-}5),$$

$$H + CH_3^* \longrightarrow CH_4 \qquad (2\text{-}6),$$

$$CH_3 + CH_3^* \longrightarrow C_2H_6 \qquad (2\text{-}7),$$

$$(CH_3)_xGa + CH_3^* \longrightarrow (CH_3)_{x-1}GaCH_2^* + CH_4 \qquad (2\text{-}8),$$

$$\longrightarrow ((CH_3)_{x-1}GaCH_2)_n \qquad (x=3,2,1),$$

$$(CH_3)_xGa + H \longrightarrow (CH_3)_{x-1}Ga^* + CH_4 \qquad (x=3,2,1) \quad (2\text{-}9).$$

The decomposition in N_2(non-reacting carrier gas) can also be discussed by ignoring the reactions originating from the presence of H_2. The reaction (2-8) is included to account for the methane formed when TMGa decomposes in N_2. More reactions may be added to account for small amount of C_2H_4 and higher mass hydrocarbons (m/e=40-44) seen in the spectra, but they are ignored here because of their low relative concentrations.

The inclusion of methyl radicals in the intermediates demands a few words of explanation. Butler and co-workers reported the observation of free CH_3^* from TMGa thermal decomposition over a hot susceptor using infrared-diode laser spectroscopy[15]. Although the direct observation of free methyl radicals by mass spectroscopy was claimed in the publications of Eltenton[30] from thermally decomposed mixture of tetramethyllead and ethane and Lossing and Tickner[31] from thermal decomposition of dimethylmercury in He, respectively, recent application of the technique is rare. We attempted to detect the net CH_3^* signal over the parent background of TMGa, CH_4, and C_2H_6 using a very low ionization voltage,

nominal 18 V and the lowest reasonable value for this gas analyzer. As can be seen from the results in the Table 2.1, AP(CH_3^+/TMGa) of 12.7 ev is only greater by a small margin than IP(CH_3) of 9.83 ev.[28] This is to be compared to the corresponding differences (AP(CH_3^+/M) - IP(CH_3^*)) for M = CH_4, 4.6 ev, and M = C_2H_6, 4.4 ev. Consequently, there will always be appreciable contribution to the m/e=15 signal from the ionization cracking pattern of molecular TMGa. At an appropriate low ionization voltage where the appearance of CH_3^+ from CH_4 and C_2H_6 can basically be avoided, only the contribution from TMGa is important relative to the contributions from CH_4 and C_2H_6 which are present as the products of the thermal decomposition. By operating the mass spectrometer at low ionization voltage we are able to obtain a net m/e=15 signal after subtracting the contribution from the remaining molecular TMGa. The net m/e=15 signal starts to appear at the temperature at which decomposition occurs appreciably. It increases with T at first and then decreases after passing a maximum, resembling the behavior of CH_3^* observed by Butler *et al.* [15] Methyl radicals also manifest themselves in the formation of such observed low mass hydrocarbon products as CH_4 and C_2H_6. These products are not likely to be formed directly from TMGa molecules through bond rearrangement. The additional energy in distorting the simple near planar structure of TMGa is too great to make this a favorable path. The molecular orbital calculation of Tsuda *et al.* [32] also showed process (2-1a) as the initial step in TMGa decomposition.

The temperature at which the decomposition becomes appreciable is related to the contact time . In Fig.2.5, we compare the decomposition in H_2

and N_2 for the same contact time. TMGa decomposition in H_2 commences at lower temperatures than in N_2. This shift of the curve to lower temperatures in Fig.2.5 is occasionally disputed as the effect of the difference in thermal and hydrodynamic properties of the carrier gases[17]. The change in relative amount of CH_4 versus C_2H_6 generated for different $TMGa/N_2/H_2$ mixtures as shown in Fig.2.7(a) is, however, a strong indication of the involvement of H_2 in the reactions. This confirms the result by Larsen *et al*[20]. Here the data are presented in terms of $[TMGa]_0/([TMGa]_0 + [H_2]_0)$ since an analysis by taking only the eqn.s (2-1a) through (2-1c) and the eqn.s (2-5) through (2-7) assumes a neat form when the $[CH_4]/3[TMGa]_0$ and $[C_2H_6]/1.5[TMGa]_0$ are expressed as functions of the effective TMGa mole fraction $X_{eff} = [TMGa]_0/([TMGa]_0 + [H_2]_0)$. Such analysis shows that the Eqn.s (2-1a) through (2-1c) and the eqn.s (2-5) through (2-7) describe the basic behavior of TMGa thermal decomposition in presence of H_2 as is shown in Fig.2.7(b), where the $q = k_{1a}k_r/k_{abst}^2$ with the k_{1a} being the rate constant of the reaction (2-1a), k_r being that of the reaction (2-7), and k_{abst} that of the reaction (2-5). Only at high X_{eff} does the experimental data differ from the simulation, where the eqn.(2-8) has to be considered. The direct reaction between H_2 and TMGa is ruled out by energy considerations. However, reaction (2-5) has a low activation energy around 10 kcal/mol.[33]-[35] It will compete with reactions (2-6) through (2-8) for the supply of CH_3^* and generate atomic H. The kinetics of attack on $(CH_3)_xGa$ by atomic H, reaction (2-9), is not known. It is considered as an important path in the destruction of atomic H because the activation energy for radical-molecule reaction is generally low.

At low concentration of H_2, the recombination of methyl radicals to form C_2H_6 dominates. A small amount of CH_4 forms from the abstraction of H by CH_3^* from Ga containing hydrocarbons, most likely $Ga(CH_3)^*$, i.e. x=1 in the reaction (2-8) because at this later stage of TMGa decomposition, the probability that a gallium containing species will collide with methyl radicals is the highest. A reasonable carbon balance supports this point. Since we did not observe the accumulation of either $Ga(CH_2)^*$ or CH_2^* species in the gas phase, we have to assume that the $Ga(CH_2)^*$ is not volatile and the Ga-CH_2 bond is stable. This accounts for the dark deposit on the reactor wall at the entrance of the hot zone, especially after TMGa decomposition in N_2. This deposit dissolves partially in mixture of HF and HNO_3 with films of polymer-resembling residue. At high H_2 concentration, reactions (2-5), (2-6), and (2-9) will dominate and CH_4 is then the primary low mass hydrocarbon species.

Frequently, a direct test of the effect of carrier gas on properties of the grown epilayers by conventional MOCVD hydride growth shows little dependence on carrier gas[36].[37]. This occurs because AsH_3 is a more effective source of atomic H than H_2 itself and facilitates the removal of CH_3 from the surface. It may also be pointed out that the decomposition behavior discussed here is obtained with moderate contact time. It is expected that with very short contact time the reactions between intermediates and carrier gas will be diminished. The effect of carrier gas on TMGa thermal decomposition becomes less perceptible.

The attack on TMGa by atomic H could explain the variation of the apparent activation energies with TMGa to H_2 ratios. In the extreme of TMGa thermal decomposition in N_2, only reactions (2-1a), (2-1b), (2-1c), (2-7), and (2-8) are to be considered. The apparent rate constant is obviously k_{1a} and the measured apparent activation energy can be taken as the activation energy for reaction (2-1a), i.e. E_{1a} = 64.6 kcal/mol. The determination of first order rate parameter from temperature dependence of the reactants does not involve any assumption on reaction details in producing products. Neither does it require an absolute calibration of the monitoring system. This type of measurement and analysis is easier and probably be more reliable than that from the temperature dependence of the products. The reported values for the E_{1a} are 59.5 kcal/mol[6] and 58 — 62 kcal/mol.[14] A molecular orbital calculation resulted in 64.9 kcal/mol.[32] The agreement is reasonable.

Since all the methyl radicals released from TMGa eventually form volatile hydrocarbon species, It is possible to measure experimentally the equivalent moles of CH_3 released from each mole of TMGa decomposed by monitoring the low mass volatile hydrocarbon species, as is defined in eqn.(2-4). A dynamic analysis considering only eqn.s (2-1a) through (2-1c) will relate the same quantity PRD(CH3) to the rate parameters $k_{1a}(A_{1a},E_{1a},T)$, $k_{1b}(A_{1b},E_{1b},T)$, and $k_{1c}(A_{1c},E_{1c},T)$. In principle, the apparent Arrhenius parameters for successive release of the three methyl radicals can be found independently by a multiple parameter least square curve fit to the data displayed in the Fig.2.8. To avoid the inaccuracies that result from the peculiar functional behavior of the Arrhenius expressions

for the rate constants, we choose to use the rate constant expression found from the temperature dependence of the remaining reactant (TMGa) as the apparent rate constant for the breakage of the first Ga-methyl bond, k_{1a}. We also estimate the Arrhenius pre-exponential factors for the unimolecular reactions of the rupture of the second and third Ga-methyl bonds, A_{1b} and A_{1c}, to be as $4x10^{14}$ sec^{-1} and $1x10^{14}$ sec^{-1} respectively by adopting a statistical thermodynamics approach as given, for example, by Benson.[38] The entropy changes from the original states to the transition states are calculated using the structural and spectroscopic information summarized in the section 2.1 and assuming that the excited bond elongates to ~2.8 times the original length.[38] The two parameter least square fits to the data as plotted in Fig.2.8 give the activation energies for the reactions of the rupture of the second and the third Ga-methyl bonds as E_{1b} = 52.6 kcal/mol and E_{1c} =54.1 kcal/mol respectively. The sum of the squared errors between the fitted expression and the experimental data has single sharp minimum with respect to E_{1b} and E_{1c}. The values of E_{1b} and E_{1c} are not very sensitive to the changes in A_{1b} and A_{1c}. It is important to note that the sum of the three activation energies thus determined independently is 171.3 kcal/mol, in agreement with the 172.4 kcal/mol thermochemical measurement of Long[39], the value of 175.7 kcal/mol summarized by Tuck[4], the value of 183.9 kcal/mol that is derived according to the compilation of Pilcher and Skinner[5], and the value of 176.1 kcal/mol that is calculated from the compilation of Tirtowidjojo and Pollard[1]. An electron impact study also gave a value of 166.8 kcal/mol for this quantity[29].

In Ref.[6], the rate of the reaction (2-1b), k_{1b}, was assumed to be much slower than that of the reaction (2-1a) in high temperature range such that all input TMGa is converted to DMGa in a small fraction of the contact time. A low activation energy for the reaction (2-1b) was deduced from the data analysis using this assumption. The result that E_{1b} is much lower than E_{1a} would generally mean that the rate of the reaction (2-1b) should be much faster than that of the reaction (2-1a) — contradicting the original assumption — unless the reactions (2-1a) and (2-1b) proceed by a totally different mechanism. Not only is this self inconsistency noteworthy, but also the absence of large quantities of $Ga(CH_3)_2^*$ and $Ga(CH_3)^*$ species from various diagnostic techniques would suggest that they are in relatively low concentrations. An equilibrium analysis of MOCVD[1] using these available kinetic data, however, predicts $Ga(CH_3)^*$ at more than quarter of the CH_4 concentration. This high level of $Ga(CH_3)^*$ has never been observed experimentally. The accuracy of the kinetic data used is in question. Our values of E_{1a}, E_{1b}, and E_{1c} are consistent with the picture that TMGa decomposes by releasing successively its three methyl radicals along the whole length of the hot zone and the intermediate species $Ga(CH_3)_2^*$ and $Ga(CH_3)^*$ do not survive for long, a life time probably determined by the rate of energy transfer, the environment that has caused the rupture of the first Ga-methyl bond. The stability of $Ga(CH_3)_2^*$ and $Ga(CH_3)^*$ are different only by a small margin in favor of the last Ga-methyl bond. Finally the presence of atomic Ga in the final products also points out the complete breakdown of TMGa above about 610 °C.

2.7 Conclusions and Their Implications to ALE Using TMGa

A detailed study has been carried out on thermal decomposition of TMGa in H_2, N_2, and their admixtures by using molecular beam sampling mass spectrometry. Methane and ethane are found as the primary volatile hydrocarbon products. At high enough temperatures, the relative amounts of CH_4 and C_2H_6 formed in the gas phase are affected by the presence of H_2. The amount of CH_4 increases and C_2H_6 decreases while the mole fraction of H_2 increases in a TMGa/H_2/N_2 mixture. The measured apparent activation energies from the temperature dependence of the remaining reactant differ for decomposition occurring in H_2 and N_2. This difference is explained qualitatively by the participation of H_2 in the reaction specifically by the attack of TMGa by atomic H. The apparent activation energy obtained from the temperature dependence of remaining reactant for TMGa in N_2 is taken as the activation energy for the process of rupturing the first Ga-methyl bond, i.e. E_{1a} = 64.6 kcal/mol. The activation energies for the reactions of breaking the second and the third Ga-methyl bond are also estimated independently to be E_{1b} = 52.6 kcal/mol and E_{1c} = 54.1 kcal/mol from the temperature dependence of the volatile hydrocarbon products. Our data reinforce a radical mechanism where TMGa decomposes by way of releasing successively its three methyl radicals. The rupture of the first Ga-methyl bond is, by far, the rate limiting step.

It is seen from the review and our study that TMGa decomposes appreciably at $T \geq 430$ °C in H_2 for a contact time of several seconds. For ALE performed at atmospheric pressure with TMGa injection time in the

order of 1s, gas phase decomposition is clearly one of the causes for the failure of ALE self limiting behavior. Since gas phase decomposition depends critically on the time at which TMGa molecules traverse the hot zone, the operable ALE window (T, injection time, TMGa mole fraction etc.) will depend on reactor geometry and operating hydrodynamic parameters although the thickness uniformity is insensitive to the hydrodynamics. A fast gas stream and capable of short TMGa exposure are desirable to operate at high temperature, which should be kept in mind for ALE reactor design.

The dehydrogenation of Ga containing hydrocarbon species, eqn.(2-8) or an analogous reaction on the surface, could be responsible for carbon incorporation in the growing GaAs film. The existence of reactive H donating species from the group V precursors (e.g. AsH) is desirable for reducing the carbon incorporation. In the case of conventional MOCVD, the reduction of carbon may be expected to be in effect through the gettering of CH_3 and partial reversal of the reaction (2-8), while in ALE where the injection of TMGa and AsH_3 is temporally separated, only partial reversal of the reaction (2-8) can be expected, which leads to higher carbon background level.

References for Chapter Two

[1] M.Tirtowidjojo and R.Pollard, "Equilibrium Gas Phase Species for MOCVD of $Al_xGa_{1-x}As$," J. Cryst. Growth, Vol.77, 200(1986).

[2] B.K.Chadwick, "Equilibrium Analysis of the MOCVD $Ga(CH_3)_3$-AsH_3-H_2 System," J. Cryst. Growth, Vol.96, 693(1989).

[3] M.Tirtowidjojo and R.Pollard, "The Influence of Reactor Pressure on Rate-Limiting Factors and Reaction Pathways in MOVPE of GaAs," J. Cryst. Growth, Vol.98, 420(1989).

[4] D.G.Tuck, in "Comprehensive Organometallic Chemistry," Vol.1, Eds., G.W.Wilkinson, F.G.A.Stone, and E.W.Abel, Pergamon Press, 1982, pp693.

[5] G.Pilcher and H.A.Skinner, in "Chemistry of the Metal-Carbon Bonds," Eds., F.R.Hartley and S.Patai, John Wiley & Sons Ltd., 1982, pp57.

[6] M.G.Jacko and S.J.Price, "The Pyrolysis of Trimethyl Gallium," Can. J. Chem., Vol.41, 1560(1963).

[7] V.R.McCrary and V.M.Donnelly, "The Ultraviolet Absorption Spectra of Selected Organometallic Compounds Used in the Chemical Vapor Deposition of Gallium Arsenide," J. Cryst. Growth, Vol. 84, 253(1987).

[8] H.Itoh, M.Watanabe, S.Muka, and H.Yajima, "Ultraviolet Absorption Spectra of Metalorganic Molecules Diluted in Hydrogen Gas," J. Cryst. Growth, Vol.93, 165(1988).

[9] M.Sasaki, Y.Kawakyu, and M.Mashita, "UV Absorption Spectra of Adlayers of Trimethylgallium and Arsine," Jpn. J. Appl. Phys. Vol.28(1), L131(1989).

[10] B.Beagley, D.G.Schmidling, and I.A.Steer, "An Electron-Diffraction Study of the Molecular Structure of Trimethylgallium," J. Mol. Struct., Vol.21, 437(1974).

[11] G.E.Coates and A.J.Downs, "The Vibrational Spectrum and Structure of Trimethylgallium," Spectrochim. Acta, Vol.20, 3353(1964).

[12] M.R.Leys and H.Veenvliet, "A Study of the Growth Mechanism of Epitaxial GaAs as Grown by the Technique of Metal Organic Vapor Phase Epitaxy," J. Cryst. Growth, Vol.55,145(1981).

[13] J.Nishizawa and T.Kurabayashi, "On the Reaction Mechanism of GaAs MOCVD," J. Electrochem. Soc., Vol.132(3), 413(1983).

[14] S.P.DenBaars, B.Y.Maa, P.D.Dapkus, A.D.Danner, and H.C.Lee, "Homogeneous Thermal Decomposition Rates of Trimethylgallium and Arsine and Their Relevance to the Growth of GaAs by MOCVD," J. Cryst. Growth, Vol.77, 188(1986).

[15] J.E.Butler, N.Bottka, R.S.Sillmon, and D.K.Gaskill, "In Situ, Real-Time Diagnostics of OMVPE Using IR-Diode Laser Spectroscopy," J. Cryst. Growth, Vol.77, 163(1986).

[16] M.Yoshida, H.Watanabe, and A.Uesugi, "Mass Spectrometric Study of $Ga(CH_3)_3$ and $Ga(C_2H_5)_3$ Decomposition Reaction in H_2 and N_2," J. Electrochem. Soc., Vol.132(3), 677(1985).

[17] P.W.Lee, T.R.Omstead, D.R.Mckenna, and K.F.Jensen, "In Situ Mass Spectroscopy and Thermogravimetric Studies of GaAs MOCVD Gas Phase and Surface Reactions," J. Cryst. Growth, Vol.85, 165(1987).

[18] N.Pütz, H.Heinecke, M.Hegen, and P.Balk, "A Comparative Study of $Ga(CH_3)_3$ and $Ga(C_2H_5)_3$ in the MOMBE of GaAs," J. Cryst. Growth, Vol.74, 292(1986).

[19] M.Mashita, S.Horiguchi, M.Shimizu, K.Kamon, M.Mihara, and M.Ishii, "The Pyrolysis Temperature of Trimethylgallium in the Presence of Arsine or Trimethylaluminum," J. Cryst. Growth, Vol.77, 194(1986).

[20] C.A.Larsen, N.I.Buchan, and G.B.Stringfellow, "Reaction Mechanisms in the Organometallic Vapor Phase Epitaxial Growth of GaAs," Appl. Phys. Lett., Vol.52 (6), 480(1988). This work is reviewed and a more complete compilation of the work of this group is presented in "Organometallic Vapor Phase Epitaxy" by G.B.Stringfellow (Academic Press, San Diego CA, 1989).

[21] H.Suzuki, K.Mori, M.Kawasaki, and H.Sato, "Spatially and Time-Resolved Detection of Gallium Atoms Formed in the Laser Photochemical Vapor Deposition Process of Trimethylgallium by Laser-Induced Fluorescence: Decomposition in the Adsorbed State," J. Appl. Phys., Vol.64(1),371(1988).

[22] A.Kantrowitz and J.Grey, "A High Intensity Source for the Molecular Beam. Part I. Theoretical," Rev. Sci. Instrum., Vol.22 (5), 328(1951).

[23] M.A.A.Clyne and W.S.Nip, in "Reactive Intermediates in Gas Phase: Generation and Monitoring", D.W.Setser, Ed., Academic Press, (1979), p38.

[24] R.Pertel, "Molecular Beam Sampling of Dynamic Systems", Int. J. Mass Spectr. Ion Phys., Vol.16, 39(1975).

[25] H.Parker, A.R.Kuhthau, R.Zapata, and J.E.Scott,Jr., in "Rarefied Gas Dynamics," F.M.Devienne, Ed., Pergamon Press, (1958), p69.

[26] J.W.Warren, "Measurement of Appearance Potentials of Ions Produced by Electron Impact Using a Mass Spectrometer," Nature, Vol.165, 810(1950).

[27] C.A.Mcdowell and J.W.Warren, "The Ionization and Dissociation of Molecules by Electron Impact," Discuss. Faraday Soc., Vol.10, 53(1951).

[28] In "Handbook of Chemistry and Physics", 68TH, R.C.Weast Ed., CRC (1987-1988), E-84.

[29] F.Glockling and R.G.Strafford, "Electron Impact Studies on Some Group III Metal Alkyls," J. Chem. Soc., (A), 1761(1971).

[30] G.C.Eltenton, "The Study of Reaction Intermediates by Means of a Mass Spectrometer," J. Chem. Phys. , Vol.15(7), 455(1947).

[31] F.P.Lossing and A.W.Tickner, "Free Radicals by Mass Spectrometry. I. The Measurement of Methyl Radical Concentrations," J. Chem. Phys., Vol.20(5), 907, (1952).

[32] M.Tsuda, S.Oikawa, M.Morishita, and M.Mashita, "On the Reaction Mechanism of Pyrolysis of TMG and TEG in MOCVD Growth Reactors," Jpn. J. Appl. Phys., Vol.26(5), L564, (1987).

[33] G.L.Pratt, in "Gas Kinetics", John.Wiley, (1969), p159.

[34] P.C.Kobrinsky and P.D.Pacey, "The Reaction of Methyl Radicals with Molecular Hydrogen," Can. J. Chem., Vol.52, 3655(1974).

[35] G.L.Pratt and D.Roger, "Homogeneous Isotope Exchange Reactions: Part 2.–CH_4/D_2," J. Chem., Soc., Faraday Trans. I, Vol.12, 2769(1976).

[36] T.F.Kuech and E.Veuhoff, "Mechanism of Carbon Incorporation in MOCVD GaAs," J. Cryst. Growth , Vol.68, 148(1984)

[37] G.Arens, H.Heinecke, N.Pütz, L.Lüth, and P.Balk, "On the Role of Hydrogen in the MOCVD of GaAs, "J. Cryst. Growth, Vol.76, 305(1986).

[38] S.W.Benson, in "Thermochemical Kinetics: Methods for Estimation of Thermochemical Data and Rate Parameters", 2nd Ed., J.Wiley (1976).

[39] L.H.Long, "Dissociation Energies of Metal-Carbon Bonds and the Excitation Energies of Metal Atoms in Combination," Pure Appl. Chem., Vol.2, 61(1961).

CHAPTER THREE

LALE Growth and Optimization Using TMGa and AsH_3

The advantages of LALE as an in situ processing tool in optoelectronic integration has been discussed in Chapter One. In this chapter, our experimental results on the growth of GaAs by LALE using TMGa and AsH_3 as precursors will be presented in detail. The success in ALE using TMGa and AsH_3 and the relative wealth of information on the self limiting nature of ALE growth using these two precursors make them the first choice for a detailed study in LALE. As a matter of fact to mention, the very first attempt of ALE using TMGa and AsH_3 was carried out under low levels of light illumination, though the light intensity was not enough to cause appreciable localized growth enhancement.[1]

3.1 Approaches to LALE and Reactor Design Issues

In our experiments, maintaining a clean optical path during the alternate exposure to TMGa and AsH_3 is achieved through two different reactor designs: a rotating susceptor design and a switching flow design as are shown in Fig.3.1 In the rotating susceptor design, the substrate is rotated on a pyramidal graphite susceptor. TMGa and AsH_3 are passed continuously into their respective chambers separated by two H_2 purge chambers. A laser beam with λ=514.5nm from an argon ion laser is directed through the quartz window on the TMGa chamber onto the

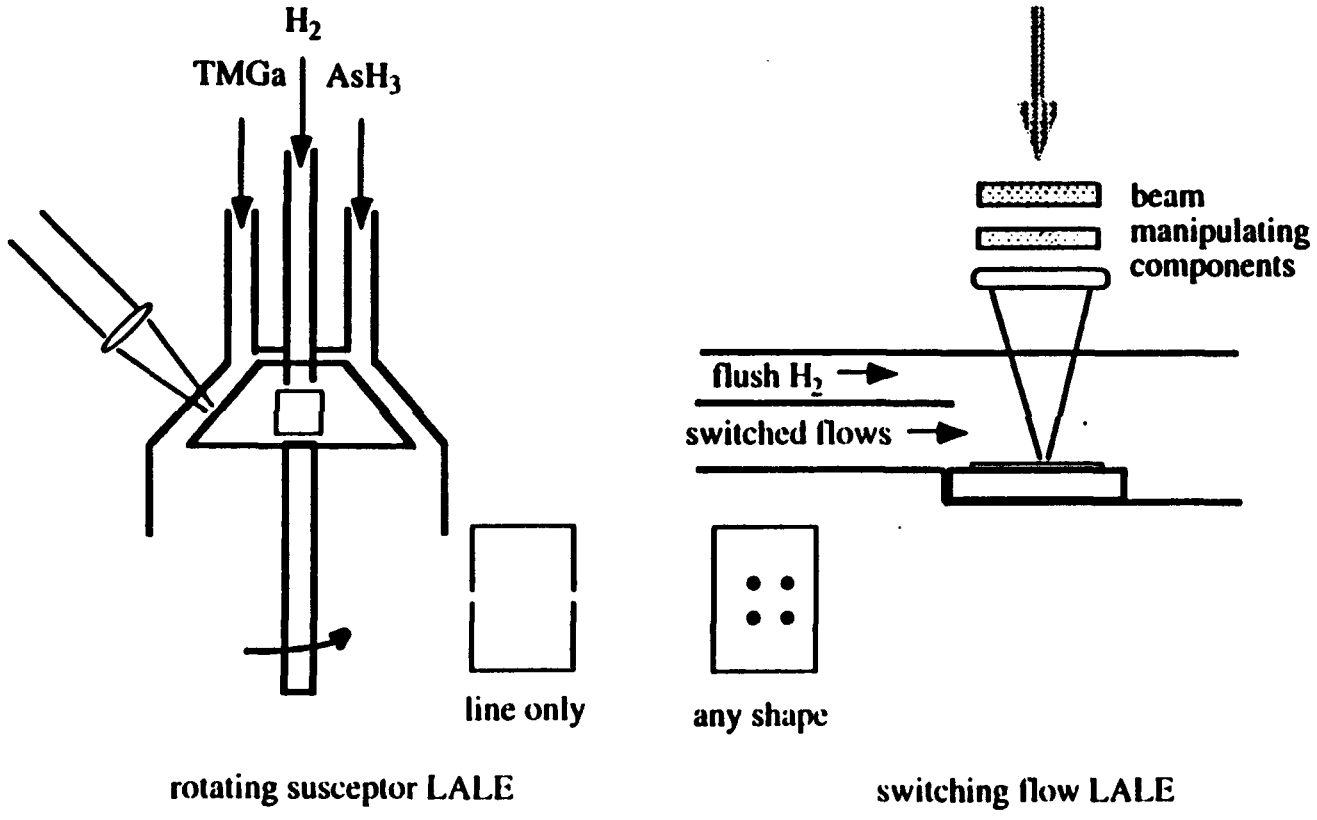

Fig.3.1 L ALE experimental approaches.

substrate while it is exposed to TMGa. A complete LALE cycle occurs once every revolution, writing single line where the path of the beam traverses the substrate. Notice here that the average residence time of the laser spot is D/v, where the D is the beam diameter of the laser spot and v the linear scan speed, which is about 0.2 second in most of our experiments.

As an alternative approach, the LALE in the switching-flow reactor proceeds as the TMGa and AsH_3 is switched into the manifold with a continuous H_2 carrier gas flow and a laser beam is directed through a quartz window flushed with another stream of H_2 flow to keep the window from fogging. With this approach, patterns of arbitrary shapes can be deposited. Optics have been employed to form the desired pattern, such as a shadow mask-imaging lens combination or a planar beam splitter-focusing lens combination. In the latter case, about 94% of the laser power is utilized. A chopping mechanism consisting of a computer controlled stepper motor allowed intentional variation of the delay time between the initiation of the laser illumination and the TMGa injection and the duration of the illumination. This gives us the opportunity to obtain kinetic information concerning the LALE mechanism. An important, probably unique, feature that comes with both reactor designs is their full compatibility with conventional MOCVD. This allows us to grow double heterostructures (DH's) and quantum wells (QW's) with the central layer grown by LALE, and yet perform photoluminescence PL and capacitance-voltage (C-V) measurements on the thin and small area deposits.

Common to ALE and LALE, a reactor with fast gas transients is desirable to achieve short cycle time (high ALE growth rate) and to obtain wide ALE self limiting operation range. With the rotating susceptor configuration, fast gas transients are guaranteed by the rotation of the susceptor. A practical problem here is rather to devise a good sample mounting mechanism which prevents the sample from flying away during rotation and at the time of exposure mode change without interfering with the desired hydrodynamics (flow pattern). In the case of the switching flow reactor, the gas velocity is the main concern. Although a low pressure operation can increase the volumetric flow rate at the same input mass flow, it is not available in our reactor. For a convenient total carrier flow of 5 L/min and a reactor cross section area of 1x3.2 cm^2, the gas velocity is about 26 cm/s. At this velocity, TMGa molecules traverse the 3.6 cm-long hot susceptor in about 0.14 s. The average decomposition time constant of TMGa in H_2 at 480 °C, on the other hand, is ~15 s (see Chapter Two). This order of magnitude estimation indicates that ALE and LALE in this reactor will not suffer severely from premature gas phase decomposition. At higher temperature, e.g. 550 °C, the TMGa decomposition time constant is ~0.8 s. ALE self limiting growth in a regular horizontal laminar flow reactor is difficult, if not impossible. This exercise illustrates that although the thickness uniformity in ALE is not severely affected by reactor geometry and hydrodynamics, the successful ALE operation is affected. "Designing an ALE reactor to do ALE" may not be an overstatement.

One important task in performing LALE is to maintain a clean window for the intense laser beam. Two schemes used quite satisfactorily

are to keep the chamber with the window at low temperature at all times when there is a reactant in the flow or to protect the window with a separate stream of H_2. In the first case, care must be taken so as not to allow the focal point to fall too close to the window because photolysis of TMGa by visible light may occur via multiphoton processes. The coating of the window in the presence of a high intensity light beam quickly leads to permanent damage to the window. Since the reactor tube has to be cleaned with strong acidic solutions, it is found latter that shallow but visible micro-scratches develops on the inner surface of the window. It is therefore recommended that a dismountable window assembly should be considered.

The desire for full compatibility with conventional MOCVD presents a more stringent requirement on the reactor design. Several design considerations for achieving uniform MOCVD growth may actually be in conflict with the objective of having a wide range of self limiting ALE operation. Although there is no universal scalable optimal design available, there are guidelines that can be followed. These guidelines come from theoretical analysis using the basic principles of flow dynamics[2][3] and from the direct visualization of flow patterns by TiO_2 smoke[4]-[7] and more elegantly by interference holography.[8] From these reported works, it can be appreciated that an "ideal" horizontal reactor should operate at a stable laminar flow regime free from convective flow even at high flow velocity to promote uniformity. It should have a fully developed temperature profile. These requirements can be met with a rectangular cross section vessel of low free height/width ratio and of an appropriately designed entrance expansion geometry. One suitable engineering approach is to first evaluate

several dimensionless groups of quantities for a design. By comparing these evaluations with the experimentally established criteria, one can obtain some idea on the operation behavior of the design and, if necessary, modifications are made accordingly.

The most important quantity to characterize the dynamic behavior of a gas flow in a tube at a given temperature is the Reynolds number as defined by

$$N_{Re} = \frac{u_\infty \rho h}{\mu} = \frac{u_\infty h}{\nu} \qquad (3\text{-}1),$$

where the u_∞ is the free stream velocity (m/s), ρ the gas density (kg/m^3), h the height of the flow channel (which can also be replaced by the hydraulic diameter d = 4 x channel area/ perimeter), μ the dynamic viscosity (kg/ms), and $\nu = \mu/\rho$ is the kinematic viscosity (m^2/s). An established criterion for laminar flow requires that $N_{Re} < 2300$.[9] The dimensions given above give rise to a N_{Re} ~24 for H_2 at 300 K (ν = 1.10 cm^2/s [8]) and 3 at 1000 K (ν = 8.33 cm^2/s). A laminar flow is quite possible.

When the cold gas passes over a hot susceptor, a buoyancy force will be exerted on the gas. This effect is appreciated by defining a Rayleigh number as

$$N_{Ra} = \frac{\alpha g C_p \rho^2 h^2 \Delta T}{\mu \kappa} \qquad (3\text{-}2),$$

where the α is the thermal expansion coefficient (K^{-1}, = 1/T for idea gas), g the gravitational acceleration (9.81 m/s^2), $\Delta T = T_{susceptor} - T_{ambient}$, κ the thermal conductivity ($Jm^{-1}s^{-1}K^{-1}$), and C_p the specific heat ($Jk^{-1}g^{-1}K^{-1}$). The criterion for the occurrence of free convection is that Ra > 1707.[10] For our design, N_{Ra} = 7 using a $q = (\mu\kappa/\alpha g C_p \rho^2)$ = 98.54 (cm^3K) for H_2[8] and at ΔT = 1000 K- 300 K. Thus our design is far from the critical value.

Even if the criteria for N_{Re} and N_{Ra} are met, recirculating flow may still occur in the inlet region where the gas is injected into the reactor vessel and expands to the full size of the vessel. A straight forward way avoiding this problem is to restrict the angle of expansion from the size of the inlet to the full width of the flow channel. A recommended critical angle of expansion without breakaway of the gas from the side wall of the vessel is about 7°.[11] The expansion from 0.8 cm to 3.2 cm width will then take a transition length ~9.8cm. This increases the total volume as well as the inner surface area upstream of the susceptor, which is not desirable for obtaining abrupt interfaces in MOCVD and for minimum transient time in ALE operation. Goodings *et al.*[12] have tackled this problem by designing a parabolic expansion of the type

$$W = \frac{W_0}{CX^{0.95} + 1} \qquad (3\text{-}3),$$

where the inlet of width (diameter) W_0 (mm) expands to a width of W (mm) at an axial distance X (mm). Their smoke test result identified C= -0.012 as an optimum choice for N_{Re} up to ~42 at 300 K. This still requires an expansion distance ~7.8 cm in our case. This length is still too long for a

small volume ALE reactor and some compromise has to be made. In addition, the small head height used in our reactor reduces the N_{Re} and a greater absolute C value may be used. Thus we have chosen the distance from the inlet to the susceptor to be 6.8 cm. Unfortunately, the shaping of the quartz ware could not be made to the specification. Instead, the transition becomes linear across ~2.3 cm axial distance. Growth evaluations of the reactor have not revealed severe problems; however.

The flow velocity profile in a tube will be varying until up to a distance X_f where the profile stabilizes. This defines an entrance length,[9]

$$X_f = 0.04 \frac{h^2 u}{\nu} = 0.04\, hN_{Re} \qquad (3\text{-}4).$$

Beyond this distance the flow is said to be fully developed. Since our susceptor is at the same height as the leading tube wall, it follows immediately that the flow is fully developed by the time it reaches the susceptor.

The temperature profile, however, will take a distance X_T measured from the front edge of the susceptor. The entrance length for temperature profile development is given by Hwang and Cheng[13] as

$$X_T = 0.28 hN_{Re} = 7X_f \qquad (3\text{-}5).$$

It is apparent that the temperature profile in this reactor is not fully developed. Adding upstream preheating can help establishing fully

developed temperature profile but this is certainly unwanted for ALE growth.

The protection of the window is achieved by a stream of H_2 flowing through a parallel channel of cross section hxW = 0.4x3.2 cm^2. With a flow ratio $Q_{window}/Q_{carrier}$ = 1/2.5, the window has no obvious coating after two hours of GaAs/AlGaAs deposition at 750 °C.

3.2 LALE Growth Phenomena

The ALE mode of operation in both types of reactors can be described by an exposure mode. The exposure mode of 1s of TMGa exposure, 4s of H_2 purge, 4s of AsH_3 exposure, and another H_2 purge of 4s will be designated as a 1-4-4-4 exposure mode. The laser illumination mode is described by the laser intensity (W/cm^2) and the duration of the pulse (or laser resident time). LALE was performed at 380 °C with varying TMGa mole fractions, exposure modes, and illumination modes. The thickness of the LALE stripes was measured by stylus profilometer.

The most important control parameter in LALE is the laser intensity. As can be seen from Fig.3.2, the laser intensity dependence of the LALE growth rate (in monolayer/cycle or ML/cycle) exhibits three regimes of different characteristics. In the low laser intensity regime, regime (I), the growth rate increases with increasing intensity. Above a threshold value of intensity, one ML/cycle is reached and the rate remains close to one ML/cycle upon further increase in the laser intensity. Here, in regime (II),

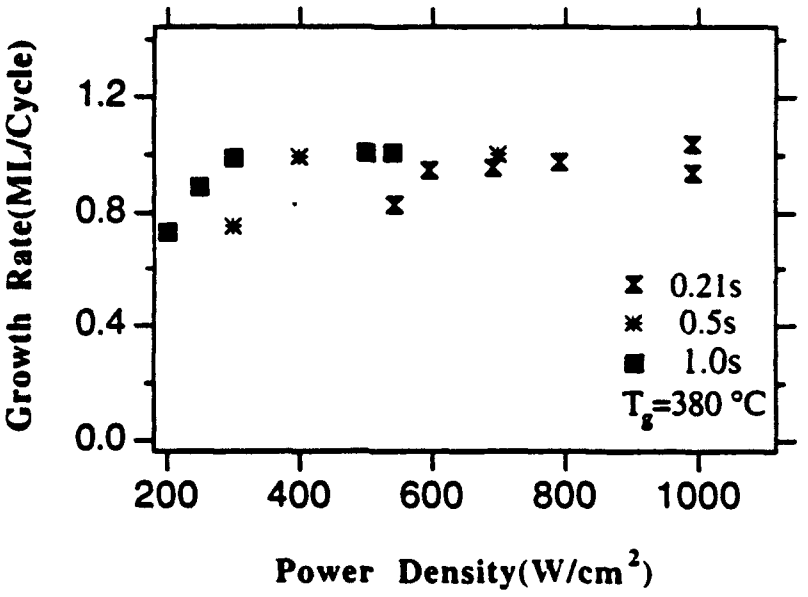

Fig.3.2 LALE growth rate as a function of laser intensity

we have attained th self limiting monolayer growth regime. There is a finite range of laser intensities over which the regime (II) extends – the laser intensity "window". At even higher intensity, the whole system becomes unstable. For example, if excess intensity causes a small amount of excess Ga, the formation of amorphous or polycrystalline deposits or simply particulates on the growth area will increase the effective absorption of the laser light, This, in turn, causes more polycrystallites to form. The final morphology of the LALE deposit will be polycrystalline. This regime should be avoided.

Because of the proportionality between the laser intensity and the growth rate in the low intensity regime, the growth thickness profile will be

more or less a replication of the intensity distribution as is shown in Fig.3.3 (I). Within the LALE intensity window, the intensity profile will be truncated to result in a nearly flat top thickness profile shown in Fig.3.3(II). In both the regimes (I) and (II), single crystalline GaAs of smooth morphology is obtained.

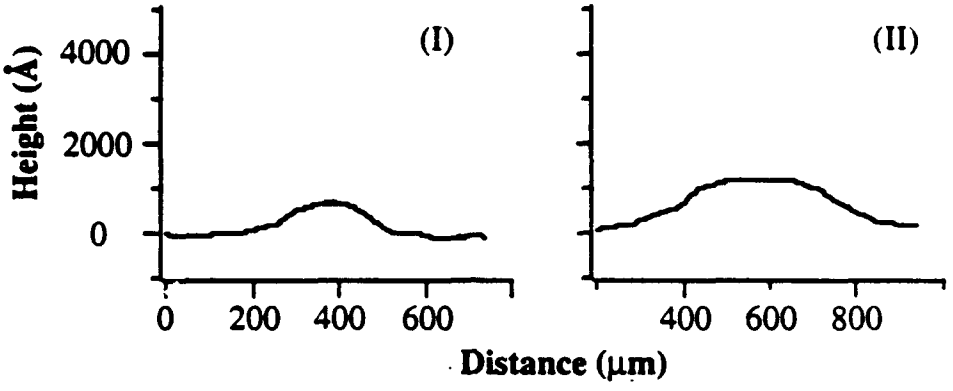

Fig.3.3 Typical thickness profiles across LALE stripes,
(I) below ML/cycle and (II) ML/cycle.

It can also be seen from the Fig.3.2 that the threshold intensity for achieving monolayer self limiting growth is a function of the illumination duration (laser pulse length). The product of the threshold intensity $I_{th}(W/cm^2)$ times the illumination duration τ (s) gives the threshold energy deposit in unit area, Φ_{th}. The Φ_{th} is plotted as a function of the illumination duration in Fig.3.4. The approximate upper boundary of the LALE intensity window is outlined with a dashed line. In analogy to a phase diagram, the area between the two lines in Fig.3.4 represents the range of operation within which the self limiting LALE "phase" can be obtained. There are

two degrees of freedom, i.e. both Φ and τ may be varied independently without losing self limiting LALE operation.

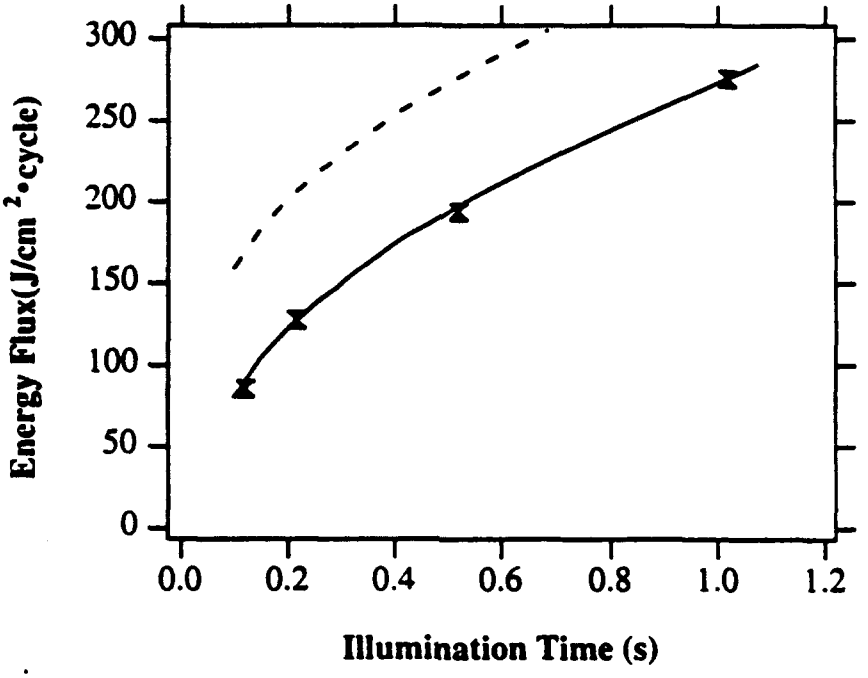

Fig 3.4 Threshold illumination versus illumination durations in LALE using TMGa and AsH_3.

It follows from Fig.3.4 that the Φ_{th} is not a constant with varying illumination duration. Photons are more efficiently utilized on average in the growth with shorter laser pulses and higher intensities. For a pure photochemical reaction via a single photon process and with essentially constant source (TMGa) supply, the rate is expected to be in direct proportion to the total photon fluence. The Φ_{th} is then expected to be a constant. In addition, the number of photons required to effectively lay down one lattice site is in the order of 10^5:1. Our observations indicate that it is not likely that LALE proceeds by a pure photochemical reaction via a single photon process.

As a test whether the self limiting mechanism is operative under our experimental conditions, LALE growths were performed with varying TMGa mole fraction under the same exposure and illumination modes. The growth rates are plotted against the TMGa injected/cycle for the same TMGa exposure time in Fig.3.5. Since the laser pulse is shorter than the TMGa exposure time, it is the TMGa concentration not the duration of the exposure that matters. The use of TMGa injected/cycle without specifying the exposure time causes confusion. The Fig.3.5 shows that monolayer self limiting growth can be achieved in wide ranges of TMGa input. The flow

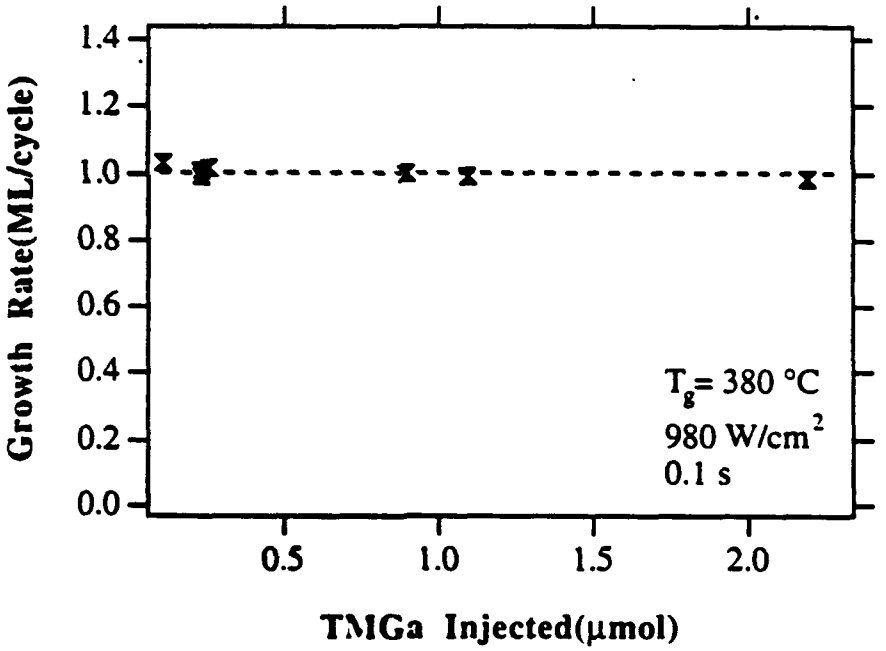

Fig.3.5 The effect of TMGa injection on LALE growth rate, indicating self limiting growth. The laser illumination is 0.1s at 980 W/cm^2

range exceeds an order of magnitude and is basically limited by the readily achievable flow rate in our gas handling system. Because of the lower substrate bias temperature used in LALE than in ALE, this range is expected to extend into higher flow rate than that could be used in ALE.

By varying the delay time between the TMGa injection and the initiation of laser illumination, kinetic information concerning the adsorption and desorption of TMGa on GaAs can be obtained. Fig.3.6 shows the growth rate as a function of such delay time. In this series of experiments, the laser pulse is 0.1s long. It is seen that the coincident of

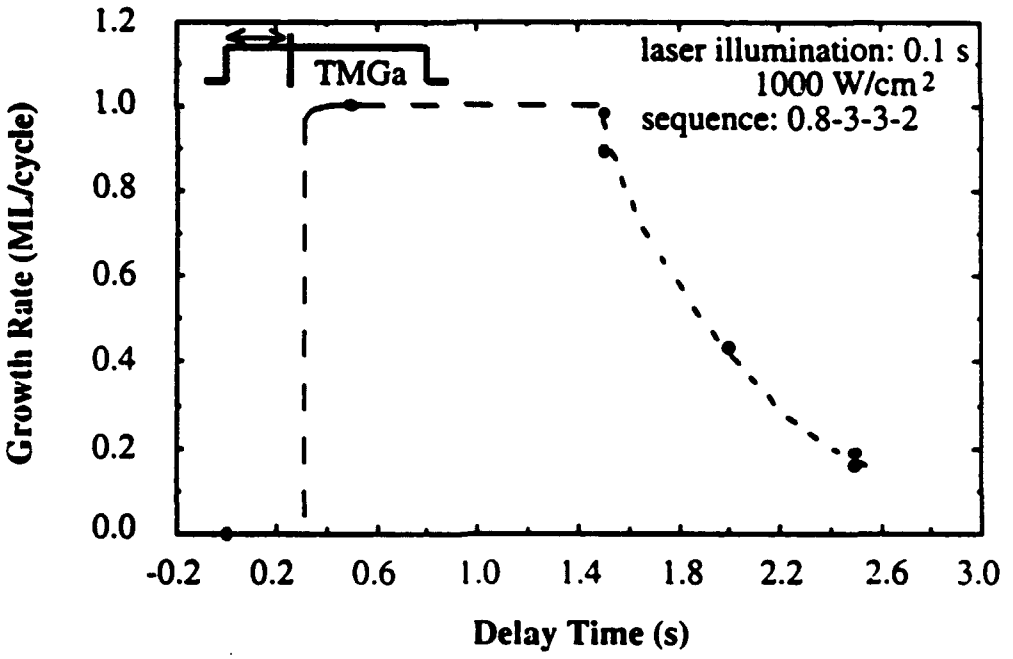

Fig.3.6 The effect of delay in laser illumination on LALE growth.

photons and the TMGa molecules is required for LALE growth to occur. From 0 to 0.4 s, a delay is required to accommodate the intrinsic time constant of the gas handling system. Monolayer self limiting LALE can be achieved as long as the laser illuminating the substrate in presence of TMGa. As soon as the laser pulse arrives later than the trailing edge of the TMGa pulse, the LALE growth rate begins to decrease. The apparent 1/e fall-off time is about 0.6 s. We believe this is due to the smearing of the reactant (TMGa) pulse during the mass transfer process. Adsorption-desorption occurring on the reactor surfaces upstream of the substrate are postulated as the cause. This fall-off time places an upper limit for TMGa desorption time constant. The actual desorption time of TMGa may be much shorter (~10^{-2} s, see Chapter Six). The static picture of TMGa molecules adsorbing on the surface, waiting for the energy input from the laser illumination, and being permanently incorporated should be used with caution.

3.3 Characterization of LALE Grown GaAs

We have noted previously that the characterization of GaAs materials grown by LALE is hindered by the fact that only small area and thin deposits are available. We have devised several sample structures which allows us to perform PL, C-V, and secondary ion mass spectrometry (SIMS). The sample structures for PL and C-V measurements are shown in Fig.3.7 (a) and (b). They are basically GaAs/AlGaAs DH's. The structures are grown in a three step procedure. First, the GaAs buffer and the $Al_{0.3}Ga_{0.7}As$ lower cladding layer is grown by MOCVD at 750 °C. The

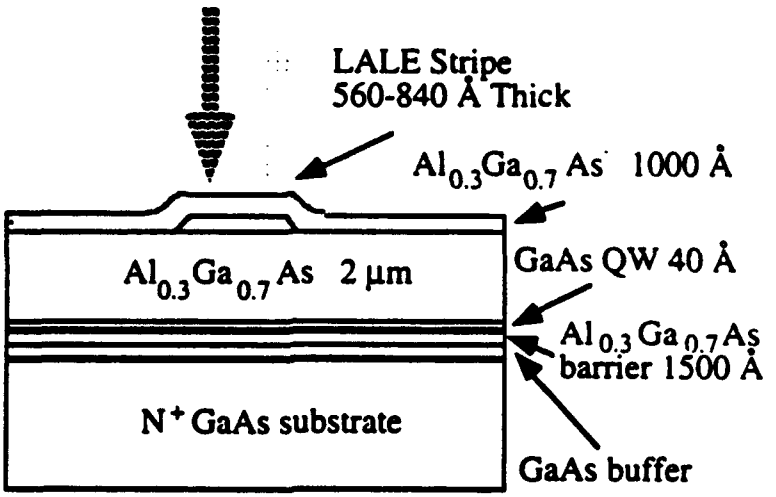

(a) LALE DH for PL

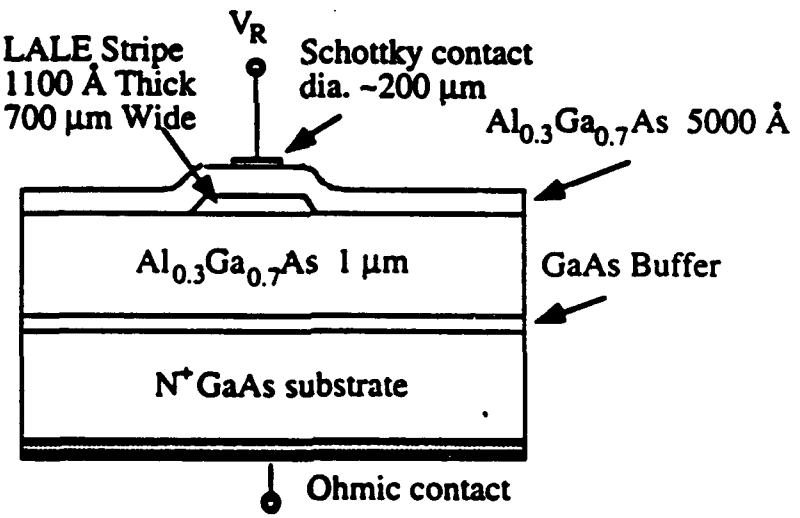

(b) LALE DH for C-V

Fig.3.7 Sample structures for the characterization of the thin and small area of GaAs grown by LALE.

substrate temperature is then reduced to 380 °C to perform LALE for 200~400 cycles. The substrate temperature is then raised again to finish the top cladding layer. The samples for PL measurements have a thin top cladding for good excitation and signal collection efficiency and a thick lower cladding to isolate the substrate from either direct excitation by the laser or from electron-hole pairs that diffuse from the photo excited AlGaAs. In either of the circumstances luminescence from the substrate could be generated that would be indistinguishable from that of the GaAs grown by LALE. A QW may be deliberately embedded below the LALE grown material to insure satisfactory isolation since any excess carriers diffusing across the lower cladding layer will be captured by the QW giving rise to a peak on the shorter wavelength side of the main GaAs peak of interest.

The top cladding layers of the samples for C-V measurement should be thicker than the depletion layer thickness in this $Al_{0.3}Ga_{0.7}As$ material, which are generally ~5000 Å for a background doping of $p \sim 10^{15}$ cm^{-3}. Au or Ag dots of diameter 200 μm are placed on stripe on top of the AlGaAs cladding layer. The GaAs layer is probed by advancing the depletion layer through increasing the reverse bias voltage. Thicker LALE GaAs layers (0.5μm) are also grown and the Schottky contacts formed directly on the LALE GaAs.

The sample structures for SIMS profiling are also DH's. Multiple layers of LALE GaAs are grown under different conditions and the carbon incorporation studied. The top most 500 Å AlGaAs is used to protect the

region of interest from ambient contamination. It also gives room for initial instrumental adjustment.

Fig.3.8 (a) shows a PL spectrum from a DH of which room temperature PL could be observed. This is the first time that room temperature PL is observed from the GaAs material grown by LALE. At low temperature (5K), Fig.3.8 (b), impurity related emission at $\lambda = 8295$ Å dominates the spectrum. This peak is assigned to the band to carbon acceptor transition according to Ozeki *et al.*[14] (A_1, 1.493 ev).

All the unintentionally doped GaAs grown by LALE using TMGa and AsH_3 exhibit p type conductivity with hole concentration ranging from $2x10^{17}$ to $3x10^{18}$ cm^{-3} as measured by C-V. The carbon impurities apparently incorporate into the As sublattice, i.e. C_{As}. SIMS measurements reveal the existence of carbon above the background level of the MOCVD $Al_{0.3}Ga_{0.7}As$ from our system. Since no internal reference was used in the SIMS measurements, the total amount of carbon was not quantified. It is then impossible to tell whether all the carbon is electrically active. It is worth mentioning that, in highly carbon doped GaAs grown by MOMBE using TMGa as a dopant, evidences were reported for the incorporation of H[15] simultaneously with the carbon and the passivation[16] of the carbon through the formation of C_{As}-H complex.[15]

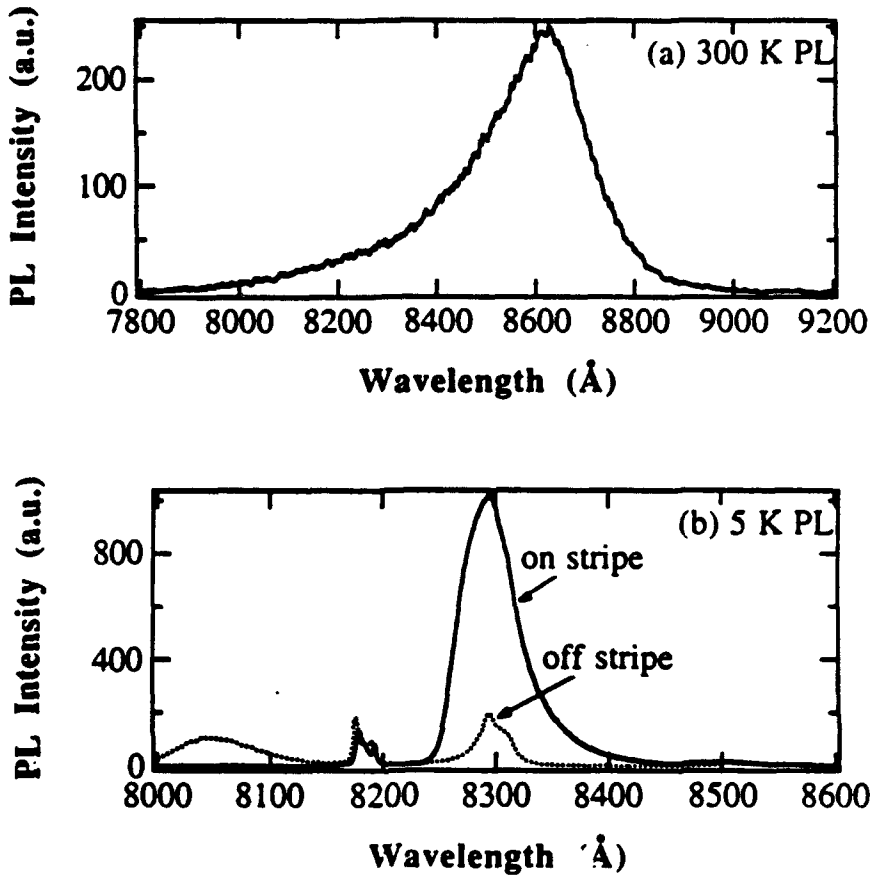

Fig.3.8 Typical PL spectra from DH's grown by LALE using TMGa and AsH_3 taken at (a) 300 K and (b) 5 K.

3.4 LALE Growth Optimization

The ability to characterize the thin and small area of GaAs grown by LALE provides valuable information for process control to obtain high quality materials. The influence of growth parameters on the material quality can thus be studied.

We have seen in the section 3.2 that monolayer self limiting LALE can be obtained within a finite laser intensity window. In Fig.3.9, room temperature PL spectra from DH's with the GaAs grown by LALE under different laser intensities are shown. The low and the high intensities correspond closely to the lower and higher ends of the LALE intensity window. The PL efficiency is enhanced by growing under higher laser intensity. Since an increase in the laser intensity increases both the photon density and local heating (see Chapter Six), the contributions from multiphoton enhanced impurity reduction and from the local heating can not be differentiated in this experiment.

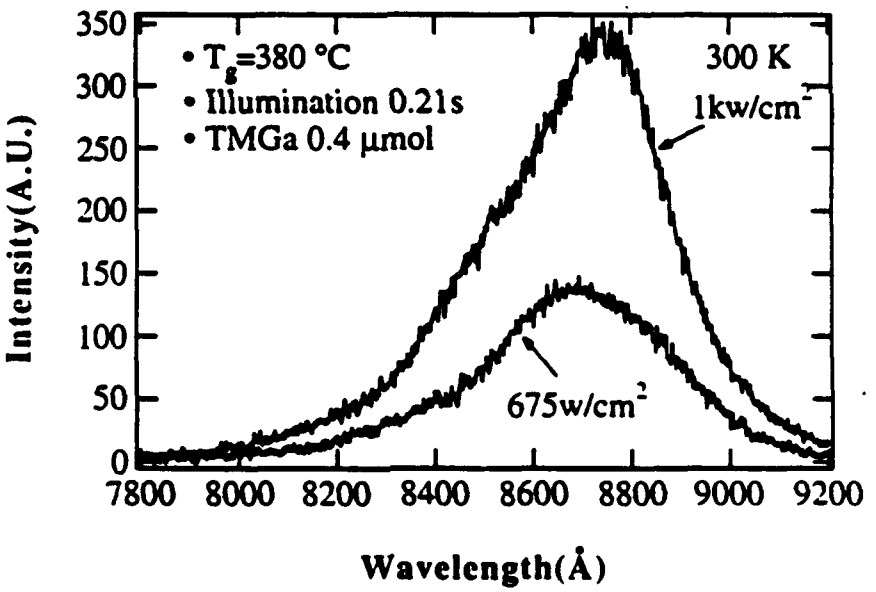

Fig.3.9 PL spectra from LALE DH's grown at different laser intensities.

Since self limiting LALE can be achieved with two degrees of freedom as regards to the laser intensity and the illumination time, the mode

of laser illumination was varied to study its influence on the material quality. The spectra shown in Fig.3.10 is from the samples grown at laser illumination modes of 600 W/cm^2 for 0.1s and 176 W/cm2 for continuous illuminations. Although the maximum temperature rise is higher in the former case, longer illumination seem to result in better GaAs probably due to an "annealing effect" that promotes perfect lattice site registry.

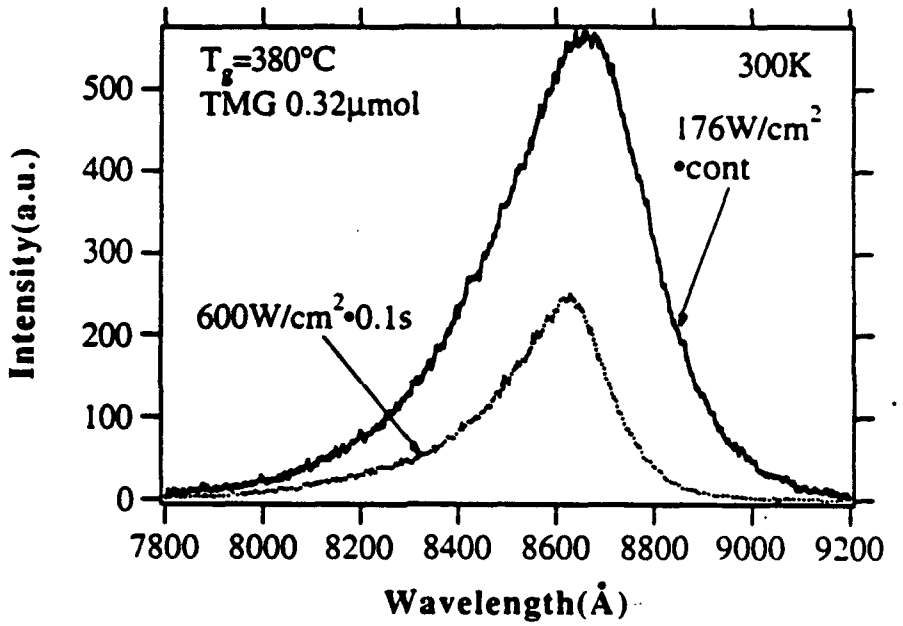

Fig.3.10 Dependence of PL efficiency on laser illumination modes.

The effect of TMGa exposure on carbon contamination in the film can be seen from the SIMS profiles shown in Fig.3.11. The exposure modes for the three layers are the same, i.e. 1.5-2-4-2. The laser resident time is 0.2 s at 700 W/cm2. The substrate bias temperature during LALE is 380 °C. The drawing above the traces is used to locate the approximate boundaries between the layers. The numbers over each region indicate the moles of

TMGa injected per cycle for that layer. Carbon incorporation is clearly reduced with lower TMGa injection level, i.e. lower concentration at a given exposure duration. This implies that the reactions leading to the carbon incorporation has direct connection to the gas phase concentration of TMGa. We speculate that the surface analogy of the equation (2-8) is the likely path for C_{As} upon further dehydrogenation. It should also be pointed out that there is no interface accumulation of the carbon impurities according to the SIMS profile.

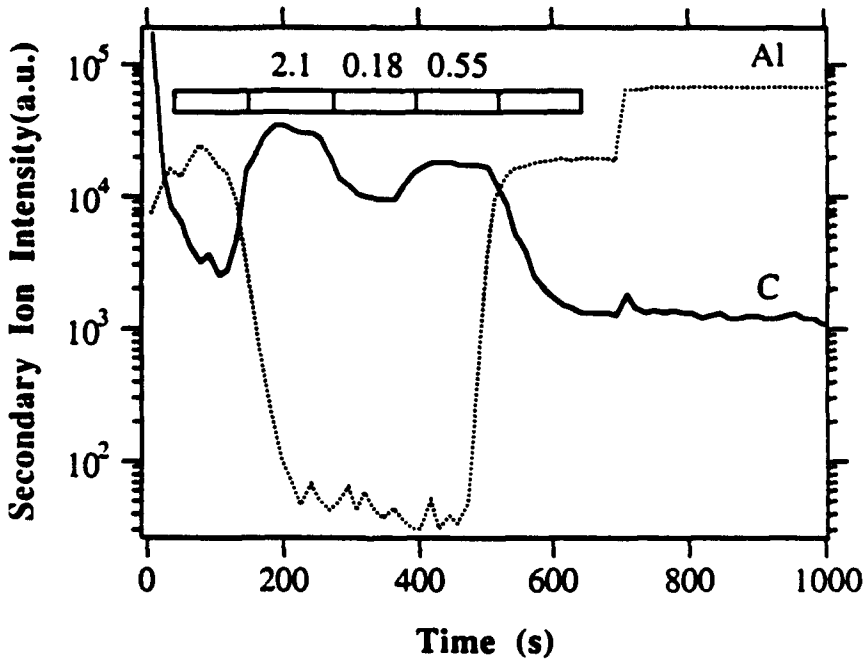

Fig.3.11 The influence of TMGa mole fraction on carbon contamination in LALE.

The AsH_3 exposure time has subtle influence on the carbon contamination and material quality. As is shown in Fig.3.12, the carbon level decreases monotonously as the AsH_3 exposure time increases. On the other hand, as is summarized in the Table 3.1 along with other

aforementioned results, the PL efficiency increases with increasing AsH_3 exposure time from 3 s to 5 s. The use of longer exposure time did not seem to have further effect on the PL efficiency. One possible explanation is that at short AsH_3 exposure time, the PL efficiency is limited by impurity induced defects and complexes which reduce the radiative recombination rate. At long AsH_3 exposure times, the native defects due to low temperature growth set the limit to efficient radiative recombination.

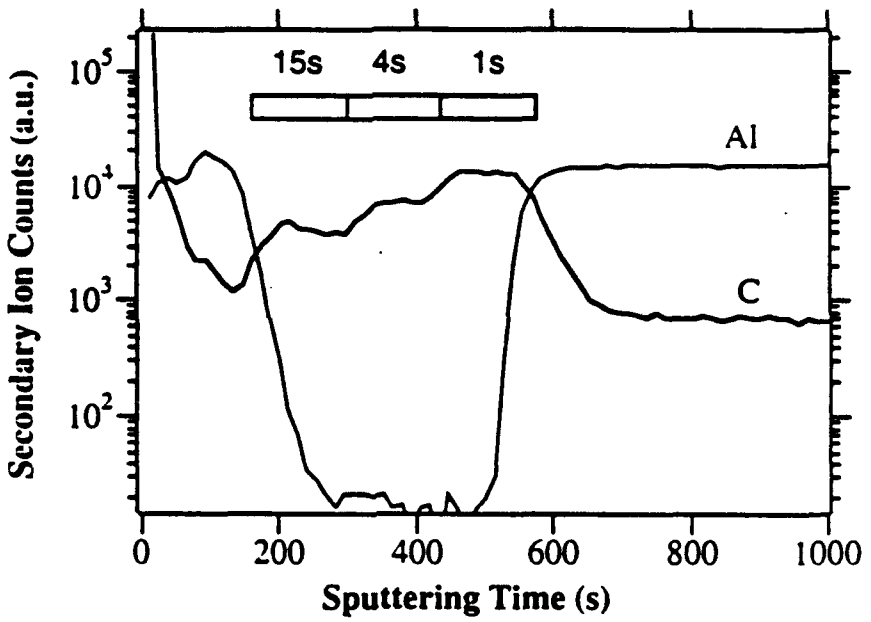

Fig.3.12 The carbon and aluminum traces of the SIMS profile from a multiple layer DH with the GaAs grown by LALE at AsH_3 exposure times of 15, 4, and 1s.

From the Table 3.1, it can be said that the best material may be obtained by growing at higher laser intensities and longer illumination durations with as low a TMGa concentration as possible and at a reasonably long AsH_3 exposure time. We have used these optimal conditions to form

laser structures with the single QW grown by LALE. The results on the device fabrication and test will be presented in Chapter Seven.

Table 3.1 Summary of LALE growth optimization using TMGa and AsH_3.

Effect On / Parameters	PL Efficiency	Carrier Concentration	C Counts From SIMS
↑ Laser Power	↑	↓	
↑ TMGa Mole Fraction	↓	↑	↑
↑ AsH_3 Exposure Time	↗		↓
Mode of Illumination	Higher for longer illum.		

3.5 LALE Doping

Doping is an integral part of a growth technique. Localized doping gives additional strength to LALE for in situ processing. We have explored the possibility of doping during LALE. The doping is performed within the LALE self limiting regime, i.e. ALE mode of 1-3-4-3, laser illumination mode of 900 W/cm^2 for 0.1 s, and at T_{sub} = 380 °C. TMGa and AsH_3 were used for GaAs LALE growth and diethylzinc (DEZn) and disilane (Si_2H_6) were used for the p and n dopants , respectively. The dopants were injected at the same time as the TMGa injection. The molar ratios of the dopants to

TMGa are such that a doping level of ~$2x10^{18}$ cm^{-3} will result in conventional MOCVD growth. The total growth is 100 cycles on semi-insulating (100) GaAs substrates.

Localized doping is achieved since only the laser illuminated areas experience changes in the electrical characteristics. The doped thin LALE stripes exhibit high conductivity as is evidenced by the almost Ohmic current-voltage (I-V) characteristics across two needle probes in contact with the stripes, Fig.3.13 (a) and (b), as opposed to the definitely rectifying characteristic on the undoped LALE GaAs stripe, Fig.3.13 (c).

To asses the contact resistance for possible device application, a row of Au contacts of 100x100 μm size is formed on the LALE GaAs by standard lithography. The uniform space between the contacts is 508 μm. The resistance across two contacts is measured as a function of the distance between them. The results are plotted in Fig.3.14 (a) for the p doping and (b) for the n doping. The resistance across two contacts at distance L apart can be expressed as

$$R = 2R_c + \frac{\rho}{A}L \qquad (3\text{-}6),$$

where the R_c is the contact resistance, ρ the resistivity of the doped GaAs stripe and A the cross section area of the stripe. By extrapolating to $L \rightarrow 0$, we find the R_c for the p and n dopings are ~4 Ω and 40 Ω. From the slope of the straight lines, we estimated the resistivities for the p and n cases to be ~ 0.0062 Ω•cm and 0.029 Ω•cm, respectively. Using the resistivity versus impurity relationship given in Sze,[17] we can estimate the effective doping

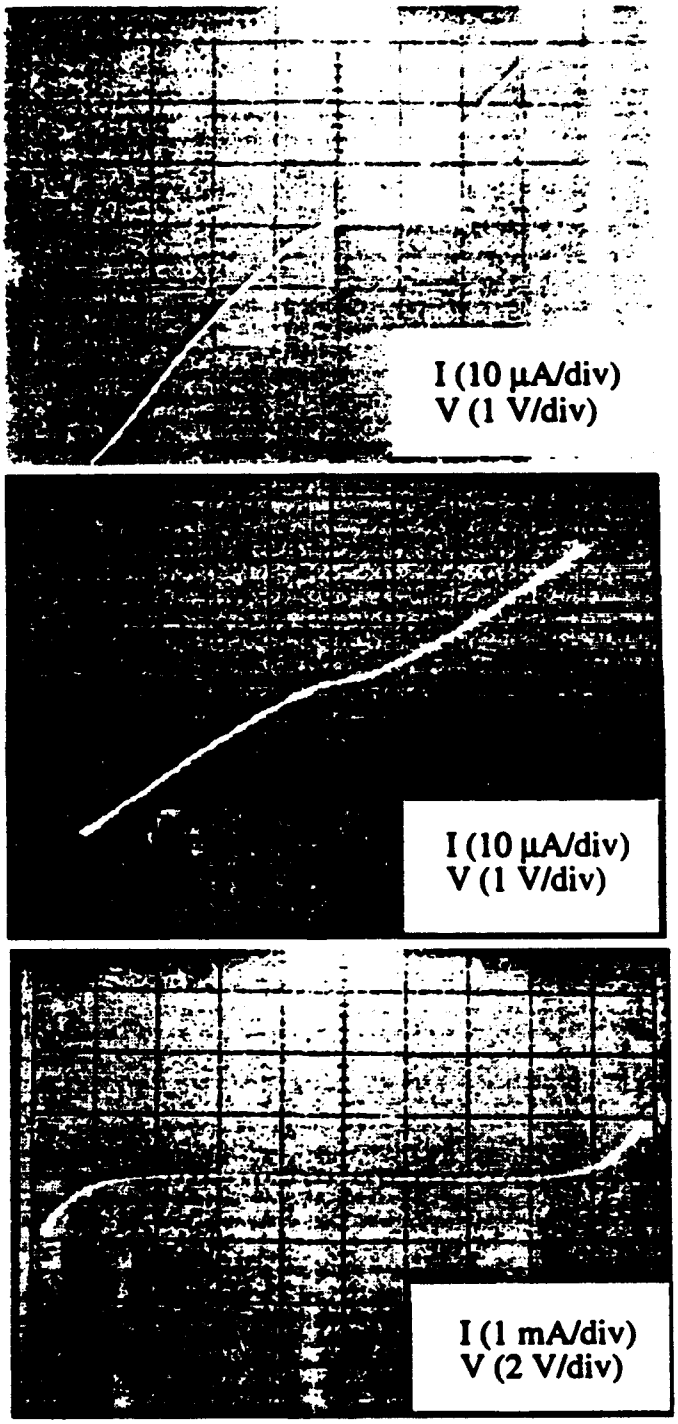

Fig.3.13 I-V characteristics of contacts across two probes on LALE stripes (a) doped using DEZn, (b) doped with disilane, and (c) undoped.

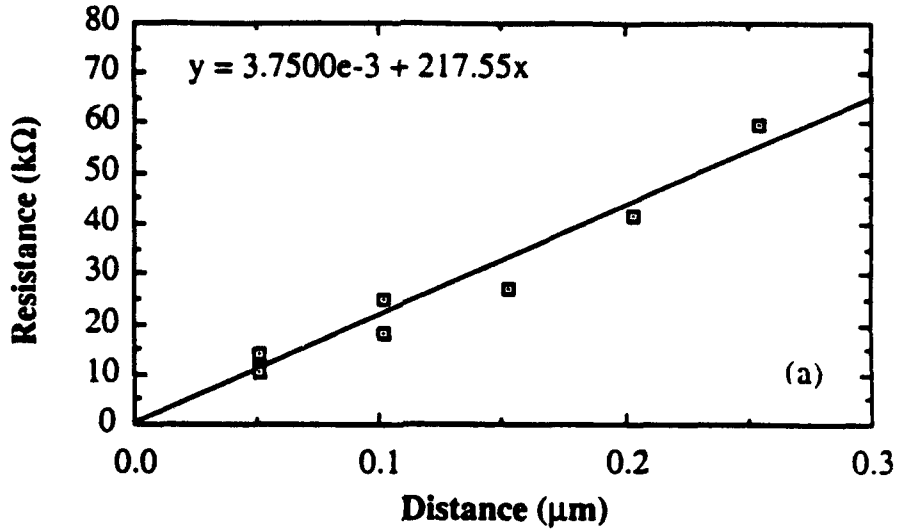

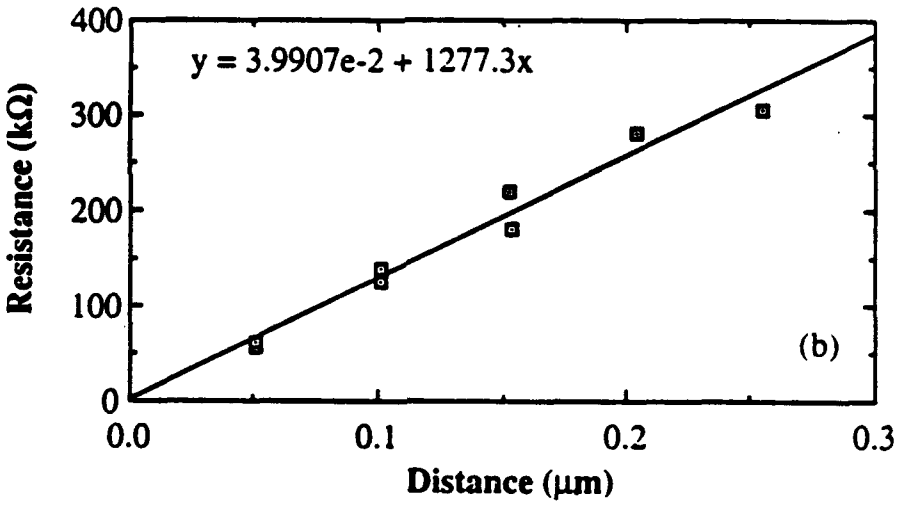

Fig.3.13 Contact resistance measurement of LALE GaAs doped with (a) DEZn and (b) disilane.

level to be ~1.3×10^{19} cm^{-3} for the p doping and ~8×10^{16} cm^{-3} for the n doping. It is not surprising that high doping using DEZn can be achieved at this low temperature since the vapor pressure of metallic Zn is reduced at low temperature. A reduced doping efficiency with Si_2H_6 at low temperature is also expected. The carrier concentration of $<10^{17}$ cm^{-3} seems

to be low in view of the almost Ohmic I-V displayed by the material. We speculate that in ALE mode of operation, gas phase stoichiometry is different from that of conventional MOCVD. The tendency for Si to occupy the Ga sites is reduced so that the material is highly self compensated. An amphoteric dopant may not be suitable for doping in ALE mode of operation. Nevertheless, our results show that LALE doping using DEZn is suitable for device application.

3.5 Conclusions and the Limitations to LALE of GaAs Using TMGa and AsH_3

The growth of GaAs by LALE using TMGa and AsH_3 has been studied in detail. Monolayer self limiting growth can be achieved within wide ranges of TMGa exposure, laser intensities, and laser illumination duration. Room temperature PL, CV, and SIMS are used for the first time to characterize the GaAs grown by LALE. Carbon is identified as the main impurity incorporated into the LALE grown GaAs layer. The correlation between the growth parameters and the material quality led to a growth procedure optimization. According to our results it is recommended that LALE growth be carried out at a low TMGa exposure, reasonably long AsH_3 exposure time, high laser intensity, and long illumination duration to achieve localized GaAs deposits of good optical quality and reasonably low carbon contamination.

It should be mentioned, though, that the intensity of ~600 W/cm^2 is relatively high for readily available light sources, which limits the total area

of the deposits and may limit, to some extent, the usefulness of the technique. In addition, the carbon impurity level in GaAs amounts to ~10^{17} cm^{-3} which is still relatively high for certain device applications. In the following two chapters, the work is described in searching for alternative precursors in LALE to produce GaAs of low carbon contamination.

References for Chapter Three

[1] J.Nishizawa, H.Abe, and T.Kurabayashi, "Molecular Layer Epitaxy," J. Electrochem. Soc., Vol.132(5), 1197(1985).

[2] K.J.Klingman and H.H.Lee, "Design of Epitaxial CVD Reactor I, Theoretical Relationships for Mass and Heat Transfer," J. Cryst. Growth, Vol.72, 670(185).

[3] I.A.Toor and H.H.Lee, "Design of Epitaxial CVD Reactors II, Design Considerations and Alternatives," J. Cryst. Growth, Vol.72, 679(1985).

[4] F.C.Eversteyn, P.J.W.Severin, C.H.J.v.d.Brekel, and H.L.Peek, "A Stagnant Layer Model for the Epitaxial Growth of Silicon from Silane in a Horizontal Reactor," J. Electrochem. Soc., Vol.117(7), 925(1970).

[5] V.S.Ban and S.L.Gilbert, J. Cryst. Growth, Vol.31, 284(1975).

[6] R.Takahashi, Y.Koga, and Kugawara, "Gas Flow Pattern and Mass Transfer Analysis in a Horizontal Flow Reactor for Chemical Vapor Deposition," J. Electrochem. Soc., Vol.119(10), 1406(1972).

[7] J.I.Davies, G.Fan, and J.O.Williams, "Metal-Organic Chemical Vapor Deposition (MOCVD) of Compound Semiconductors Part 1. – Optimization of Reactor Design for the Preparation of ZnSe," J. Chem. Soc., Faraday Trans. I, Vol.81, 2711(1985).

[8] L.J.Giling, "Gas Flow Patterns in Horizontal Epitaxial Reactor Cells Observed by Interference Holography," J. Electrochem. Soc., Vol.129(3), 634(1982).

[9] H.Schlichting, in "Boundary Layer Theory," McGraw-Hill, New York, 6th edn, 1968.

[10] B.J.Curtis and J.P.Dismukes, "Effect of Natural and Forced Convection in Vapor Phase Growth Systems," J. Cryst. Growth, Vol.17, 128(1972).

[11] L.J.Giling and J.Van de Ven, in "Advances in Crystal Growth," eds., P.M.Dryburgh, K.G.Barraclough, and B.Cockayne, (Prentice-Hall, Englewood Cliffs, NJ, 1987), p309.

[12] C.Goodings, N.J.Mason, P.J.Walker, and D.P.Jebb, "A New Inlet Design for Horizontal MOVPE Reactors," J. Cryst. Growth, Vol.91, 13(1989).

[13] G.J.Hwang and K.C.Cheng, J. Heat Transfer, Trans. ASME, Vol.95, 72(1973).

[14] M.Ozeki, K.Nakai, K.Dazai, and O.Ryuzan, Jpn. J. Appl. Phys., Vol.13(7), 1121(1974).

[15] D.M.Kozuch, M.Stavolar, S.J.Pearton, C.R.Abernathy, and J.Lopata, "Hydrogen in Carbon-Doped GaAs Grown by Metalorganic Molecular Beam Epitaxy," Appl. Phys. Lett., Vol.57(24), 2561(1990).

[16] N.Pan, S.S.Bose, M.H.Kim, G.E.Stillman, F.Chambers, G.Devane, C.R.Ito, and M.Feng, Appl. Phys. Lett., Vol.51, 596(1987).

[17] S.M.Sze, in "Physics of Semiconductor Devices," 2nd. edn. (John Wiley & Sons, Inc., 1981), p33.

CHAPTER FOUR

The Use of Tertiarybutylarsine in ALE and LALE for Low Carbon and High Quality GaAs

It can be concluded from the review carried out in the Chapter One and our investigation described in the Chapter Three that a persistent problem in low temperature ALE and LALE growth involving an organometallic precursor is the reduction of carbon background impurity levels that is believed to result from the incomplete decomposition of the metal alkyls on the surface. A key ingredient to reducing the incorporation of carbon in the pervious studies has been the minimization of the TMGa exposure and extended exposure to AsH_3[1]-[3] However, the minimization of TMGa exposure can not be carried so far as to jeopardize the self limiting growth feature of ALE and LALE. Extended exposure to AsH_3 is undesirable from both economical and environmental point of views. A complete change in the growth chemistry is then a logical alternative.

In this chapter, we describe the first result on the use of tertiarybutylarsine (TBAs) in ALE and LALE growth of high quality GaAs. TBAs was chosen for the study because it is known to decompose at lower temperatures[4]-[6] than AsH_3[7][8] and is believed to remove methyl radicals more efficiently from the growing surface than AsH_3[9] The difference in growth chemistry at low temperatures involving TBAs will be exploited to

obtain GaAs of low carbon contamination. In addition, the lower toxicity of TBAs compared to AsH_3 offers further advantage in its usage.

4.1 Basic Chemistry of TBAs

The formation of a TBAs molecule can be viewed as the replacement of one of the H from an AsH_3 molecule by the tertiarybutyl group as is depicted in Fig.4.1. As a result, the heavier and asymmetric TBAs molecules exhibit stronger intermolecular interactions and a much lower vapor pressure than that of AsH_3 but yet is still in a convenient physical state to handle and use. Under normal condition, TBAs is a liquid with a vapor pressure of 60.3 mmHg at 0°C as is listed in Table 4.1 along with several group V sources for MOCVD and CBE.

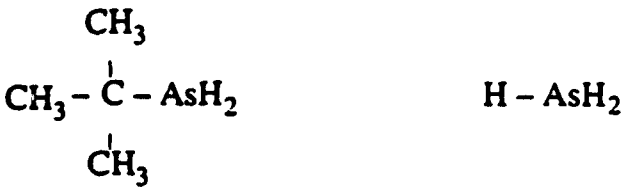

Fig.4.1 Structural formulars of TBAs and AsH_3

Not much is known of the possible addition reaction between TBAs and the commonly used group III metalorganics such as TMGa, TEGa, and TMIn. Since adduct formation in the intermixing stage of MOCVD generally results in the loss of useful reactant, it is certainly a major concern in the search for a new precursor. From the dissociation entropy of the adducts between TEGa and ammonia or amines, the apparent donor

Table 4.1 List of vapor pressures for selected group V sources used in vapor phase growth. of III-V materials.[10][11]

Compounds	P(mmHg)/T(°C)	logP(Torr) = B - A/T(K)	
		B	A
As(s, 440-815°C)	1/370	10.80	6946.59
AsH_3	205 PSIG/20		
DEAs	40.6/20	7.339	1680
TBAs	60.3/0	7.50	1562.3
TEAs	6.2/20	8.23	2180
TMAs	97.0/0	7.405	1480
P(wht,20-44°C)	1/68.6	9.6511	3296.9
P(vlt,380-590°C)	254.9/380	11.0842	5667.48
PH_3	593 PSIG/20		
DEP	70.8/20	7.6452	1699
TBP	89.5/0	7.586	1539
TEP	10.9/20	7.86	2000
TMP	98.7/-10	7.7627	1518

strength (or the Lewis basicity) was established to be[12] $MeNH_2 > NH_3 > Me_2NH > Me_3$, where the Me represent a methyl group. According to the theory forwarded by Coates *et al.*,[13] there are two effects contributing to the strength of the bond formed between a Lewis acid (electron pair acceptor) and a Lewis base (Electron pair donor), i.e. the inductive and the steric effects. For example, an adduct may form between a metalorganic boron of the type R_3B and an amine of the type NR'_3:

$$R_3B + NR'_3 \rightarrow R_3B{\leftarrow}NR'_3 \qquad (4\text{-}1),$$

where the R and R' are the groups (such as alkyls and hydrogen) attached to the B and N, respectively. The small arrow indicates the direction of

electron pair transfer. The stability of a co-ordination adducts will be enhanced by the extent to which (a) negative charges tend to be removed from the acceptor atom by the attached group R and (b) positive charge tend to be removed from the donor atom by the attached group R'. This is the so called inductive effect. From the inductive effect alone, the order of acceptor strength (acidity) will be $BF_3>BCl_3>BBr_3>BH_3>BMe_3$ and the order of donor strength (basicity) will be $NH_3<RNH_2<R_2NH<R_3N$. Bulky groups attached to both B and N atoms will, however, interact to reduced the tendency of electron pair transfer from the donor to the acceptor (base to acid), therefore reduce the bonding strength of the adduct. This is the so called steric effect. A quantitative prediction is still not possible. Some experiments have to be done in order to establish the Lewis basicity of TBAs towards several important group III metalorganics of interest.

Because of the potential use of TBAs in MOCVD, thermal decomposition of TBAs was studied by two groups[5][6] since it provides a quick evaluation of the new source. In both studies, mass spectrometry was used. Larsen *et al.*[5] used the classic ex situsampling approach and Lee *et al.*[6]. used molecular beam sampling similar in principle to that described in the Chapter Two of this writing. The sampling techniques dictated the convenient operating pressures of the decomposition reactors, i.e. 1 atm in Ref.[5] and ~10^{-3} Torr in Ref.[6].

TBAs was fund to decompose to 50% of its input concentration at $T_{50\%}$ ~375 °C in deuterium (D_2). In the presence of GaAs surfaces, this $T_{50\%}$ reduced to ~320 °C. Lee *et al.* reported a lower $T_{50\%}$ (~287 °C) in H_2,

He, and D_2. In spite of this difference which may not be readily explained by the difference in the operating pressure alone, the $T_{50\%}$ for TBAs is considerably lower than those reported for AsH_3, i.e. 540~565 °C[8] and ~690 °C.[7]

The major stable gas phase products of TBAs decomposition was found by Larsen *et al.* to be isobutane (C_4H_{10}), isobutene (C_4H_8), AsH_3, and H_2. At all temperatures, C_4H_{10} was the dominant species but the difference in the quantity of C_4H_{10} and C_4H_8 was reduced as more C_4H_8 was produced at T above ~420 °C. The proposed dominant reaction pathway was an intramolecular coupling described as

$$TBAs \rightarrow C_4H_{10} + AsH \qquad (4\text{-}2).$$

The second of the two pathways is the β-elimination,

$$TBAs \rightarrow C_4H_8 + AsH_3 \qquad (4\text{-}3),$$

which was believed to occur more rapidly at higher temperatures. Lee *et al.*, on the other hand, found that the relative abundance of C_4H_8 was higher than that of C_4H_{10} at high temperatures. Accordingly, a radical mechanism was proposed where the main reaction pathway was the simple scission of the carbon-arsenic bond,

$$TBAs \rightarrow C_4H_9 + AsH_2 \qquad (4\text{-}4).$$

The subsequent radical disproportionation and recombination were then believed to produce the detected stable species. Both studies found no deuterated hydrocarbon (HC) species in the product with D_2 as the carrier gas, indicating that any intermediate radical species are not reactive enough to abstract a D atom from the D_2. The alkyl radicals will convert to a stable volatile HC species through processes rather than abstracting H from other HC species resulting in the dehydrogenation of the latter and the carbon contamination problem. Therefore, the bulky tert-butyl radicals contained in TBAs are expected to be less of a problem as a source of carbon contamination. The presence of species such as AsH and AsH_2 is expected to be beneficial for removing alkyl radicals produced from the metalorganics, especially at low temperature growth. At higher temperatures where AsH_3 decomposes, TBAs may be viewed as an in situ source of AsH_3 which subsequently undergoes thermal decomposition to give appropriate As containing species for arsenide growths. The hazard associated with handling AsH_3 is reduced, however.

In many cases, a major obstacle to the use of AsH_3 in MOCVD particularly in populated areas is the toxic hazard of the chemicals (AsH_3 and PH_3) under high pressure. The threshold limit values (TLVs) are 0.05 ppm and 0.3 ppm for AsH_3 and PH_3[14], respectively. No value could be found for the lethal concentration for 50% of the rat population under test (LC_{50}) for AsH_3. The LC_{50} for PH_3 is 11 ppm. PH_3 is considered less toxic than AsH_3. The LC_{50} has been given for TBAs to be 70 ppm,[15] which is then much less toxic than PH_3 and AsH_3 at least in view of the immediate toxicological effect.

4.2 TBAs in MOCVD

The pioneering work of Chen *et al.*[4] using TBAs in MOCVD produced quite encouraging results even with the source contaminated by relatively high level of Ge. Most notable was the ability to grow GaAs of excellent and fair morphology at a V/III ratios as low as ~2 and ~1, respectively. Further purification of the TBAs source resulted in GaAs of quality comparable to that obtainable from using AsH_3.[16] Total impurities (N_a+N_d) as low as $6.6x10^{14}$ cm^{-3} and μ_{77K} and μ_{300K} as high as 80700 and 7600 cm^2/vs were reported. Sharp and well resolved excitonic features in low temperature PL spectra also indicated high quality of the GaAs material. $Al_xGa_{1-x}As$ with x up to 0.6 was also grown using TBAs.[17] The PL spectra of the QW's grown entirely by MOCVD using TMGa, TMAl, and TBAs showed sharp QW peaks with the intensity and line shape comparable to those using AsH_3. The device quality of GaAs and AlGaAs materials was demonstrated by the characteristics of QW lasers fabricated on the graded-index separate-confinement heterostructures(GRIN-SCH) grown using TBAs. Threshold current density as low as 180 A/cm^2 was obtained.

An interesting feature in the growth using TBAs is the conduction type conversion from n to p upon reducing the V/III ratio,[16][17] similar to that of the growth using TMGa and AsH_3. This has usually been explained as being the compensation effects caused by the variations of gas phase stoichiometry between the carbon acceptors and donor impurities

commonly existing in the precursors (e.g. Si, Ge, S, etc.). For a given amount of donor impurities carried by the precursors and at a given growth temperature, the lower is the V/III at which the material converts from n to p and the better is the group five source in its role of getting rid off carbon. There is yet no a complete study.which compares AsH_3 and TBAs in this manner. Typical conversion points reported were V/III ~10 for TBAs[16] at 660 ° and ~22 for AsH_3.[18]

In a thermogravimetric study of MOCVD using TMGa, TEGa, and TBAs, Omstead *et al*[19] found that the growth rate in the case when TMGa and TBAs were injected through different ports into the reactor was three times higher that when the precursors were injected through a common manifold. This could be the evidence of prereaction between TMGa and TBAs that depletes the reactants available for the growth. Similar but more severe phenomenon was observed for TEGa and TBAs, in which case the growth rate dropped an order of magnitude when the V/III increased from 2 to 5. Parasitic reactions between TMGa and TBAs were also noted[17] by observing a decrease in the solid composition (x) of $Al_xGa_{1-x}As$ for a fixed V/III and TMGa/TMAl ratios within the same run. In the ALE mode of operation, the III and V precursors are injected separately, this parasitic reaction may be avoided to large extent.

4.3 ALE and LALE Using TBAs

The ALE and LALE work described here was carried out in the same switching flow reactor described in the Chapter Three. Alternate

exposure of the substrate to TMGa and TBAs was achieved by temporal switch of the TMGa and TBAs into the carrier flow. TBAs injection is through a separate manifold so that the point of mixing in the conventional MOCVD sense is at ~30 cm upstream of the substrate. ALE was carried out at 480 °C and LALE at 380 °C. The 514.5 nm line of an Ar ion laser was used for the LALE growth. The laser beam was first expanded and then focused with a cylindrical lens to obtain suitable intensity over a narrow line of typical dimensions as 300 μm wide and 2~4 mm long.

For ALE study, suitable ALE exposure modes obtained from previous growth using TMGa and AsH_3 were used directly in the experiments using TBAs. QW's and a DH's were grown with the central GaAs region by LALE using TBAs at nominal V/III ratios 3 and 3.6. It is more reasonable now to define a V/III ratio pertaining to the ALE mode of operation, i.e. $(V/III)_{ALE}$ = (moles of group V injected per cycle)/(moles of group III injected per cycle). The corresponding $(V/III)_{ALE}$ ratios at a 1-4-4-4 mode are 12 for the QW's and 14.4 for the DH's. PL was utilized to asses the material quality.

PL and CV measurements are the same as those described in the Chapter Three. For SIMS profiling, multiple layer DH's were grown, whereby each LALE GaAs layer of thickness ~700 Å was grown using a different combination of precursors and the carbon incorporation was studied.

The final morphology of the QW's and DH's up to 200 ML thick with the central GaAs grown by ALE (without laser) using TBAs are featureless as viewed by the naked eye and under x1000 optical microscope, indicating a layer-by-layer growth even at $(V/III)_{ALE}$ ~12. The samples grown by LALE using TBAs are specular on and off the LALE stripes for conditions (20 cc/min TMGa at -7 °C for 1s and 10 cc/min of TBAs at 0 °C for 4s) which corresponds to a nominal V/III of ~0.64 if the TMGa and TBAs were to be injected simultaneously into the reactor and an $(V/III)_{ALE}$ as low as 2.5. This result is in accord with the results from MOCVD using TMGa and TBAs where a V/III of approximately unity could be used to produce GaAs layer of good morphology[4][15] Consequently, most of our LALE growth using TBAs were carried out at $(V/III)_{ALE} < 30$. This is to be compared to the $(V/III)_{ALE} \geq 150$ used in most of our LALE growths using AsH_3 in order to obtain material of suitable quality.

Shown in Fig.4.2 is the laser intensity dependence of the growth rate for LALE growth of GaAs using TBAs along with that using AsH_3. The growth using TBAs is performed on bare N^+ GaAs substrates oriented 2° off (100) at a TMGa mole fraction of 1.2×10^{-4} for an injection duration of 1s. The laser illumination time is 0.1s. The data for LALE using AsH_3 were obtained in our previous study in the four-chamber rotating susceptor reactor with TMGa mole fraction of 1.8×10^{-4} on a freshly grown $Al_{0.3}Ga_{0.7}As$ surface. In these experiments, the laser beam was swept across the moving substrate so that each position was illuminated for approximately 0.2s. It is seen from these data that self limiting LALE using

TBAs occurs in a similar range as that using AsH_3. TBAs is considered a direct replacement as regards to achieving monolayer self limiting growth. The difference in the laser intensities at the lower end of the LALE intensity widow for these two cases is due partially to the difference in the illumination duration and partially the difference in the optical and thermal properties of the starting surface.

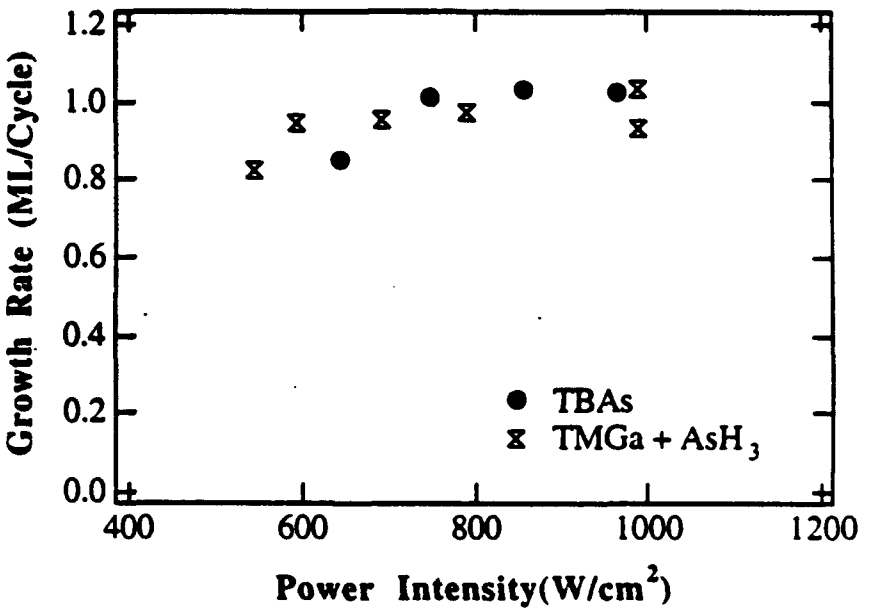

Fig.4.2 Laser intensity dependence of LALE using TBAs in comparison to that using AsH_3. Monolayer self limiting is achieved in similar ranges of intensities.

4.4 Materials Characteristics

Intense room temperature PL can be observed from the QW's and DH's grown by ALE using TBAs at moderate excitation as is shown by the dashed trace in Fig.4.3 for a DH, indicating good quality of the ALE material and the interfaces in the structure. As a means of testing the quality

of the material for device applications, such a QW is incorporated into the GRIN-SCH laser structures. Broad area laser diodes have been successfully fabricated. Threshold current density as low as 300 A/cm^2 is obtained under pulsed testing condition at 10 kHz repetition rate. This is the first demonstration of the device quality of GaAs QW grown by ALE using TMGa and TBAs.

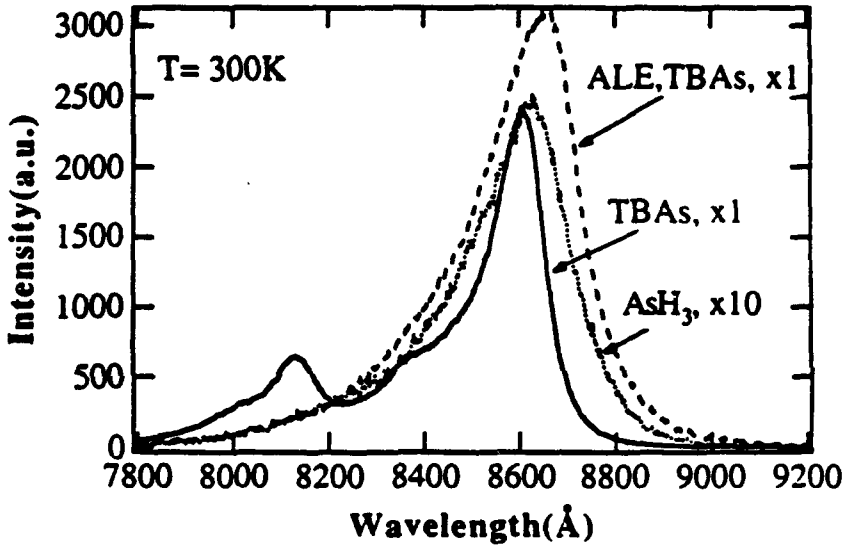

Fig.4.3 Room temperature PL from DH's with the central GaAs grown by ALE and LALE.

Thin GaAs layers (~565 Å) grown by LALE using TMGa and TBAs and sandwiched between conventional $Al_{0.3}Ga_{0.7}As$ layers also show intense photoluminescence emission at room temperature. A typical PL spectrum is shown as the solid line in the Fig.4.3 in comparison to one from a DH by LALE using TMGa and AsH_3, dotted line. For both cases, the exposure modes are 1-5-5-4 and the laser illumination durations are 0.1 sec. The fact that room temperature PL is routinely observable indicates good

quality of GaAs grown by LALE. GaAs layers using TBAs show about ~7-10 fold higher PL efficiency than films grown using AsH_3. In addition, the whole $Al_{0.3}Ga_{0.7}As/GaAs/Al_{0.3}Ga_{0.7}As$ structure for the TBAs case exhibits a much lower rate of nonradiative recombination as evidenced by the QW peak in the short wavelength side of the main peak, originating from the excess carriers diffusing through the ~1.7 μm isolation layer and being captured by the conventional MOCVD QW deliberately imbedded in the lower part of the DH structures designed for PL measurement. This is a result of a low nonradiative recombination rate either in the LALE GaAs or at the interfaces or both. Complete isolation was possible when the $Al_{0.3}Ga_{0.7}As$ layer thickness was increased to about 2.5 μm.

In Fig.4.4 (a), the carrier concentration profile from C-V measurements on a DH with the central GaAs layer grown by LALE using TBAs is compared to that obtained from a similar DH grown by LALE using AsH_3. In the first case, no acceptor related impurity is detected above the background level of the conventionally grown $Al_{0.3}Ga_{0.7}As$, i.e. $p\sim3\times10^{15}$ cm^{-3}. This is in contrast to the appreciable amount of acceptors in the GaAs grown using TMGa and AsH_3. The CV data from the measurements performed directly on the 0.5 μm-thick GaAs grown by LALE are also included in Fig.4.4 (b). The hole concentration is $3–4\times10^{17}$ cm^{-3} for the material grown using AsH_3 and between $1–2\times10^{16}$ cm^{-3} using TBAs.

This low carbon contamination in the GaAs grown by LALE using TBAs is further confirmed by SIMS measurement. Fig.4.5 shows the C, Al,

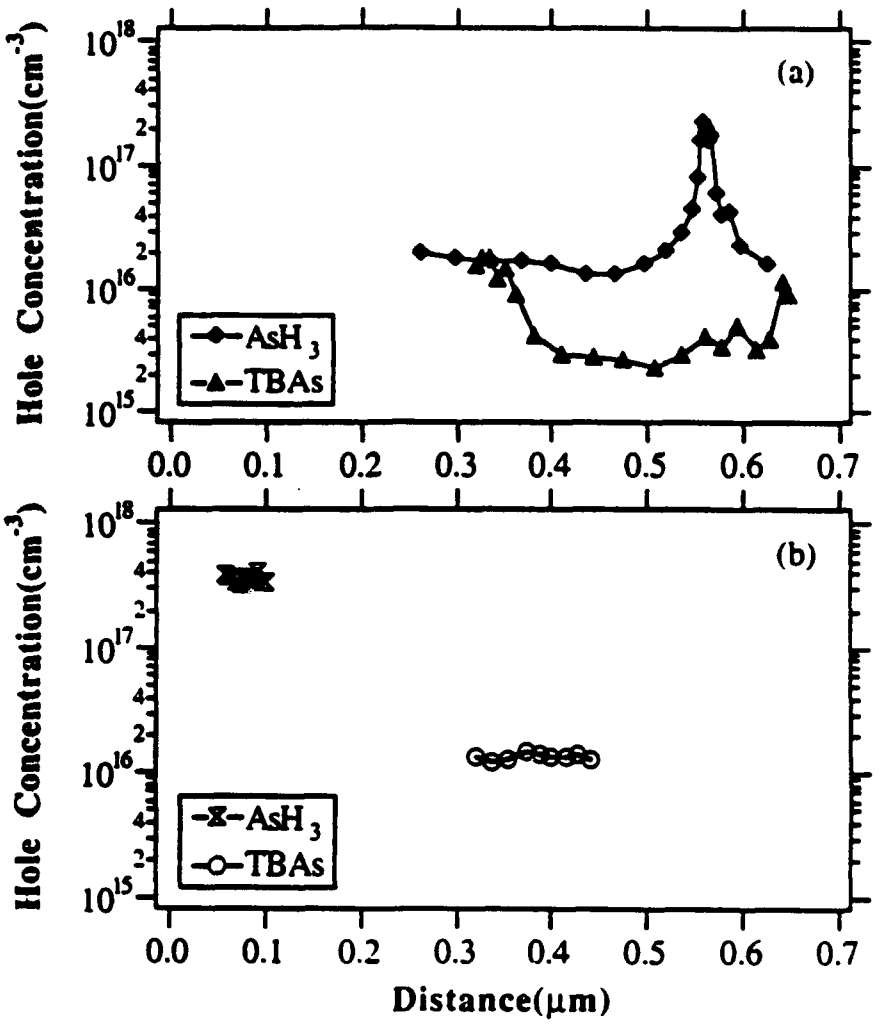

Fig.4.4 C-V profiles of (a) DH's and (b) thick GaAs grown by LALE.

and H traces of SIMS profiles on a three layer DH. Only the GaAs layer grown by LALE using TMGa and AsH_3, layer (III), shows appreciable amounts of carbon relative to the background level in the MOCVD grown $Al_{0.3}Ga_{0.7}As$ layers. The GaAs layer grown by LALE using TMGa and TBAs, layer (II), contains, at most, a level of carbon within the background of the conventional MOCVD $Al_{0.3}Ga_{0.7}As$ layer on which the LALE is

performed. The drawing over the traces is meant to locate the approximate boundaries of each layers. The spreading at the GaAs/AlGaAs interfaces is believed to be an measurement artifact because of the high acceleration potential of the primary Cs beam that enhances the ion beam mixing yet is necessary for sensitive carbon detection. In addition, the sputtered area is larger than the dimension of the LALE stripe. The observed reduction in carbon contamination with the use of TBAs may be attributed to the abundance of species like AsH_x (x=1, 2) on the growing surface from the decomposition of TBAs[5][20]. Unsaturated carbon containing species are saturated through reacting with the AsH_x and largely removed as stable and volatile molecules.

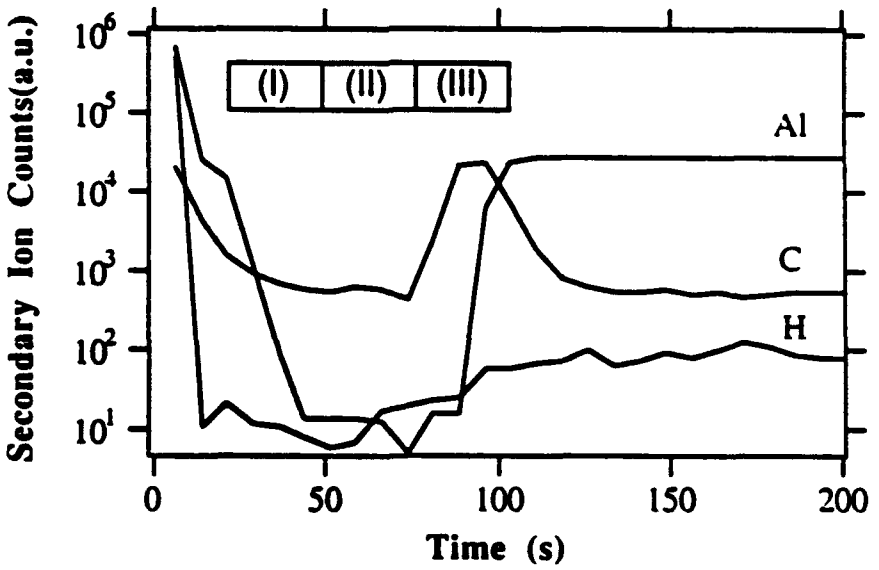

Fig.4.5 SIMS profiles through a multilayered structure with GaAs grown by LALE using (I) TEGa and AsH_3, (II) TMGa and TBAs, and (III) TMGa and AsH_3.

4.5 Growth Optimization in LALE Using TBAs

The influence of growth parameters on the qualities of the material grown by LALE using TBAs was also studied. Shown in Fig.4.6 are the room temperature PL spectra from DH's grown with different illumination durations. The enhanced PL efficiency at longer illumination time is similar to the case when AsH_3 was used. Notice that in this set of experiments, the laser intensity is the same. The increase in the illumination time increases both the flux of photons and the time of heating. It is more likely that the enhancement in the PL efficiency is due largely to the longer heating that promotes perfect lattice site registry.

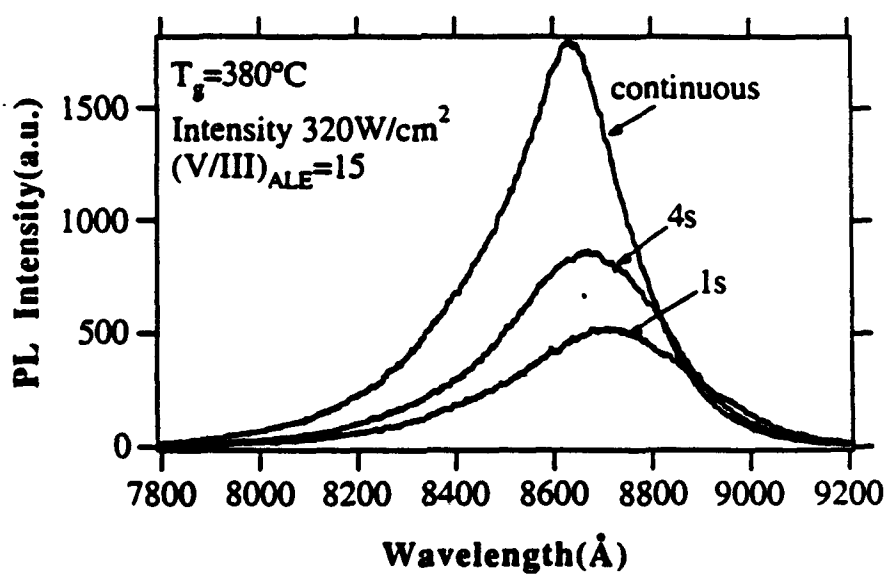

Fig.4.6 The influence of illumination duration on PL efficiency of GaAs grown by LALE using TBAs.

It is difficult to compare the room temperature PL obtained from samples grown at short illumination time but with high intensity with that at long illumination time with low intensity since similar line shape and comparable PL efficiency were observed. There are differences in the PL spectra at 5 K as is shown in Fig.4.7. First of all, the low temperature PL of GaAs grown by LALE using TBAs, (the solid line) is dominated by a peak at a shorter wavelength than the carbon related peak displayed by GaAs grown using AsH_3, (the dotted line). In addition, there is at least another peak which appears as a shoulder in the even shorter wavelength side of the main peak. The energy position of this second peak varies with the mode of

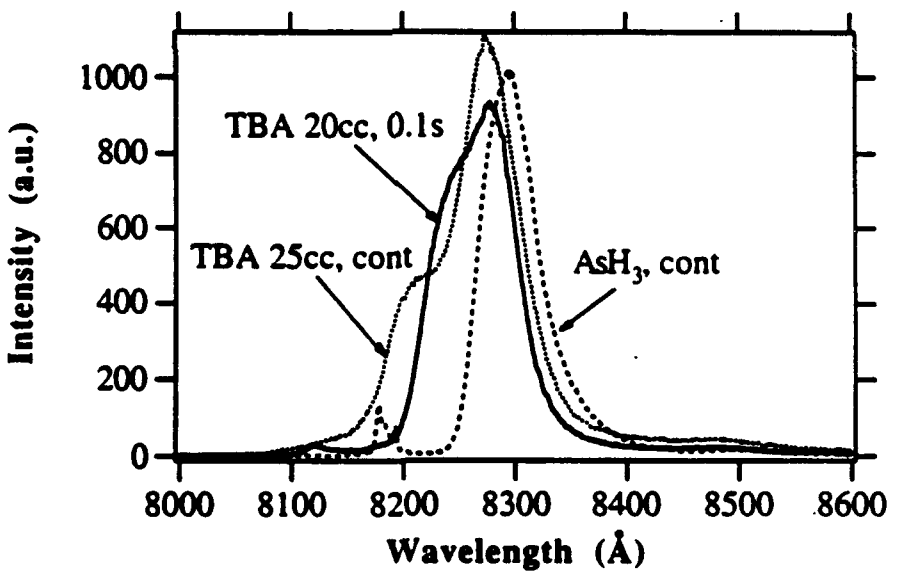

Fig.4.7 Low temperature (5 K) PL spectra from DH's grown by LALE: the solid line, using TBAs at 20cc/min and laser illumination for 0.1s; the dotted line, TBAs at 25cc/min under continuous illumination; the dashed line, using AsH_3 under continuous illumination.

laser illumination, being closer to the near-band-edge emission at longer illumination with correspondingly lower intensity. The exact assignment of these peaks is still unclear.

Finally as is expected, the increase in TBAs flow rate (or concentration) also enhances the PL efficiency as is seen from the spectra shown in Fig.4.8. The 100 cc/min of TBAs in this case would correspond to $(V/III)_{ALE}$ ~71 and V/III ~18. Device quality GaAs has been obtained with mostly $(V/III)_{ALE}$ between 10~20 when other conditions are optimized. Our results show that TBAs is an efficient arsenic source in LALE.

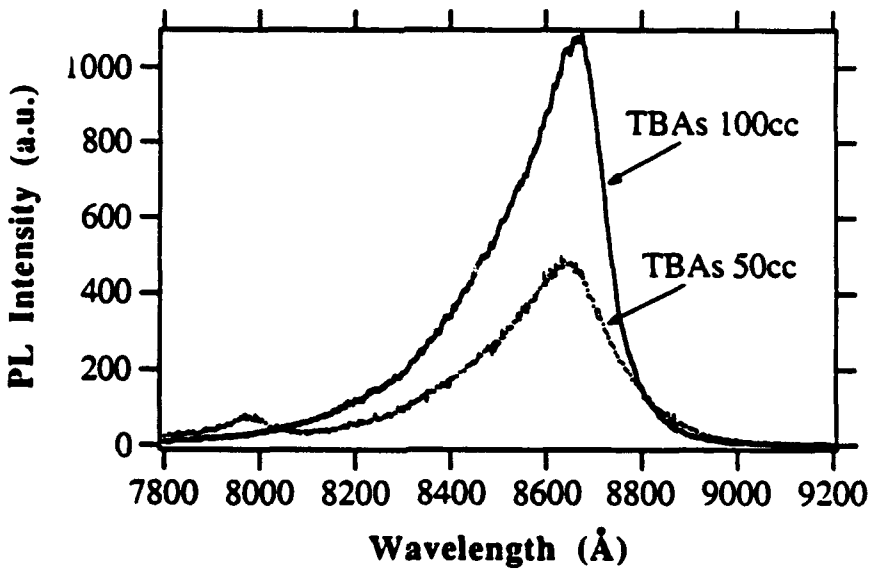

Fig.4.8 Room temperature PL from DH's Grown by LALE using different TBAs flow rates.

4.6 Concluding Remarks

We have succeeded in growing GaAs by ALE and LALE using a combination of TMGa and TBAs for the first time. TBAs is observed to be a direct and efficient replacement for AsH_3 in ALE and LALE. GaAs materials grown by LALE using TBAs exhibit low carbon contamination as is evidenced by C-V and SIMS measurements. Intense room temperature PL response is observable from DH's grown by ALE and LALE using TBAs, indicating good optical quality and suitable interfaces for device applications. The device application of the GaAs/AlGaAs QW with the central GaAs grown by ALE using TBAs is demonstrated. The details in the device application of GaAs grown by LALE will be presented in Chapter Seven.

References for Chapter Four

[1] Q.Chen, J.S.Osinski, and P.D.Dapkus, "Quantum Well Lasers with Active Region Grown by Laser Assisted Atomic Layer Epitaxy," Appl. Phys. Lett. 57(14), 1437 (1990).

[2] K.Mochizuki, M.Ozeki, K.Kodama, and N.Ohtsuka, "Carbon Incorporation in GaAs Layer Grown by Atomic Layer Epitaxy," J. Cryst. Growth, Vol.93, 557(1988).

[3] P.C.Colter, S.A.Hussien, A.Dip, M.U.Erdogan, W.M.Duncan, and S.M.Bedair, "Atomic Layer Epitaxy of Device Quality GaAs with 0.6 μm/h Growth Rate," Appl. Phys. Lett, Vol.59(12), 1440(1991).

[4] C.H.Chen, C.A.Larsen, and G.B.Stringfellow, "Use of Tertiarybutylarsine for GaAs Growth," Appl. Phys. Lett. 50(4), 218 (1987).

[5] C.A.Larsen, N.I.Buchan, S.H.Li, and G.B.Stringfellow, "GaAs Growth Using Tertiarybutylarsine and Trimethylgallium," J. Cryst. Growth 93, 15 (1988).

[6] P.W.Lee, T.R.Omstead, D.R.Mckenna, and K.F.Jensen, "In situ Mass Spectroscopy Studies of the Decomposition of Organometallic Arsenic Compounds in the Presence of $Ga(CH_3)_3$ and $Ga(C_2H_5)_3$," J. Cryst. Growth, Vol.93, 134(1988).

[7] J.Nishizawa and T.Kurabayashi, J. Electrochem. Soc., Vol.130, 413(1983).

[8] S.P.DenBaars, B.Y.Maa, P.D.Dapkus, A.D.Danner, and H.C.Lee, "Homogeneous Thermal Decomposition Rates of Trimethylgallium and Arsine and Their Relevance to the Growth of GaAs by MOCVD," J. Cryst. Growth, Vol.77, 188(1986).

[9] B.Y.Maa and P.D.Dapkus, "Reaction Mechanisms of Tertiarybutylarsine on GaAs (001) Surface and Its Relevance to Atomic Layer Epitaxy and Chemical Beam Epitaxy," J. Electron. Mat. 20, 589 (1991).

[10] "Handbook of Chemistry and Physics," 71th edn., Ed. by D.R.Lide, (CRC Press, 1990-1991), p6-71.

[11] According to the product notes available from Morton International, Inc., 148 Andover street, Danvers, Massachusetts 01923.

[12] D.G.Tuck, in "Comprehensive Organometallic Chemistry," Vol.1, Eds., G.W.Wilkinson, F.G.A.Stone, and E.W.Abel, (Pergamon Press, 1982), pp693.

[13] G.E.Coates, J.H.S.Green, and K.Wade, "Organometallic Compounds: Vol.1, The Main Group Elements," (Methuen & CO, LTD), p204.

[14] "CRC Handbook of Laboratory Safety," Ed. by N.V.Steere, (Chemical Rubber Co., Cleveland, Ohio, 1967).

[15] G.B.Stringfellow, "Non-Hydride Group V Source for OMVPE," J. Electron. Mat. 17(4), 327 (1988).

[16] G.Haacke, S.P.Watkins, and H.Burkhard, "Metalorganic Chemical Vapor Deposition of High-Purity GaAs Using Tertiarybutylarsine," Appl. Phys. Lett., Vol.54(20), 2029(1989).

[17] S.G.Hummel, C.A.Beyler, Y.Zou, P.Grodzinski, and P.D.Dapkus, "Use of Tertiarybutylarsine in the Fabrication of GaAs/AlGaAs Quantum Wells and Quantum Well Lasers," Appl. Phys. Lett. 57(7), 695 (1990).

[18] J.Hallais, Acta, Electronica, Vol.21, 129(1978).

[19] T.R.Omstead, P.M.Van Sickle, P.W.Lee, and K.F.Jensen, "Gas Phase and Surface Reactions in the MOCVD of GaAs from Trimethylgallium, Triethylgallium, and Tertiarybutylarsine," J. Cryst. Growth, Vol.93, 20(1988).

[20] A.V.Annapragada, S.Salim, and K.F.Jensen, Presented in the 1991 Spring Materials Research Society Meeting, April 17–May 1, Anaheim, California, U.S.A., Symposium D. Full paper in " Atomic Layer Growth and Processing ", Materials Research Society Symposium Proceedings Vol.222, Eds., T.F.Kuech, P.D.Dapkus, and Y.Aoyagi, p81.

CHAPTER FIVE

A Comparative Study of LALE Using TEGa and TMGa

Triethylgallium (TEGa) is an important group III precursor now widely used in MOCVD, MOMBE, and chemical beam epitaxy (CBE). The replacement of TMGa by TEGa in MOCVD resulted in GaAs of considerably low carbon incorporation.[1] In the case of MOMBE and CBE where the process occurs predominantly on the surface, only TEGa can be used to obtain GaAs material of low carbon background[2]-[4] as opposed to TMGa which becomes a carbon dopant source.[5][6]

Although self limiting growth in LALE using TEGa and AsH_3 has been demonstrated, the material is not well characterized, if at all. This fact makes it impossible to asses the suitability of TEGa in LALE as compared to TMGa. In this chapter, a comparative study of LALE using TEGa and TMGa is described. The evidence of lower carbon impurity levels in GaAs grown using TEGa than those using TMGa is reported for the first time.

5.1 Some Important Facts Concerning TEGa

Structurally, as is depicted in Fig.5.1, TEGa is similar to TMGa except that the three methyl groups are now replaced by the ethyl groups in TEGa. This gives a liquid with somewhat lower vapor pressure than that of TMGa but is still at a convenient value for mass transfer, e.g. 4.4 mmHg at

20 °C given by logP(mmHg)= 8.224 - 2222/T(K), without heating the gas lines.

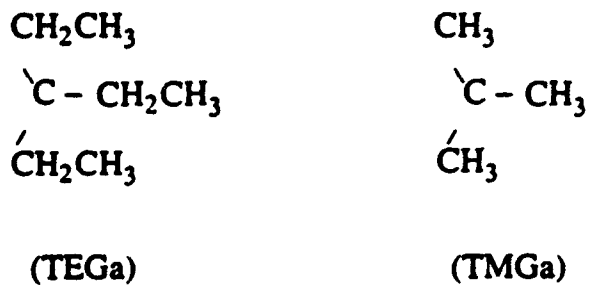

(TEGa) (TMGa)

Fig.5.1 Structural formulars of TEGa and TMGa.

The thermal stability and decomposition of TEGa have been studied extensively by infrared spectroscopy (IR)[7] and by mass spectroscopy.[3][7]-[10] TEGa has been found to decompose to 50% completion at ~320 °C, much lower than TMGa ($T_{50\%}$ ~470 °C, see Chapter Two). This lower decomposition temperature is more compatible with trimethylindium (TMIn) for alloy growth by LALE. The major hydrocarbon product in TEGa decomposition is C_2H_4, supporting a mechanism whereby the TEGa decomposes via a β-elimination process. These thermal decomposition studies indicate that the bulkier ethyl groups have weaker Ga-C bonds. In addition, the longer C-C chain allows the flexibility in the transition state of the reaction such that the hydrogen atom on the carbon atom that is not bonded to the Ga atom (the β carbon) is transferred to the Ga atom. The C_2H_4 is produced according to the reaction

$$(C_2H_5)_2GaCH_2CH_3 \rightarrow (C_2H_5)GaH + C_2H_4 \qquad (5\text{-}1).$$

The β-elimination can proceed further to possibly result in GaH_3 which, in turn, is quite unstable and converts immediately to metallic Ga and hydrogen. This reaction scheme was also identified as an energetically favorable process with an activation energy of 43.51 kcal/mol (after the zero point energy correction) as compared to the simple scission process by Tsuda *et al.*[11] using a molecular orbital calculation. Furthermore, this reaction path results in largely stable volatile C_2H_4 molecules instead of radicals. The carbon contamination problem associated with the use of TMGa is expected to be alleviated.

The vapor of TEGa exhibits appreciable light absorption only in UV range with a weak band at wavelength ~260 nm and a stronger band at ~211 nm.[12] The whole absorption band is shifted to longer wavelength by at least 25 nm relative to that of the TMGa. From these reported data, it is then expected that LALE using TEGa with the 514.5 nm laser line is still dominated by surface processes.

5.2 LALE Growth Behaviors

The LALE growth using TEGa is performed in the switched flow reactor described earlier. The TEGa bubbler is kept at 20 °C. The bias temperatures of the substrate are 330 and 340 °C due to the lower stability of the TEGa molecules in the gas phase. For most cases, a narrow line up to 300 ML thick is grown and the thickness profile measured by a stylus profilometer. The sample structures for PL, C-V, and SIMS measurements are the same as those used in the work described in the Chapter Three and

Chapter Four. The Ga source for the conventional MOCVD growth of AlGaAs barrier layers is TMGa. It should be mentioned at this point that number of attempts (5 runs) in LALE using TEGa in combination with TBAs met with the disappointment of hazy surfaces on and off LALE stripes. The DH's thus grown exhibited no PL response at all at highest excitation possible. It seems that certain reaction between TEGa and TBAs occurred before reaching the substrate. The fact that the TEGa and TBAs in our system share the same sub-manifold and that the system operates at atmospheric pressure makes this problem more apparent. Consequently, we have used AsH_3 as the group V source in all the growth discussed below.

The surface morphology of the samples grown using TEGa at around 330 ° is mirror-like on and off the LALE stripes. The ALE mode of operation using TEGa above 350 °C generally result in hazy surface covered with Ga droplets and polycrystallites. The overlapping between the TEGa exposure and the laser illumination is again found to be necessary for LALE growth in this case. Either the information contained in the Fig.3.6 of Chapter Three or a calculation based on the total flow and the geometry can be used to decide the timing of the laser pulse in relation to the injection of TEGa so that the overlap is ensured.

Shown in Fig.5.2 is the growth rate dependence on the laser power intensities, similar to the LALE using TMGa (cf. Fig.3.2). There exists a laser intensity window within which monolayer self limiting growth can be achieved. Below a threshold intensity, the growth rate decreases with decreasing laser intensity. Above the intensity widow, Ga droplets and

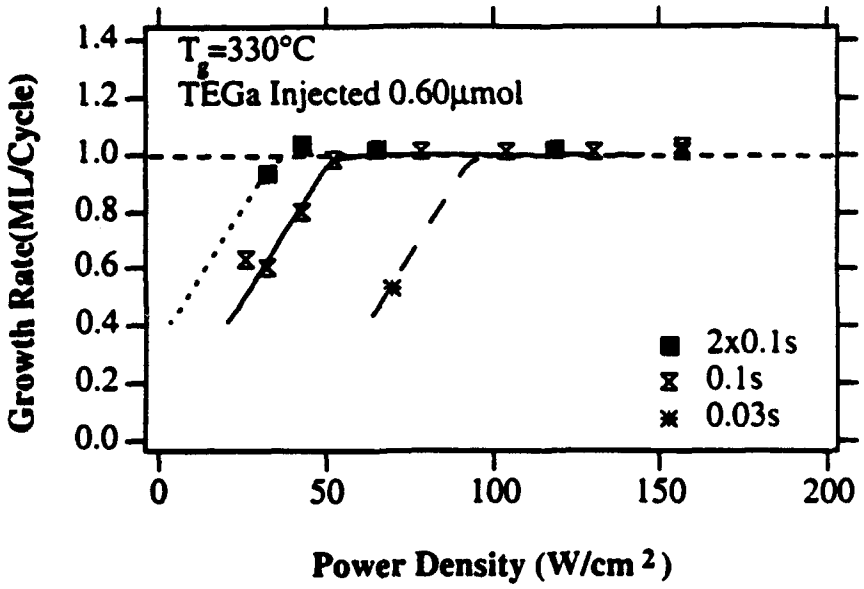

Fig.5.2 LALE growth rate as a function of laser intensity using TEGa. Notice that the intensity required to obtain ML/cycle is an order of magnitude lower than that using TMGa.

polycrystallites tends to form, resulting in a hazy LALE stripe in sharp contrast to the non-illuminated area. Most noticeable is that the threshold laser intensity for monolayer growth in this case is an order of magnitude lower than that using TMGa, namely 54 W/cm^2 (0.1s illumination) using TEGa as compared to 700 W/cm^2 (0.1s illumination) using TMGa. The extent of this reduction in the required laser intensities to obtain monolayer growth could by no means be accounted for simply by the reduced thermal stability of TEGa compared to TMGa. The laser heating effect in this case is negligible, i.e. ~5 °C at 100 W/cm^2 (see Chapter Six). The difference in the reaction rates based on the local temperatures will be so small that it is impossible to choose a bias temperature to grow a measurable stripe. We speculate that in LALE, there are three major factors contributing to the

decomposition of group III source on the surface: local heating, light induced reduction of activation energy (photocatalytic effect), and direct photodissociation of species for which the molecular orbital is greatly altered nearing the surface (photochemical effect, more likely a multiphoton process). The first factor contributes to the thermal enhancement of the growth and the last two factors contribute to the photo-enhancement of the growth. In the case of LALE using TEGa, the photo-enhancement is more pronounced than that in the case of TMGa.

From the Fig.5.2, we can obtain the threshold laser intensities (I_{th}) for each illumination duration (t). The threshold energy flux, which is the product of I_{th}•t, is plotted in Fig.5.3 as a function of the illumination duration. The approximate upper bound of the LALE laser intensity window is outlined with the dashed line. The point labeled with the closed square is from Meguro *et al.*[13] Similar to the case of using TMGa, the laser intensity and the illumination duration can be varied independently within the area bounded by the solid and the dashed lines to obtain monolayer self limiting growth, except that now the energy flux is an order lower. From the growth point of view, it will be more efficient to deliver the photons at a intense package for a short time.

The reduced thermal enhancement in the case of using TEGa is also evidenced by a more abrupt lateral transition in the thickness cross section profile as is shown in Fig.5.4. Although the laser intensity distribution was not measured, it is not believed to be a step function of distance. The profile exhibits an appreciable shoulder even in the case of using TEGa.

The shoulder in the profile for the stripe grown using TMGa is wider due to a greater degree of laser heating at the higher intensity and the dissipation of the energy via conduction. This result implies that TEGa may be a better choice for LALE in achieving ultimate spatial resolution.

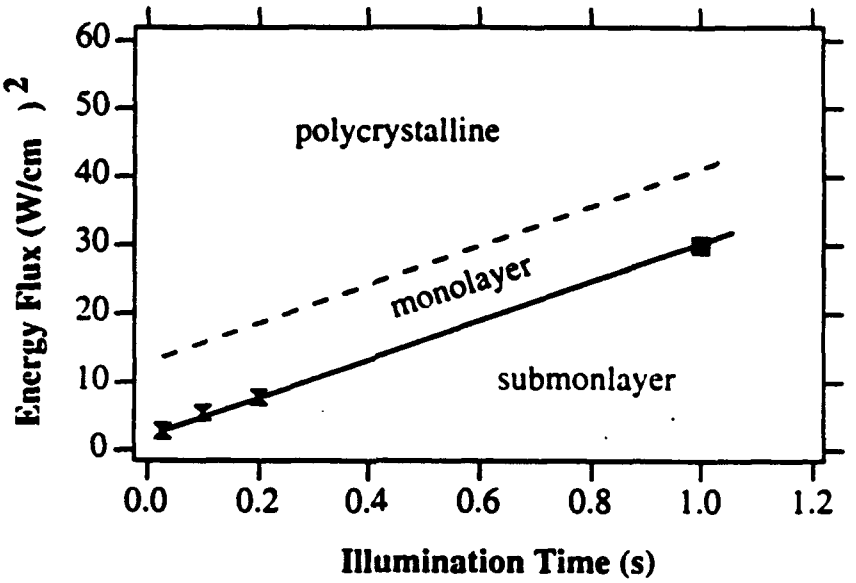

Fig.5.3 Threshold energy flux versus laser illumination time in LALE using TEGa. The point labelled with the square is from Meguro et al. The dashed line defines the approximate upper bound of the LALE intensity window.

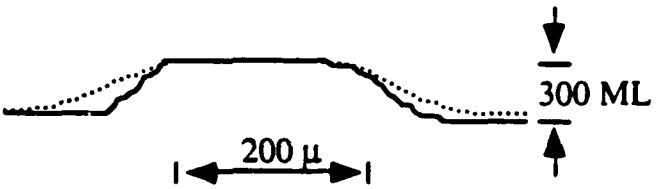

Fig.5.4 Typical thickness profiles of LALE Stripes grown using TEGa, solid line and TMGa, dotted line.

Earlier work in ALE (without laser) using TEGa resulted in no apparent self limiting feature with respect to the increasing TEGa exposure.[14][15] This different behavior displayed by TEGa as compared to TMGa is now believed to be the consequence of the different thermal decomposition mechanisms. In LALE, on the other hand, perfect self limiting is observed for TEGa as is shown in Fig.5.5 where the LALE growth rate is plotted as a function of TEGa injected per cycle with the same TEGa exposure time of 1.5s and laser illumination of 0.1s. Since the

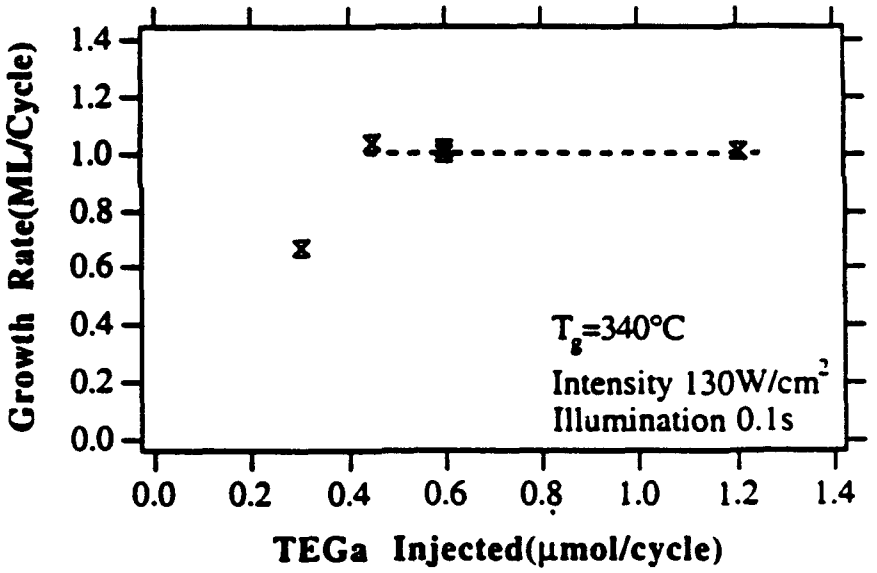

Fig.5.5 Self limiting of LALE growth rate with respect to TEGa exposure.

vapor pressure of TEGa is an order of magnitude lower than that of TMGa, the region of material delivery limited growth is readily observed. This data confirms the result reported by Aoyagi and co-workers.[16] This is also a

strong support to the point of view that LALE growth using TEGa proceeds largely via photo-enhancement (photocatalytic or/and photo chemical effects) instead of local heating.

5.3 GaAs material Quality by LALE Using TEGa

Even grown at temperatures as low as 330 °C, the GaAs material possess a reasonable good quality. Intense room temperature PL response can be obtained from the DH's with the central GaAs grown by LALE using TEGa as is shown by the solid line in Fig.5.6. Typical PL spectra from samples grown using TMGa and AsH_3, dotted line, and TMGa and TBAs, dashed line are also plotted for comparison. The GaAs grown using TEGa generally shows a better PL response than that using TMGa and AsH_3.

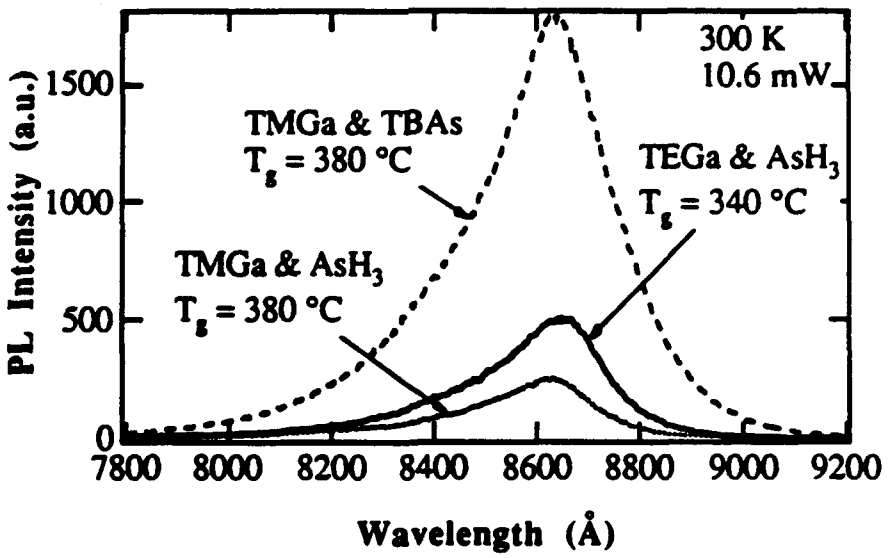

Fig.5.6 PL spectra of DH's with the GaAs region grown by LALE using TEGa and AsH_3 (solid line), TMGa and AsH_3 (dotted line), and TMGa and TBAs (dashed line).

At low temperature (5 K), the PL spectra of GaAs by LALE using TEGa, Fig.5.7, is dominated by an impurity related emission at 1.4826 ev that is at a lower energy (longer wavelength) than the similar peak from samples grown using TMGa and AsH_3. This peak is tentatively assigned as due to the donor-to-acceptor transition (D-A). If carbon were to be identified as the responsible acceptor, which has a level 26.5 mev above the valence band of GaAs, the measured energy position of this peak would require a donor level 10.4 mev below the conduction band using an Eg= 1.5195 ev for GaAs.[17] It is well tabulated that donors in GaAs are mostly shallower than 6 mev. One or more deeper acceptors, such as Cd or Si (34.5 and 35.1 mev above valence band when incorporated as acceptors), is the likely origin of this peak. More work is needed to clarify this issue.

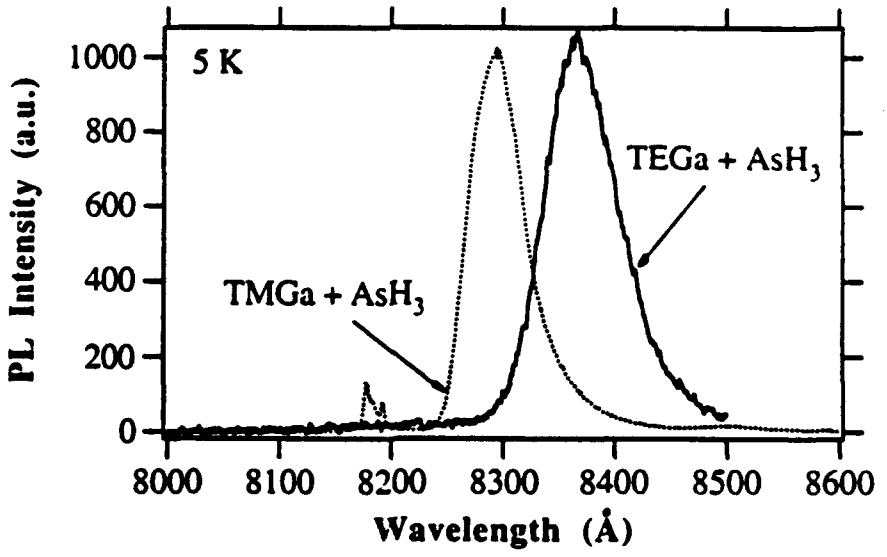

Fig.5.7 Low temperature PL spectra from GaAs grown by LALE using TEGa and AsH_3 (solid line) and TMGa and AsH_3 (dotted line).

Shown in Fig.5.8 is the C-V profile through GaAs layers grown by LALE using TEGa sandwiched by conventional MOCVD $Al_{0.3}Ga_{0.7}As$ cladding layers. The carrier concentration in the GaAs is equal or below the background of the MOCVD $Al_{0.3}Ga_{0.7}As$ layers. The C-V data obtained from the measurement performed directly on thick (0.5 μm) GaAs grown using TEGa is also included. Since the first point exceeds already a distance of 0.5 μm, the GaAs layer is just completely depleted through. From the zero bias capacitance of ~5 pF, we estimated the carrier concentration in the GaAs layer to be $p \leq 4x10^{-15}$ cm^{-3}. This is in sharp contrast to the material grown using TMGa and AsH_3 where $p \geq 2x10^{17}$ cm^{-3} could only be obtained. Our data suggests a greatly reduced total impurity contamination and carbon incorporation in GaAs grown using TEGa. This low doping level is consistent with the excellent Schottky contacts that can be formed

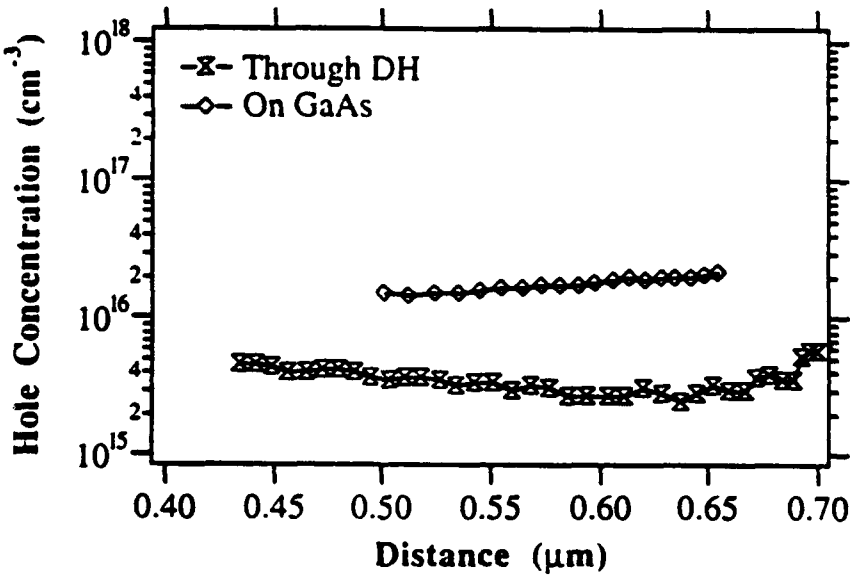

Fig.5.8 CV profiles of GaAs grown by LALE using TEGa and AsH_3.

on top of the GaAs grown using TEGa with a reverse breakdown voltage as high as 20 V.

The direct evidence of carbon reduction comes from our SIMS measurement as has been shown in the Fig.4.5 of Chapter Four. The carbon level in the layer grown using TEGa (layer (I)) was not observed above the background level in the MOCVD $Al_{0.3}Ga_{0.7}As$ layers. On the other hand,an appreciable amount of carbon was detected in the layer grown using TMGa and AsH_3. The growth chemistry is shown to have a great influence on the carbon incorporation in LALE as well as MOCVD. LALE using TEGa is an alternative way of reducing carbon contamination compared to the case of using TBAs where the abundance of AsH_x is believed to saturate and remove the dehydrogenated carbon species.

5.4 The Influence of Growth Parameters on Material Quality

Although the very first DH structure grown by LALE using TEGa had a reasonable PL response, material quality can be further improved by a careful optimization of the growth conditions. Shown in Fig.5.9 is the PL spectra from samples grown at different laser intensities. Both the 76 and 119 W/cm^2 are within the self limiting regime. Other critical parameters are the same, i.e. exposure mode of 1.5-4-4-3 and laser illumination time of 0.1s. The growth at higher intensity is seen to improve the PL efficiency of the DH structure. The additional energy delivered to the surface could, on the one hand, make the reaction more complete that reduces carbon

contamination and, on the other hand, increase the mobility of the surface species to reduce defects.

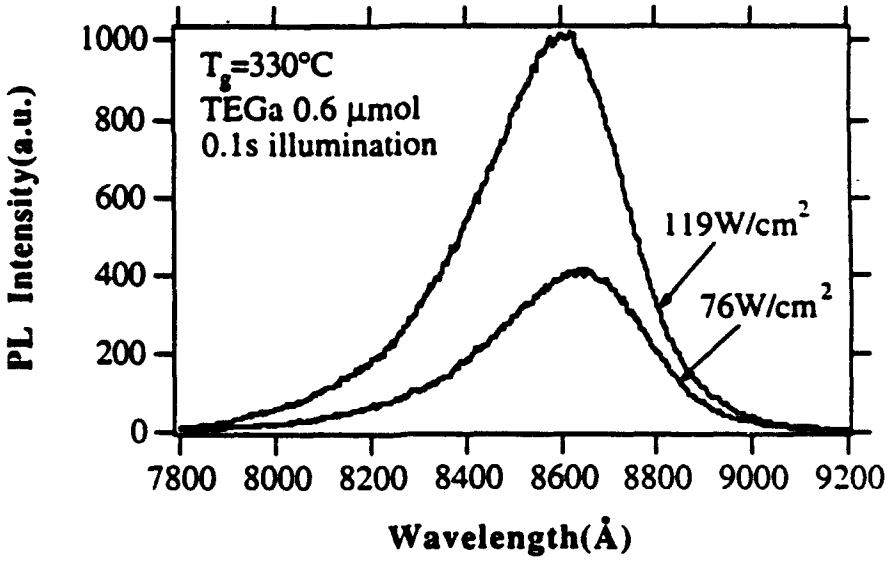

Fig.5.9 The effect of laser intensity on PL efficiency in the case of LALE usingTEGa.

The excess energy can also be supplied in a different manner, i.e. a different mode of illumination. In such an experiment, two laser pulses (0.1s long) of equal intensity are used with a 0.5s time spacing between them so that both pulses are still overlapping with the TEGa exposure. The 0.5s time spacing is long enough compared to the thermal transient phenomenon in most semiconductors and to the desorption time constants of most species in the TEGa+AsH_3+H_2 on GaAs system. From the growth point of view, the use of two 0.1s pulses should be different from the use of one pulse of 0.2s at the same intensity since additional time is available in the first case for the reaction by-products to desorb, which reduces the interception of photons by the reaction by-products. Interestingly, the

growth result showed that the second laser pulse did not increase the thickness above 1 ML/cycle, manifesting the strong self limiting mechanism that is operative. The PL efficiency of the GaAs is, however, improved with the use of two pulses as is shown in the Fig.5.10. In the case of using TEGa for LALE growth, the substrate bias temperature has to be so low as to became a limiting factor for the improvement of the material quality. Additional energy input without losing the self limiting growth is one approach to material optimization.

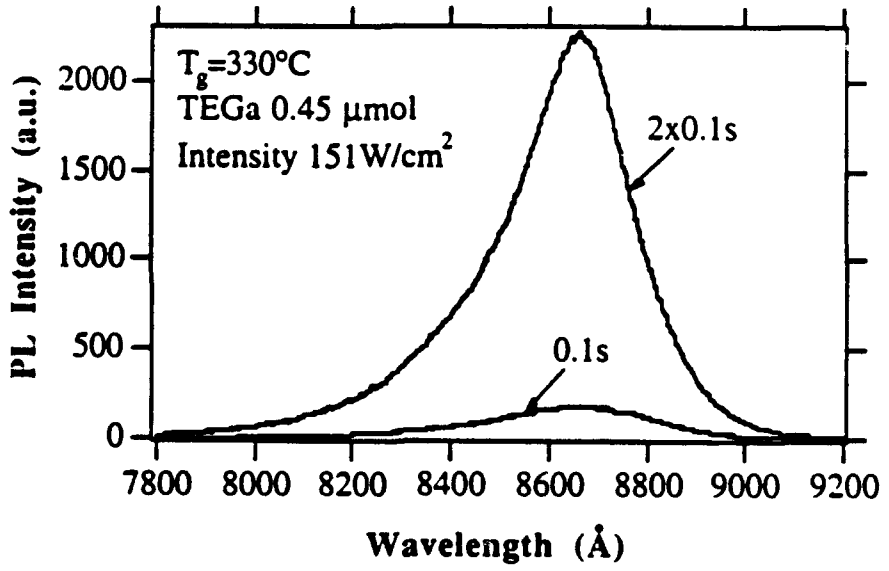

Fig.5.10 The effect of modes of illumination on PL efficiency

The PL spectra from DH's grown at different TEGa mole fraction are shown in Fig.5.11. GaAs material of better PL efficiency is obtained with less TEGa exposure. Although TEGa is expected to be less likely a source of carbon as is TMGa, increased exposure to TEGa will increase the surface population by species of relatively long resident time. A crowded surface

condition leads to reduced surface mobility necessary for perfect step flow as was observed in MBE.[18][19] More defects will be expected in the material. In addition, extreme over-exposure to TEGa ultimately leads to excess Ga formation on the surface. All these excess Ga atoms will incorporate in the film because of the low vapor pressure of Ga at the growth temperature. The stoichiometry and the crystallinity of the epitaxial film is adversely affected by extreme over-exposure.

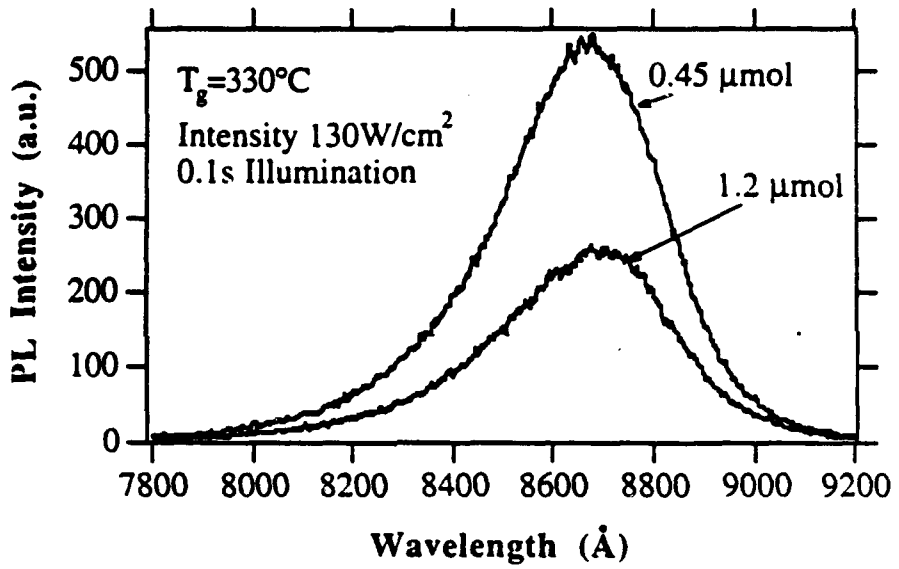

Fig.5.11 The effect of TEGa exposure on PL efficiency.

5.5 Summary and Conclusion

TEGa has been used in LALE growth of GaAs. Much lower laser intensity is required to deposit GaAs at 1 ML/cycle as compared to the case of using TMGa. Perfect self limiting is observable with respect to the TEGa exposure as compared to the result of ALE operation using TEGa without

laser. As a result of the perfect self limiting growth feature, LALE using TEGa exhibits a more desirable growth profile for improved spatial resolution. The perfect self limiting feature is explained as the increased photo-enhancement relative to local heating by the laser in the case of using TEGa. PL, C-V, and SIMS measurement techniques are used for the first time to characterize GaAs grown by LALE using TEGa. Intense room temperature PL responses from DH's with the central GaAs grown by LALE suggest good material and interface quality. Reduced impurity levels and carbon contamination are also observed compared to the material grown using TMGa and AsH_3. Based on our study of the influence of growth parameters on the material quality, GaAs material of better optical quality can be obtained with reasonably low TEGa exposure and with intense laser illumination. The use of long pulse duration or multiple pulses also improves the crystal quality.

GaAs grown by LALE using TEGa and AsH_3 has also been incorporated in a GRIN-SCH single QW laser structure. The device quality of the material is demonstrated for the first time with a threshold current density as low as 544 A/cm^2 (cavity length 570 μm) under pulsed testing condition at 10 kHz repetition rate. More details in the device application of LALE can be found in Chapter Seven.

References for Chapter Five

[1] T.F.Kuech, E.Veuhoff, T.S.Kuan, V.Deline, and R.Potemski, "The Influence of Growth Chemistry on the MOVPE Growth of GaAs and $Al_xGa_{1-x}As$ Layers and Heterostructures,' J. Cryst. Growth, Vol.77, 257(1986).

[2] E.Tokumitsu, Y.Kudou, M.Konagai, and K.Takahashi, Jpn. J. Appl. Phys., Vol.24, 1189(1985).

[3] N.Pütz, H.Heinecke, M.Heyen, and P.Balk, "A Comparative Study of $Ga(CH_3)_3$ and $Ga(C_2H_5)_3$ in the MOMBE of GaAs," J. Cryst. Growth, Vol.74, 1292(1986).

[4] K.Kimura, S.Horiguchi, K.Kamon, M.Mashita, M.Mihara, and M.Ishii, "Molecular Beam Epitaxy Growth of GaAs Using Triethylgallium and As_4," Jpn. J. Appl. Phys., Vol.26(3), 419(1987).

[5] M.Konagai, T.Yamada, T.Akatsuka, K.Saito, E.Tokumitsu, "Metallic p-Type GaAs and GaAlAs Grown by Metalorganic Molecular Beam Epitaxy," J. Cryst. Growth, Vol.98, 167(1989).

[6] D.M.Kozuch, M.Stavolar, S.J.Pearton, C.R.Abernathy, and J.Lopata, "Hydrogen in Carbon-Doped GaAs Grown by Metalorganic Molecular Beam Epitaxy," Appl. Phys. Lett., Vol.57(24), 2561(1990).

[7] J.O.Williams, R.Hoare, N.Hunt, and J.Parrott in "Mechanisms of Reactions of Organometallic Compounds with Surfaces," Eds., D.J.Cole-Hamilton and J.O.Williams, NATO ASI Series B: Physics, Vol.198, (Plenum Press, 1989), p131.

[8] M.Yoshida, H.Watanabe, and A.Uesugi, "Mass Spectrometric Study of $Ga(CH_3)_3$ and $Ga(C_2H_5)_3$ Decomposition Reaction in H_2 and N_2," J. Electrochem. Soc., Vol.132(3), 677(1985).

[9] M.Mashita, S.Horiguchi, M.Shimazu, K.Kamon, M.Mohara, and M.Ishii, "The Pyrolysis Temperature of Triethylgallium in the Presence of Arsine or Trimethylaluminum," J. Cryst. Growth, Vol.77, 194(1986).

[10] P.W.Lee, T.R.Omstead, D.R.Mckenna, and K.F.Jensen, "In Situ Mass Spectroscopy and Thermogravimetric Studies of GaAs MOCVD Gas Phase and Surface Reactions," J. Cryst. Growth, Vol.85, 165(1987).

[11] M.Tsuda, S.Oikawa, M.Morishita, and M.Mashita, "On the Reaction Mechanism of Pyrolysis of TMG and TEG in MOCVD Growth Reactors," Jpn. J. Appl. Phys., Vol.26(5), L564, (1987).

[12] H.Itoh, M.Watanabe, S.Muka, and H.Yajima, "Ultraviolet Absorption Spectra of Metalorganic Molecules Diluted in Hydrogen Gas," J. Cryst. Growth, Vol.93, 165(1988).

[13] T.Meguro and Y.Aoyagi, in "Atomic Layer Growth and Processing," Mat. Res. Soc. Symp. Proc., Vo222, Eds., T.F.Kuech, P.D.Daphus, and Y.Aoyagi, (MRS, Pittsburgh, PA, 1991), p121.

[14] M.Ozeki, K.Mochizuki, N.Ohtsuka, and K.Kodama, "Growth of GaAs and AlAs Thin Films by A New Atomic Layer Epitaxy Technique," Thin Solid Films, Vol.174, 63(1989).

[15] Y.Sakuma, K.Kodama, and M.Ozeki, "Atomic Layer Epitaxy of GaP and Elucidation for Self-Limiting Mechanism," Appl. Phys. Lett., Vol.56(9), 827(1990).

[16] Y.Aoyagi, A.Doi, and S.Iwai, and S.Namba, "Atomic-Layer Growth of GaAs by Modulated-Continuous-Wave Laser Metalorganic Vapor-Phase Epitaxy," J. Vac. Sci. Technol., B5(5), 1460(1987).

[17] M.Ozeki, K.Nakai, K.Dazai, and O.Ryuzan, "Photoluminescence Study of Carbon Doped Gallium Arsenide," Jpn. J. Appl. Phys., Vol.13(7). 1121(1974).

[18] K.Kanisawa, J.Osaka, S.Hirono, and N.Inoue, "Al-Ga Monolayer Lateral Growth Observed by Scanning Electron Microscopy," Appl. Phys. Lett., Vol.58(21), 2363(1991).

[19] T.Nishinaga, T.Shitara, K.Mochizuki, and K.I.Cho, "Surface Diffusion and Related Phenomena in MBE Growth of III-V Compounds," J. Cryst. Growth, Vol.99, 482(1990).

CHAPTER SIX

Theoretical Aspect of Laser Assisted Deposition and A Modeling of ALE and Related Growth

The experiments on laser assisted CVD can be divided into two major categories. Among the first category are those in which the precursors have no appreciable absorption of the light. Therefore, a non-parallel incidence has to be adopted and the deposited material or the substrate has to be highly absorbing. In the second category are those in which the photons used are appreciably absorbed by the precursors. In this case, the absorption of the light by the substrate is not required and a parallel incidence may be used. The use of parallel incidence then separates the contribution from the gas phase photochemical reaction. This is not so simple in the first category of experiments to which LALE also belongs. First, laser induced local heating can give rise to enhanced chemical reaction rates thus contributing to growth through thermal effects. Second, the electronic states of the solid surface may be so altered by a laser beam of suitable energy that the area illuminated by the laser becomes an efficient catalyst, contributing to the growth enhancement by a photocatalytic effect. Third, the molecular orbital of a TMGa molecule is modified while approaching the surface. Direct photolysis of such molecules by the impinging photons is also possible via single or multiphoton processes, which may be termed as a surface photochemical

effect. These effects are so tangled that a separate study of one of the effects is difficult.

Laser CVD of Ni from $Ni(CO)_4$ has been modeled by considering the thermal effect alone,[1][2] whereby the reactant diffuses towards the surface heated by the laser beam, leaving behind a metallic deposit. While this modeling can reproduce certain observed growth behaviors in laser CVD, it is not applicable to LALE. Experimental evidence in LALE indicates increased contribution from the combined photo-enhancement due to photocatalytic and surface photochemical effects. A reasonable theory for LALE could only be established after the direct experimental measurement of the temperature profiles and in situ identification of surface species before and after laser illumination. While these are still lacking, we shall, in this chapter, concern ourselves mainly to an assessment of the role of laser illumination in LALE. To do so, we shall first carry out a calculation of the heating of semiconductor substrates by laser illumination to get a feel of the magnitude of the heating effect and the time dependence of this heating. We shall then develop a quantitative model for ALE growth. Thus, the thermal enhancement effect in LALE can be estimated. The issues of spatial resolution and area deposition selectivity can then be discussed.

6.1 Laser-Solid Surface Interaction

The effects of high power laser beam irradiation on solids have been the subject of many publications, including a comprehensive book by

Ready.[3] The observable phenomena during laser light and solid interaction depend on the intensity and the wavelength of the laser beam, the property of the solid, and the preparation of the surface. Part of the energy carried by the beam is transferred into the solid through absorption within a characteristic distance δ_a (absorption depth) determined by the optical property of the solid. The absorption depth is generally estimated to be α^{-1}, where the α is the absorption coefficient. In a good conductor, it is more suitable to identify the δ_a with the penetration depth of electromagnetic wave in conductors. A major part of this absorbed energy is converted into heat so that the surface is selectively heated.

For a semiconductor, because of the low intrinsic carrier density, illumination with a light beam of photon energy greater than the energy of the band gap will alter appreciably the electronic states near the surface. Such a change in the surface electronic states due to light illumination has been shown to have an effect on enhancing either the adsorption or desorption of a gas on a semiconductor surface, depending on the nature of the gas and the semiconductor.[4] The effectiveness of light in changing the surface electronic states was also explored theoretically.[5] In the present system consisting of laser light of λ = 514.5 nm, GaAs substrates, and TMGa vapor in H_2, there is still a lack of experimental observations which allows an assessment of the contribution of this effect in LALE. We shall then be concerned primarily with the thermal effect of laser illumination on a single crystalline semiconductor solid.

6.1.1 Optical and Thermal Properties of Semiconductors

The transfer and dissipation of energy from the laser beam into a solid depends strongly on such material parameters as the reflectivity R and absorption coefficient. The local temperature rise is a measure of the energy stored in a unit mass of material of a given thermal capacity, C_p. The faster the absorbed energy can be carried away by, e.g. conduction (characterized by conductivity κ or thermal diffusivity D_T), the less will be the local temperature increase. As we shall use these parameters in a calculation of local temperature rise, it is worth while to gather them together and save the source of origin for future use. In general, for pure semiconductors, the data are mostly from the experimental values. For alloy semiconductors, not all compositions have studied by experiments and an extrapolation scheme is frequently used to estimated the properties of an alloy based on the properties of the constituent pure materials. In addition, all the material parameters used here are functions of temperature. Even though our goal is to calculate the linear temperature rise, it is more realistic to use, wherever possible, the values of these parameters at the bias temperature of the LALE growth (380 °C in our case).

Of first concern is the reflectivity of the surface, R, which predicts the percentage of the incident laser power being reflected without contributing to the heating. Aspnes *et al.* have measured the optical constants of GaAs and $Al_xGa_{1-x}As$ (x in 0.1 interval) at room temperature for photon energy 1.5 – 6 ev using spectroellipsometry.[6] The reflectivity at hv = 2.4 ev are 0.382 and 0.356 for GaAs and $Al_{0.315}Ga_{0.685}As$

respectively. In order to estimate the corresponding values that can be used at 380 °C, we recall that the reflectivity is related to the refractive index and the extinction factor k by the Fresnel expression at normal incidence from air to a semiconductor of n and k:

$$R = \frac{(n-1)^2 + k^2}{(n+1)^2 + k^2} \qquad (6\text{-}1).$$

From the theory of dielectric response of semiconductor to light,[7]-[10] the temperature dependence of n and k is through the changes in the energies of the critical points involved in the optical process. This change of critical point energies with temperature is in the order of 10^{-4} ev/K out of a few electron volts of the initial values. The change in n with temperature for GaAs is experimentally verified to be small, i.e. $\delta n \approx 4 \times 10^{-4} \Delta T$.[11] The use of the room temperature R values will not introduce a great error.

The measured absorption coefficients at $\lambda \sim 5145$ Å for GaAs and $Al_{0.315}Ga_{0.685}As$ were reported to be 9×10^4 and 6.2×10^4 cm^{-1}.[6] The absorption depth will be in the order of 1×10^{-5} cm. This dimension is much smaller than the dimensions of the substrate. An infinite boundary condition can be used.

Under a given absorbed laser power, local heating is mainly determined by the thermal conductivity κ and the heat capacity C_p because radiative heat loss is relatively small for the temperature rise corresponding to the LALE condition. The thermal conductivity for GaAs and AlAs at room temperature are 0.44 W/cmK[12] and 0.8 W/cmK.[12][13] The κ for

$Al_{0.3}G_{0.7}As$ at 300 K taken from Afromowitz[13] is 0.13 W/cmK. For non-degenerate semiconductors, the major contribution to thermal conduction is from the phonons. Near and above room temperature, the thermal conductivity varies as ~ 1/T. Nissim *et al.*[14] fitted the κ data for GaAs given in the Ref[12] with a function as $\kappa(T) = 91/(T-91)$ (W/cmK), where the T is in unit of Kelvin. This gives κ(380 °C) for GaAs as 0.16 W/cmK. There is no enough data available for a similar fit for AlGaAs. We shall still use the room temperature value for this quantity.

The thermal capacity can be obtained from ρc where the ρ is the density (g/cm^3) and c the specific heat (J/gK) for the material. The room temperature ρ and c for $Al_xGa_{1-x}As$ is obtained by linear extrapolation[15] to be $\rho(x) = 5.36 - 1.6x$ and $c(x) = 4.1855(0.08 + 0.03x)$. From these expressions, we find the values for GaAs and $Al_{0.3}Ga_{0.7}As$, i.e. $\rho(0) = 5.36$ g/cm^3, $\rho(0.3) = 4.88$ g/cm^3, $c(0) = 0.335$ J/gK, and $c(0.3) = 0.373$ J/gK. We shall use these values for the 380 °C case. Thus C_p values are 1.80 J/cm^{3}K for GaAs and 1.82 J/cm^{3}K for $Al_{0.3}Ga_{0.7}As$. A mathematically more convenient quantity is the thermal diffusivity $D_T = \kappa/C_p$, which has the dimension of length^2/time. The thermal diffusivities are 0.089 cm^2/s for GaAs at 380 °C and 0.071 cm^2/s for $Al_{0.3}Ga_{0.7}As$.

6.1.2 The Formulation and Solution of Thermal Diffusion Equation

If the dissipation of heat is dominated by conduction, which is true in our heating temperature range, the temperature distribution at any give instance (T(x,y,z,t)) is governed by the equation

$$\frac{\partial T}{\partial t} - D_T \nabla^2 T = \frac{Q}{C_p} \qquad (6\text{-}2),$$

where the Q is the strength of a heat source within the boundary under consideration and the D_T and C_p are assumed constant with respect to temperature. We consider a laser beam of radius r_0 illuminating normally on a semiconductor surface, see Fig.6.1. The intensity distribution is of

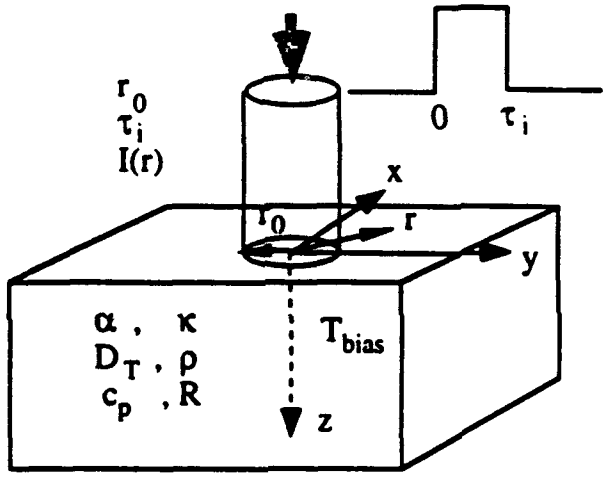

Fig.6.1 The interaction of a laser beam and a solid.

Gaussian form and the heat source strength function is then

$$Q = \frac{P(1-R)}{2\pi r_0^2} \exp\left(-\frac{x^2 + y^2}{2r_0^2}\right) f(z) \qquad (6\text{-}3),$$

where the P is the total power of the beam and the $f(z)$ is the z dependence of the absorbed intensity. Note here we have adopted the Gaussian form used by Anthony and Cline.[16] The source exists only between t=0 and τ_i since the beam is chopped on and off. Because the dimensions of the beam and its absorption depth are much smaller than the corresponding dimensions of the substrate, the problem is one of semi-infinite boundary. Following Carslaw and Jaeger,[17] the eqn.(6-2) without the source term (the right hand side set to zero) is satisfied by

$$v = \frac{Q}{8(\pi D_T t)^{3/2}} \exp\{-[(x-x')^2 + (y-y')^2 + (z-z')^2]\} \qquad (6\text{-}4),$$

which is regarded as the temperature in an infinite solid due to a quantity of heat QC_p instantaneously liberated at t=0 at a point (x',y',z'). When the source with a finite spatial extension is turned on at t=0 and off at $t=\tau_i$, the temperature rise observed at $t=\tau_i$ when the laser beam is just chopped off is

$$T_r = \int_0^{\tau_i} \int_{-\infty}^{\infty} \int_{-\infty}^{\infty} \int_{-\infty}^{\infty} \frac{Q(x',y',z',t')}{C_p} \times$$

$$\frac{\exp\left\{-\left[(x-x')^2 + (y-y')^2 + (z-z')^2\right]\right\}}{8\left[\pi D_T(\tau_i - t')\right]^{3/2}} dx'dy'dz'dt' \qquad (6\text{-}5).$$

The small absorption depth allows us to use for the $f(z)$ a $\delta(z')$ function. The integrations over x' and y' have known Gaussian forms. The final expression for the temperature rise is

$$T_r(x,y,z,\tau_i) = \frac{P}{\pi r_0^2}\frac{1-R}{C_p\sqrt{\pi D_T}}\times$$

$$\int_0^{\tau_i} \frac{\exp\left\{-\left[\frac{x^2+y^2}{2r_0^2+4D_T t''}+\frac{z^2}{4D_T t''}\right]\right\}}{\sqrt{t''}\left(2+\frac{4D_T t''}{r_0^2}\right)}dt'' \qquad (6\text{-}6).$$

Because of the cylindrical symmetry of the problem, we shall refer to the T_r as $T_r(r,z,t)$ hereafter.

6.1.3 Numerical Calculation and discussions

In LALE with a switched flow system, we shall be interested in the surface temperature distribution, $T_r(r,0,\tau_i)$ at the end of a given illumination. We are first concerned with the time scale at which the heating reaches an approximate steady state. For the thermal properties of GaAs given in section 6.1.1, the laser heating transient behavior is shown in Fig.6.2, where the calculated linear temperature rise, observed at the end of illumination, on surface and at the center of the beam ($T_r(0,0,\tau_i)$ is plotted as a function of the illumination time for a laser intensity of 1kW/cm^2. The initial increase of surface temperature takes a very short time. In this example, it takes ~2×10^{-2} s to reach an approximate steady state. This time is shorter than the laser pulse duration used in our LALE. We can speak of a fairly well defined temperature during the pulse. The major physical differences between short and long illumination time under the same laser intensity are the increased photon irradiation and a longer time at locally elevated

temperature for the latter. These will promote more complete decomposition of TMGa and perfect crystal growth. An improvement in the PL efficient is then observed for GaAs grown at longer illumination time.

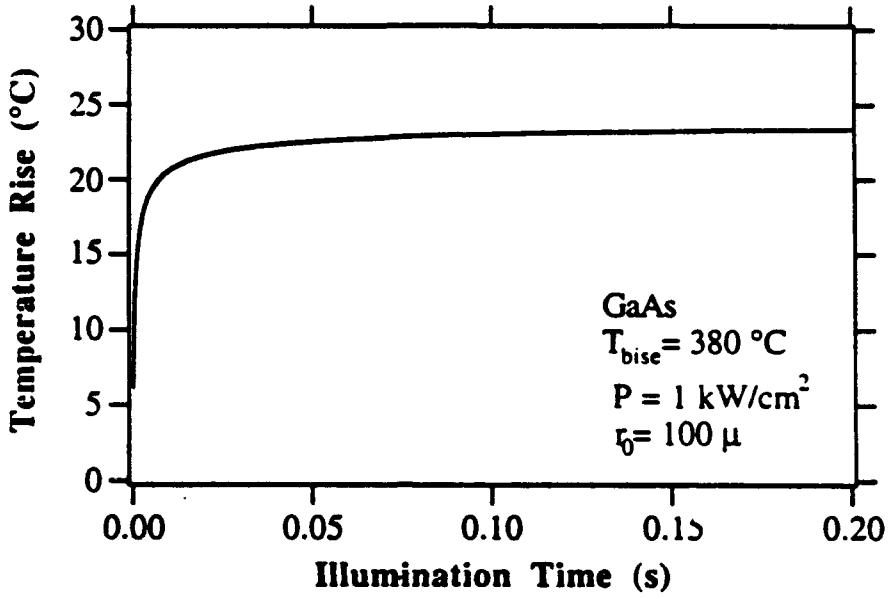

Fig.6.2 The maximum linear temperature rise as a function of laser illumination time. Notice that the time for the surface temperature to reach approximate steady state is short.

The use of long illumination time does however cause an increased over-all heating as is shown in Fig.6.3 by the distributions of surface temperature rise under 1 kW/cm^2 laser intensity for illumination time of 0.01, 0.1, and 1s. The temperatures in the area that is not illuminated by the laser is raised by about 5 °C for 1s of illumination. This is not desirable for the selectivity of the selective area growth as more deposit will occur in the non-illuminated area. One of the solutions is to reduce the bias temperature while using long illumination time. This certainly has its limits, as the

activity and thus, the efficiency of the group V source will be reduced at lower temperature.

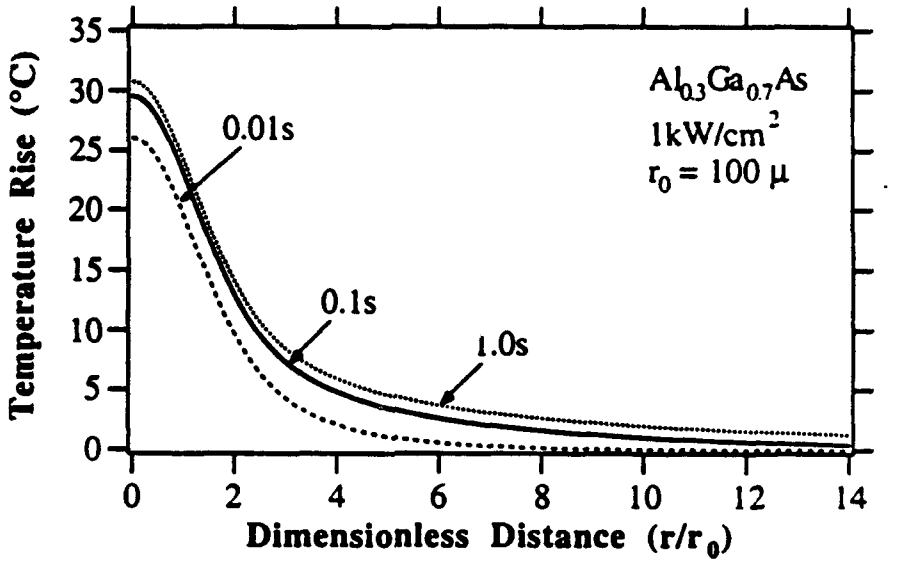

Fig.6.3 The calculated temperature rise distribution under 1kW/cm^2 illumination with a Gaussian beam radius of 100 μm for different time duration: the dashed line, 0.01s, solid line, 0.1s, and dotted line, 1.0s.

Shown in Fig.6.4 is the calculated temperature distribution under a given expected energy fluence (100 J/cm^2 per cycle) at several different delivery modes, namely, 10 kW/cm^2 for 0.01s (dotted line), 1kW/cm^2 for 0.1s (solid line), and 100 W/cm^2 for 1s (dashed line). The temperature rise is the most sensitive to the laser intensity. At 100 W/cm^2, the temperature rise is negligible. For a pure photochemical reaction proceeding via single photon events, the deposit per cycle is expected to be in direct proportion to the flux of the photons carried by the beam (photons/cm^2 per cycle). We

have seen in Chapter Three that the required energy flux for achieving monolayer growth is not a constant for different illumination duration. This suggests that the process responsible for LALE growth is not a pure photochemical reaction via single photon events. On the other hand, LALE using TEGa can generally be achieved with laser intensity below ~100 W/cm^2 for an illumination duration of 0.1s. The relative importance of heating is greatly reduced in this case.

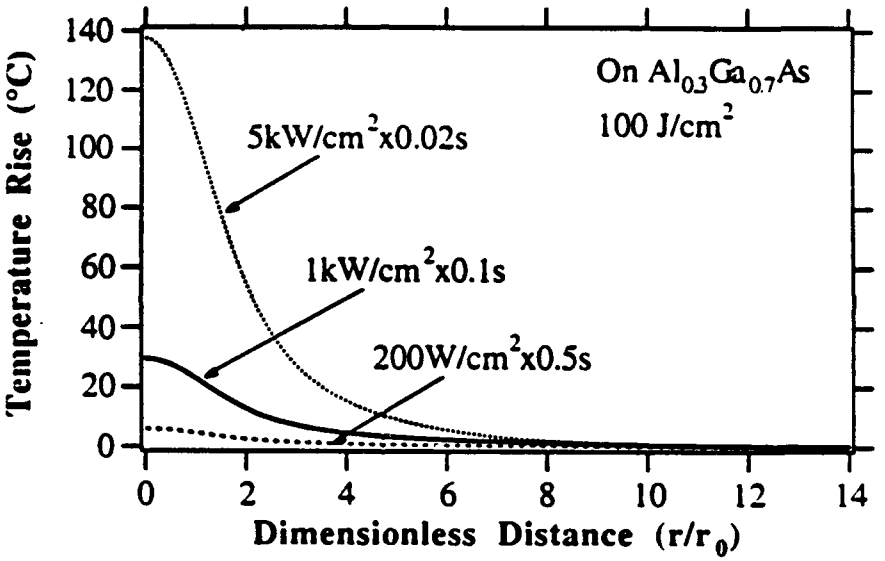

Fig.6.4 The distribution of temperature rise under 100 J/cm^2 of energy fluence at different delivery modes: the solid line, 1kW/cm^2 for 0.1s, dotted line, 5kW/cm^2 for 0.02s, and dashed line, 200 W/cm^2 for 0.5s.

From this calculation, we can appreciate a general feature of the temperature profiles resulting from heating by a laser beam of Gaussian intensity distribution, i.e. the abruptness of the lateral distribution is

scalable with the beam radius r_0. The actual dimension of the shoulder in the thickness profile will be smaller when the beam is focused tighter.

6.2 A Site Selective Reactivity Model of ALE

With the knowledge of surface temperature distribution, it is possible in principle to estimated the thermal contribution in LALE by calculating the local ALE growth rate as a function of temperature. This task will be carried out in this section.

6.2.1 The Physical Picture of ALE

The schematic representation of the current model is depicted in Fig.6.5. Consider a GaAs substrate maintained at temperature T and with its (100) surface (a polar surface) exposed to a gas stream containing TMGa of concentration C from t=0 to $t=t_e$. The time of injection in this case is identical to the time of reaction. The TMGa molecules will be supplied at a rate τ_s^{-1}, where the material arrival time constant τ_s is in the order of 10^{-4}s from a molecular dynamics calculation. The majority of the impacts are not fruitful and the molecules leave the surface within the desorption time constant τ_{ds}, which is in the order of 10^{-2}s in this case. The impact of TMGa molecules at a surface As site may result in decomposition at a rate τ_{As}^{-1} and that at a Ga site at a rate τ_{Ga}^{-1}. At any given instance, the TMGa and Ga atoms left on the surface is termed their coverage θ_{TMGa} and θ_{Ga} (in ML when scaled with the surface site density). The rate equations governing the processes can be written as

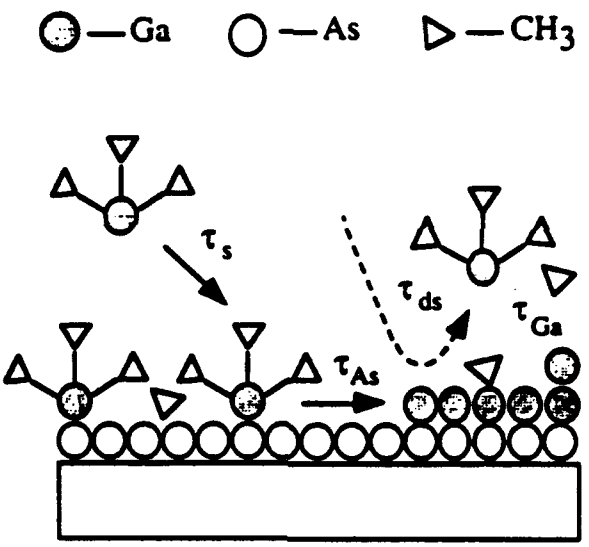

Fig.6.5 A site -selective reactivity model of ALE.

$$\frac{d\theta_{TMGa}}{dt} = \frac{(1-\theta_{TMGa})}{\tau_s} - \frac{\theta_{TMGa}}{\tau_{ds}} - \frac{\theta_{TMGa}}{\tau_{dcp}} \qquad (6\text{-}7),$$

$$\frac{d\theta_{Ga}}{dt} = \frac{\theta_{TMGa}}{\tau_{dcp}} \qquad (6\text{-}8),$$

with

$$\frac{1}{\tau_{dcp}} = \frac{S}{\tau_{Ga}} + \frac{(1-S)}{\tau_{As}} \qquad (6\text{-}9).$$

The S may be interpreted as the probability with which an impacting TMGa molecule finds itself at a Ga site. Apparently,

$$S = \begin{cases} \theta_{Ga} & \text{for } \theta_{Ga} < 1 \\ 1 & \text{for } \theta_{Ga} \geq 1 \end{cases} \qquad (6\text{-}10).$$

The initial conditions are

$$\theta_{TMGa}(0) = 0, \text{ and } \theta_{Ga}(0) = 0 \qquad (6\text{-}11).$$

One assumption tacitly used in the above formulation is that double layer adsorption of TMGa on a site that is engaged with another TMGa molecule is excluded by the term of the form $(1-\theta_{TMGa})$ in eqn.(6-6). By considering only the decomposition of TMGa, we actually assume also that all Ga atoms on the surface will eventually react with As during the subsequent exposure cycle to formed GaAs. The decomposition of TMGa in the gas phase can add a component to the ALE growth rate (in ML/cycle), which can be treated separately and is not included here.

6.2.2 Kinetics Parameters

The kinetics parameters that are used in the numerical simulation are the following:

$$\tau_{As}^{-1} = 5\text{x}10^{13} \exp(-\frac{42000}{RT}) \qquad (6\text{-}12),$$

$$\tau_{Ga}^{-1} = 5\text{x}10^{13} \exp(-\frac{51000}{RT}) \qquad (6\text{-}13),$$

and $\tau_{ds} = 5x10^{-2}$ s. The τ_s (in s) is related to the partial pressure of TMGa by

$$\tau_s = \frac{n_s\sqrt{MT_v}}{3.52x10^{22}P} \qquad (6\text{-}14),$$

where $n_s(1/cm^2)$ is the surface site density, M the molecular weight of TMGa, T_v the absolute temperature in the gas phase, and P (in mmHg) the partial pressure of TMGa in the gas stream. Since there is only one rate limiting step in TMGa decomposition, it can be treated as pseudo first order reaction with rate constants expressed as in the eqns.(6-12) and (6-13). The 42 kca/mol of activation energy is according to the experiment value of Ozeki *et al.*[18] The value of 51 kcal/mole of activation energy for TMGa at a Ga site is comparable to our previous result of TMGa decomposition in H_2 (Chapter Two).

6.2.3 Numerical Simulation and Implications

When $\theta_{Ga} < 1$, the eqns.(6-11) and (6-12) are coupled through the Ga coverage dependent τ_{dcp}. A numerical calculation has to be performed. Shown in Fig.6.6 are the simulated ALE growth rate as a function of TMGa flow rate for three substrate temperatures at an exposure time of 1s. Under a suitable temperature, 480 °C indicated by the solid line, a regime appears where ALE growth rate is saturated at one ML per cycle for further TMGa exposure. This agrees qualitative well with the experiment observation (cf. Fig.1.7 in Chapter One). At lower temperature, when the reaction time constant is much longer than the exposure time, the growth rate levels at

submonolayer per cycle. This is also experimentally observed.[19] At higher temperature, the dotted line, lack of self limiting with respect to TMGa flow rate is apparent even without including the gas phase contribution, in agreement with the results from ALE performed in vacuum.[20] With the gas phase contribution, the deviation from ML/cycle will progress faster as TMGa exposure increases. The regime of self limiting ALE growth becomes very narrow at high temperature.

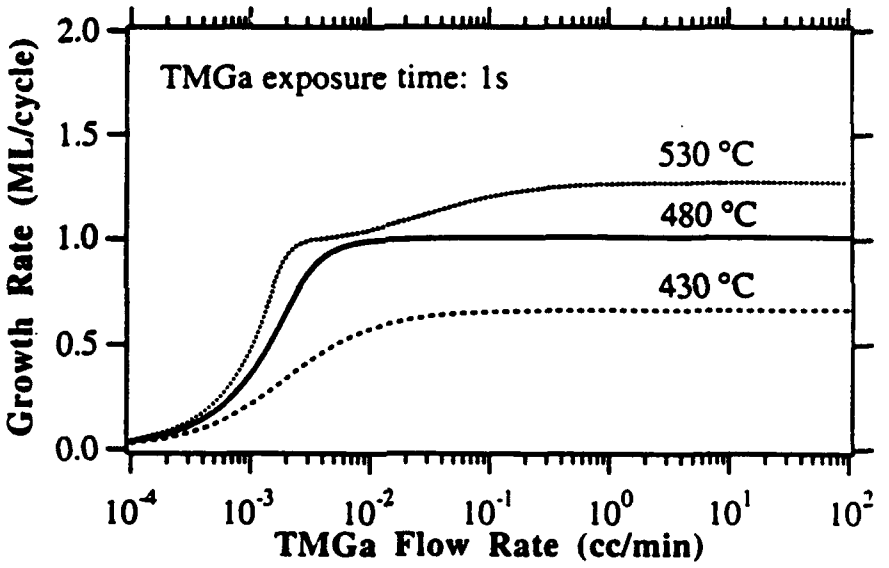

Fig.6.6 Simulated ALE growth rate as a function of TMGa flow rate at TMGa exposure time of 1.0s and growth temperatures of 430 (dashed), 480(solid), and 530 °C (dotted).

Temperature and TMGa exposure time are the most important control parameters in ALE growth. The simulated growth rate as a function of temperature is shown in Fig.6.7 for exposure time of 0.2s (dotted line),

1s (solid line), and 5s (dashed line). While varying the exposure time, the TMGa injection of 0.46 μmol/cycle is kept constant and the TMGa flow adjusted accordingly. First of all, the simulation reproduces the general ALE behavior reported in the literature with the only exception being the results observed with the pulsed-jet reactor,[18] where the growth was observed to remain at ML/cycle and even drop slightly at higher temperature. The difficult in determining a consistent true surface temperature under a high flow jet expanding from a nozzle may be one of the cause for this difference. The current model predicts the loss of self limiting growth at high temperature without resorting to the gas phase decomposition of TMGa. It can be used to explain the ALE growth results obtained in vacuum. The inclusion of gas phase decomposition will, of course, reduce the temperature at which the loss of self limiting occurs.

As we have pointed out in Chapter One, the quantity of TMGa injected per cycle is not a good and independent parameter to describe ALE growth behavior unless the time of exposure is specifically the same. Mathematically, the variables of time and the TMGa concentration are not symmetric. Growth is more sensitive to the time allowed for the reaction as long as more than a monolayer equivalent of source material is supplied. From the Fig.6.7, we see also that the curves of growth rate versus T shift towards higher temperature as the exposure time is reduced. This shows why potentially ALE may be carried out at rather high temperature if the exposure is controlled well with a short duration, e.g. 0.2s at 600 °C. A true short exposure requires an abrupt gas phase transient between exposure cycles. For a given reactor design, over exposure by TMGa (i.e. with high

TMGa concentration) actually tends to give a longer exposure time due to the adsorption-desorption inside the gas handling system. The attempts to grow at high temperatures often met with rather narrow range of self limiting with respect to TMGa flux.[21] This behavior defeats partially the one of the most important advantages offered by ALE – no accurate control of input TMGa is necessary.

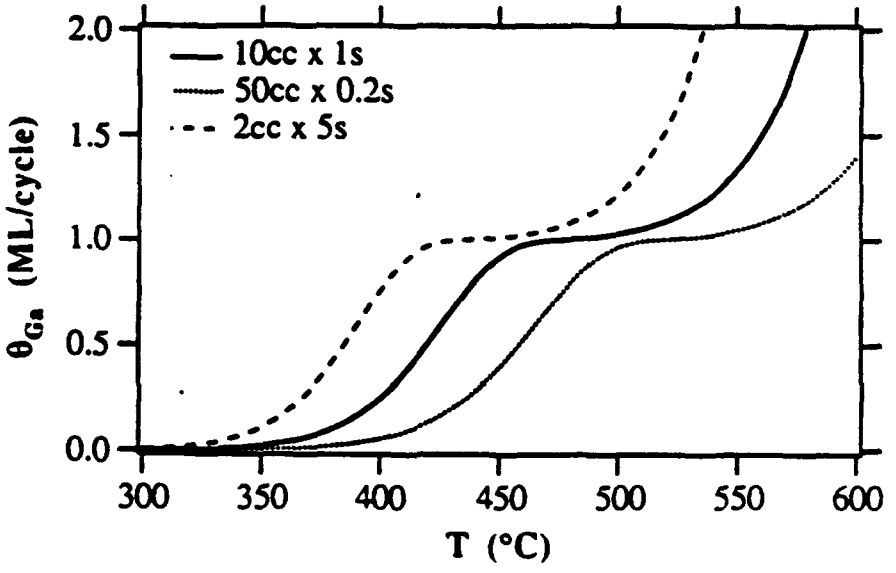

Fig.6.7 Simulated ALE growth rate as a function of substrate temperature under 0.46 μmol/cycle of TMGa exposure with different exposure modes: 50 cc/min TMGa for 0.2s (dotted line), 10 cc/min for 1s (solid line), and 2cc/min for 5s (dashed line).

The position of the curves in Fig.6.7 is not very sensitive to the value of τ_{ds} as long as the $\tau_{ds} >> \tau_s$. This is usually true because ALE is more than often carried out in TMGa flux above the material supply limited

regime. Although we have used estimated pre-exponential factors in the τ_{As}^{-1} and τ_{Ga}^{-1} expressions because they are more prone to experimental error, the quantitative agreement of the simulation and the reported growth results are reasonable. This is judged from a comparison between the inflexion point at ML on the curves shown in the Fig.6.7 and the reported growth data at 1 ML/cycle with specified growth temperature and exposure time, specifically, the monolayer growth of DenBaars and Dapkus[22] at 475-485 °C for 1s exposure and of Nishizawa *et al.*[20] at ~450 °C for 4s exposure. Considering an uncertainty of 10 K in temperature calibration in different systems, we see that this translates into an uncertainty within ~30% of the predicted growth (for rate < 0.5 ML/cycle) at a given nominal temperature. With such uncertainty or confidence, we can estimate the laser heating contribution in LALE.

In LALE, surface temperature is raised during the illumination time of τ_i. During this time laser induced local heating also contributes to LALE growth. For a typical condition of τ_i = 0.2s, laser intensity of 1 kW/cm^2, an substrate bias temperature of 380 °C, the local maximum temperature is ~410 °C. the thermal ALE growth predicted by the dotted curve in the Fig.6.7 is still below 0.2 ML/cycle. LALE using TEGa does not fit into this model since TEGa does not show self limiting growth in thermal ALE. The self limiting with respect to TEGa supply exhibited by TEGa in LALE is one of the strong indications of even lower contribution from thermal effect. The negligible laser heating in the low laser intensities used in this case leads to the same conclusion.

6.3 Spatial Resolution in LALE

Spatial resolution concerns both the smallest area and the closeness of the small areas that can be deposited. This may be limited by the size of the beam, thermal diffusion, surface species diffusion, carrier diffusion, and mechanical vibration. These issues will be discussed in order in this section.

The optical beam is shaped with the use of optical components before reaching the substrate surface. In LALE using single line of a laser source, there is no chromatic aberration. Spherical aberration can generally be corrected with a careful design of the lens. The ultimate limit to the fine size of the beam is due to the diffraction while the beam propagates through the optical system. If a lens of diameter D and focal length f is used to image a point source, the image will be finite with radius δ (from the center to the first zero of the diffracted intensity)

$$\delta = \frac{1.22\,\lambda}{D} f \qquad (6\text{-}14).$$

Different definitions in the divergence angles (e.g. half-angle at half-intensity for both circular aperture and Gaussian beam diffraction) may result in slightly different limits, but they all in the same order of magnitude. As an example, we can expand the laser beam to fill a lens of D=50 mm and f=50 mm. The focused spot at the rear focal point will be approximately 1.25 μm in diameter for λ= 514.5 nm.

Because of thermal diffusion, the area affected by heating is greater than the size of the beam. The distributions of normalized temperature rise

are plotted in Fig.6.8 along with the original intensity distribution using parameters appropriate to LALE using TMGa. The heated spot size is at most twice the beam size. It can also be concluded that the shorter is the illumination time, the better is the heated area confined and the less is the temperature rise in the region outside of the laser illumination.

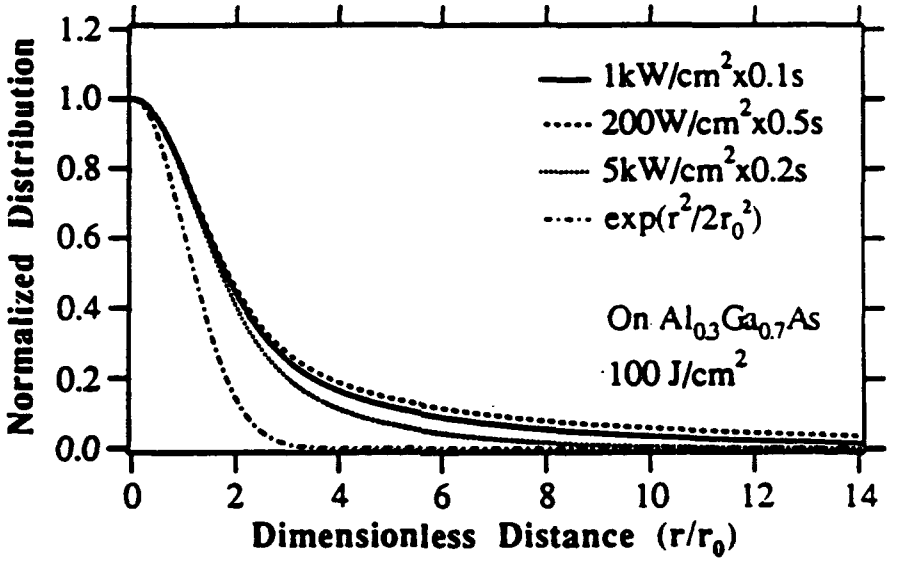

Fig.6.8 Normalized distribution of temperature rise under 100 J/cm^2 of energy fluence for different illmination modes. The original Gaussian distribution of the laser intensity is also plotted for comparison.

There is no reliable data on the surface diffusion coefficient of Ga on GaAs due to the complexity of the phenomenon that is affected by the surface conditions. Under normal MBE growth condition where As_4 and Ga are supplied simultaneously, the diffusion length (or migration length) λ_s

($=\sqrt{D_s \tau_s}$) is determined by the life time of the Ga atoms before they are captured by growth sites. In this case, Nishinaga *et al.*[23] found that λ_s (cm) = 4.0×10^{-8} exp(0.34ev/kT) for Ga on GaAs (001) surface misoriented towards the [$\bar{1}$10] . This gives a small diffusion length of 0.2 μm at 380 °C. On the other hand, when a GaAs surface is dosed with Ga flux to the point at which the excess Ga start to form droplets, the distance between the droplets is a measure of the diffusion length, ~10 μm at 580°C.[24] The estimated activation energy for the process is ~3.1 ev. The extrapolation to 380 °C results in negligibly small diffusion length (~2×10^{-5} μm). In both cases, the D_s was not determined because the τ_s could not be estimated. According to these information, we expect that surface species diffusion should not pose a limit for spatial resolution in the range of ~1 μm.

In a photocatalytic reaction, the distribution of surface excess carriers generated from laser absorption by a semiconductor needs to be examined. These carriers may be temporarily transferred to a chemical species, assisting the reaction, and are then released at the end of the reaction. For intrinsic GaAs, the bulk electron diffusion length is in the range of ~10 μm. Near the surface, however, the high surface recombination rate will reduce the carrier life time therefore the diffusion length considerably. A limit below 1 μm is quite possible. It is interesting to see what is the photon flux required to maintain a surface free carrier density (not those trapped) in the order of $10^{11}/cm^2$. Using a carrier life time near the surface τ_{rs} ~10^{-9}s and assuming every photon generates one pair of carriers, we find the photon flux in the order of $10^{20}/cm^2s$. Thus,

photocatalytic reaction, if described as due to the surface free carriers, should be a very inefficient process.

Finally, keeping the amplitude of vibration below the diffraction limit should not be a formidable task by the standards of modern optical engineering. There is practical difficult in combining a stable optical system with an MOCVD reactor. This in principle requires putting the entire MOCVD system, the light source, and the optics on an isolated energy dissipating platform. Nevertheless, one such experiment was reported recently for laser assisted MOMBE.[25] Corrugation patterns with submicron pitch (~0.85 μm) were grown directly by interfering two coherent laser beams at the substrate surface.

References for Chapter Six

[1] S.D.Allen, J.A.Goldstone, J.P.Stone, and R.Y.Jan, "Transient Nonlinear Laser Heating and Deposition: A Comparison of Theory and Experiment," J. Appl. Phys, Vol.59(5), 1653(1986).

[2] D.C.Skouby and K.F.Jensen, "Modeling of Pyrolytic Laser-Assisted Chemical Vapor Deposition: Mass Transfer and Kinetic Effects Influencing the Shape of the Deposit," J. Appl. Phys., Vol.63(1), 198(1988).

[3] J.F.Ready, "Effects of High Power Laser Radiation," (Academic Press, New York, 1971).

[4] T.Wolkenstein and I.V.Karpenko, "On the Theory of Photoadsorptive Effect on Semiconductors," J. Appl. Phys. Vol.33, 460(1962).

[5] W.C.Murphy, A.C.Beri, T.F.George, and J.Lin, "Analysis of Laser-Enhanced Adsorption/Desorption Processes on Semiconductor Surfaces Via Electronic Surface State Excitation," Mat. Res. Soc. Symp. Proc. Vol.17, (Elsevier Science Pub. Co., Inc., 1983), p273.

[6] D.E.Aspnes, S.M.Kelso, R.A.Logan, R.Bhat, "Optical Properties of AlxGa1-xAs," J. Appl. Phys. Vol.60(2), 754(1986).

[7] S.Adachi, "Model Dielectric Constants of GaP, GaAs, GaSb, InP, InAs, and InSb," Phys. Rev. B35, 7454(1987).

[8] S.Adachi, "Optical Properties of AlxGa1-xAs Alloy," Phys. Rev. B38(17), 345(1988).

[9] S.H.Wemple and M.Didomenico, Jr.,"Behavior of Electronic Dielectric Constant in Covalent and Ionic Materials," Phys. Rev. B3, 1338(1971).

[10] M.A.Afromowitz, "Refractive Index of $Ga_{1-x}Al_xAs$," Solid State Comm. Vol.15, 59(1974).

[11] H.C.Casey Jr. and M.B.Panish, in "Heterostructure Lasers," Part A, (Academic Press, 1978), p31.

[12] P.D.Maycock, "Thermal Conductivity of Silicon, Germanium, III-V Compounds, and III-V Alloys," Solid State Electron. Vol.10, 161(1967).

[13] M.A.Afromowitz, Thermal Conductivity of $Ga_{1-x}Al_xAs$ Alloys," J. Appl. Phys., Vol.44(3), 1292(1973).

[14] Y.I.Nissim, A,Lietoila, R.B.Gold, and J.F.Gibbons, "Temperature Distributions Produced n Semiconductors by Scanning Elliptical or Circular CW Laser Beam," J. Appl. Phys, Vol.51(1), 274(1980).

[15] S.Adachi, "GaAs, AlAs, and $Al_xGa_{1-x}As$: Material Parameters for Use in Research and Device Applications," J. Appl. Phys., Vol.58(3), R1(1985).

[16] H.E.Cline and T.R.Anthony, "Heat Treating and Melting Material with a Scanning Laser or Electron Beam," J. Appl. Phys., Vol.48(9), 3895(1977).

[17] H.S.Carslaw and J.C.Jaeger, in "Conduction of Heat n Solids," 2nd Edn., (Oxford, Clarendon Press, 1959).

[18] M.Ozeki, K.Mochizuki, N.Ohtsuka, and K.Kodama, "New Approach to the Atomic Layer Epitaxy of GaAs Using a Fast Gas System," Appl. Phys. Lett., Vol.53(16), 1509(1988).

[19] TH.Ohno, S.Ohtsuka, A.Ohuchi, T.Matsubara, and H.Hasegawa, "Growth of GaAs, InAs, and GaAs/InAs Superlattice Structures at Low Substrate Temperature by MOVPE," J. Cryst. Growth, Vol.93, 342(1988).

[20] J.Nishizawa, H.Abe, and T.Kurabayashi, "Molecular Layer Epitaxy," J. Electrochem. Soc., Vol.132(5), 1197(1985).

[21] P.C.Colter, S.A.Hussien, A.Dip, M.V.Erdogan. W.M.Duncan, and S.M.Bedair, "Atomic Layer Epitaxy of Device Quality GaAs with a 0.6 μm/hr Rate," Appl. Phys. Lett, Vol.59(12), 1440(1991).

[22] S.P.DenBaars and P.D.Dapkus, "Atomic Layer Epitaxy of Compound Semiconductor with Metalorganic Precursors," J. Cryst. Growth, Vol.95, 195(1989).

[23] T.Nishinaga, T.Shitara, K.Mochizuki, and K.I.Cho, "Surface Diffusion and Related Phenomena in MBE Growth of III-V Compounds," J. Cryst. Growth, Vol.99, 482(1990).

[24] K.Kanisawa, J.Osaka, S.Hirono, and N.Inoue, "Al-Ga Monolayer Lateral Growth observed In Situ by Scanning Electron Microscopy," Appl. Phys. Lett., Vol. 58(21), 2363(1991).

[25] T.Yamada, R.Iga, and H.Sugiura, "GaAs Corrugation Pattern with Submicron Pitch Grown by Ar Ion Laser-Assisted Metalorganic Molecular Beam Epitaxy," Appl. Phys. Lett., Vol.59(8), 958(1991).

CHAPTER SEVEN

LALE Applications – Selected Examples

Although LALE growth has been studied by several research groups, device applications of the material grown by LALE remained an expectation prior to this work. In order for LALE being considered as a viable technique in optoelectronic integration, it is important to demonstrate in laboratory scale some of the potential applications. Our detailed study of the influence of growth parameters on material quality in LALE has allowed us to produce GaAs material and GaAs/AlGaAs interfaces suitable for device applications. Our unique reactor design that permits LALE performed in a full function MOCVD system makes such demonstration possible.

7.1 Selective Area Deposition of Regular and Arbitrary Patterns

The simplest but the basic application of LALE is to grow islands of GaAs with regular (dots) or arbitrary shape. On these islands, different types of devices can be fabricated with good isolation (if on semi-insulating substrates), saving lithographic processing steps. The shape that has been conveniently obtained in our experiment is a line by employing either a focused scanning laser beam or cylindrically focused laser beam. A micro photograph of a GaAs LALE stripe grown by rotating the susceptor relative to the laser beam is shown in Fig.7.1(a). For depositing an arbitrary shape, a

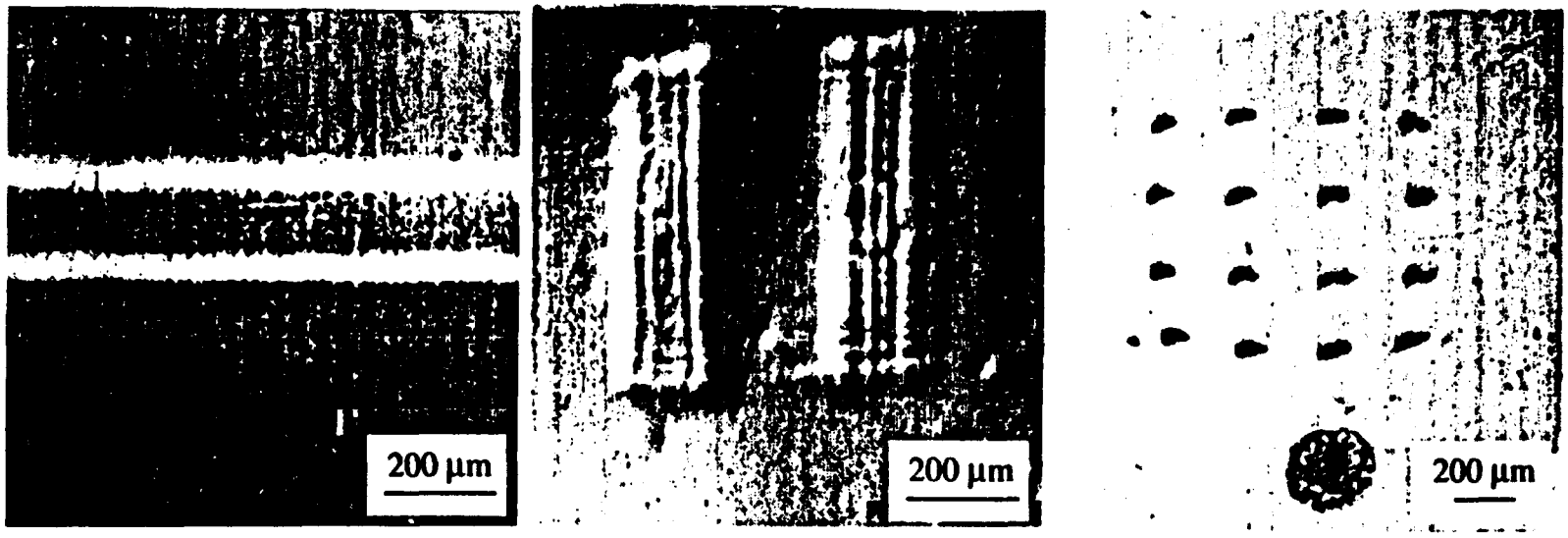

(a) Direct Writing (b) Shadow Masking (c) Beam Splitting

Fig.7.1 Selective area deposition of regular and arbitrary patterns by LALE.

straight forward way is to use a shadow mask and to project the image onto the substrate. We have used a shadow mask with two 3x1 (mm^2) openings about 1mm apart. The micro photograph of the deposit is shown in Fig.7.1(b). Because of the coherent light source illumination of the small features on the mask, diffraction and interference effects become noticeable as the parallel fine lines on the otherwise uniformly illuminated area. In this approach, an incoherent light source may be a better choice. The 4x4 array of GaAs dots shown in Fig.7.1(c) are grown at once by successive use of two 1x4 planar beam splitters. Each beam splitter will divide the original beam into four parallel and evenly spaced beams of approximately equal intensity with ~94% efficiency. The parallel beams are then focused onto the substrate, though the singlet lens gave barrel distortion of the array image. Our results show the feasibility of LALE in direct writing, shadow mask imaging, and the growth of array of GaAs islands by multiple beam projection.

7.2 LALE GaAs as the Active Medium of Laser Devices

7.2.1 Broad Area Lasers

The fabrication of broad area lasers serve also as a test vehicle for the quality of GaAs and the interfaces grown by LALE. The GRIN-SCH single QW structures are grown in a three step process in a single run. The lower part of the structure (the N region) is grown by MOCVD at 750 °C. The substrate temperature is then reduced to 380 °C for growth using TMGa and 330 °C for using TEGa and LALE QW of 100 Å thick is grown by LALE. The temperature is increased again to 750 °C to complete the

structure with the growth of the P region. The layout of the contact electrodes and the typical dimensions are shown in Fig.7.2. The bars of devices are cleaved perpendicular to the LALE stripe and the contact metal stripes. The testing is performed at room temperature without deliberate

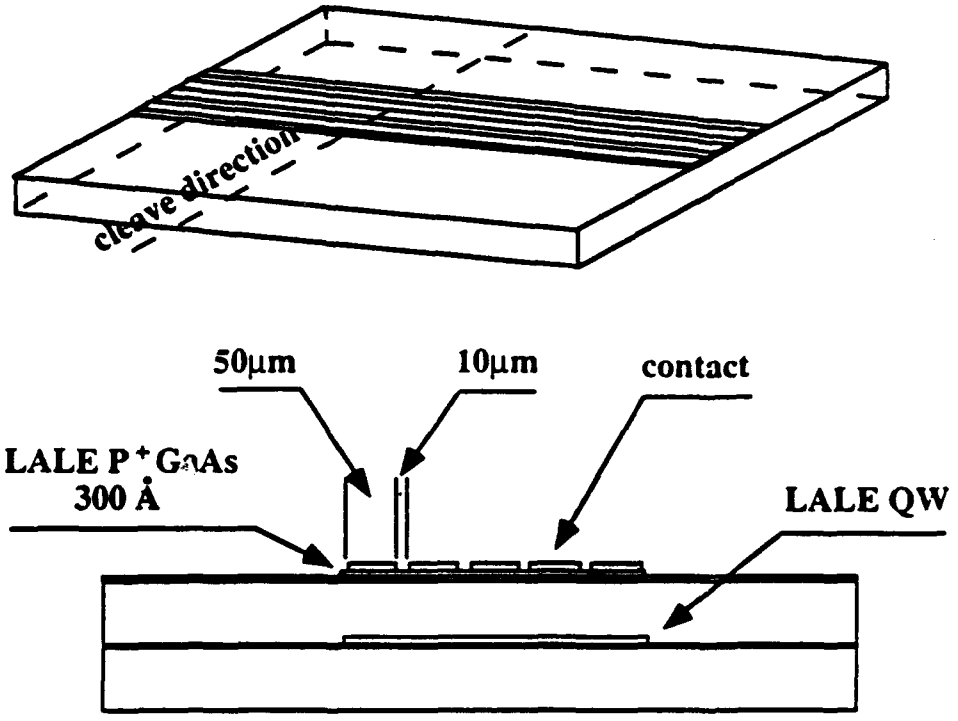

Fig.7.2 Broad area laser diodes fabricated on a LALE QW stripe.

heat sinking under pulsed condition at a repetition rate of 10 kHz. In Table 7.1, the lowest threshold current densities are summarized for structures with the single QW grown by LALE using combinations of TMGa and AsH_3, TMGa and TBAs, and TEGa and AsH_3. The data obtained from device structures with the QW grown by ALE and MOCVD in the same reactor or from literature[1][2] are also included for comparison. Considering

that practical laser devices can be made from the material exhibits threshold current densities in the range of ~500 A/cm^2, our result is not only a demonstration of the device quality of the GaAs grown by LALE but also an encouraging sign for future experimentation in realizing various novel device concepts

Table 7.1 Summary of laser device performance.

Growth Techniques	J_{th}(A/cm^2) [Cavity Length (μm)]		
	TMGa+AsH_3	TMGa+TBAs	TEGa+AsH_3
LALE	592 [735μm]	515 [675μm]	544 [570μm]
ALE	370 [544μm][1]	300 [744μm]	
MOCVD	225 [1010μm]	186 [990μm][2]	

Shown in Fig.7.3 are the threshold current density and lasing wavelength obtained at different locations across the LALE stripe. As expected, low threshold current density is obtained on the LALE stripe. It increases rapidly away from the stripe. The wavelength on top of the stripe is longer than that on the shoulder of the stripe, replicating the shape of the stripe. Of course, our ultimate goal is to reduce the size of the stripe to the dimension of a single device. In such case, lateral carrier confinement is also achieved as would otherwise achievable, with more complexity, by

growth on structured substrates and by temperature engineered growth.[3] There is, however, difficult in aligning the top contact electrodes with the LALE stripe. The experiment described in section 7.2.3 demonstrates a novel technique which provides alignment marker as well as Ohmic contact for subsequent processing.

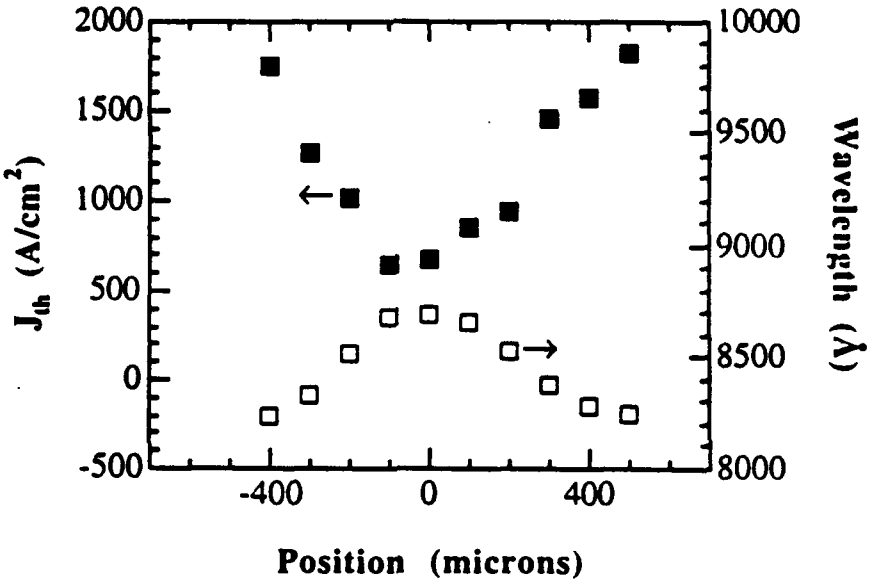

Fig. 7.3 The distribution of threshold current densities and lasing wavelengths across a LALE stripe.

7.2.2 Lasers with Sections of Transparent Wave Guide

In this case, the top contact stripes run perpendicular to the LALE stripe and cover only the portion with LALE grown QW, as is shown in the insert in the Fig.7.4. This is the basic structure of many interesting optoelectronic integration applications because it involves the active-to-passive transition in a single device. The independent choice of the length of the active region from the length of the cavity gives additional degree of

freedom in designing a low threshold current laser source of desirable lasing characteristics. The specific device has ~300 μm long LALE QW region serving as the active medium while selectively pumped by a 293 μm-long top contact electrode. An etching has been done to define a 5 μm-wide ridge wave guide perpendicular to the LALE stripe, providing also lateral confinement. The cleaving is such that the sections of passive wave guides are 35 μm long at one end and 650 μm at the other end. Fig.7.4 shows the room temperature lasing spectrum under pulsed testing condition along with the electroluminescence spectra of the device before and after cleaving off the 650 μm wave guide length to 11 μm. The threshold for the device with the 650 μm-long wave guide present is 225 mA and reduces to

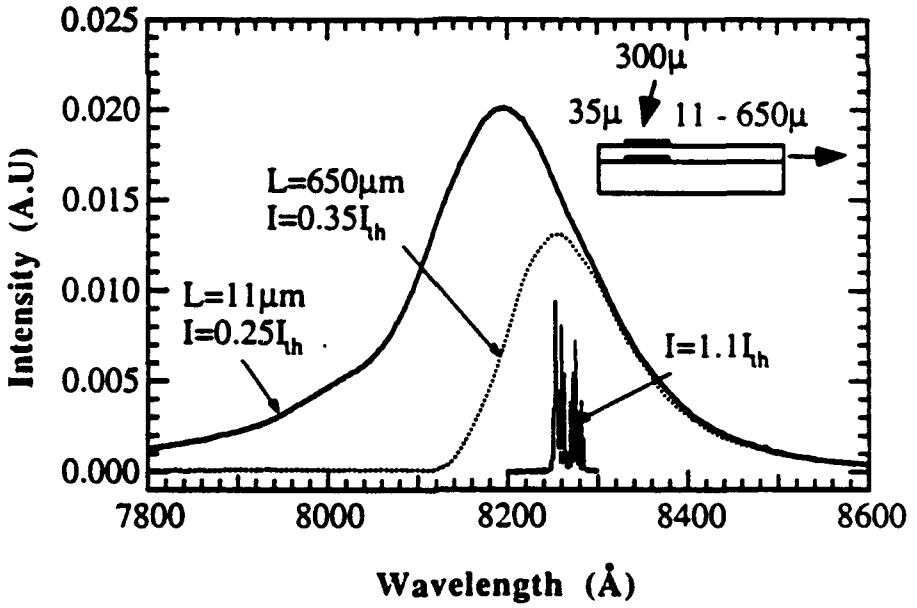

Fig.7.4 The lasing and electroluminescence spectra of lasers with sections of transparent waveguides. The insert shows the cross section (cut along the light propagation direction) of structure.

155 mA after cleaving. These high values are caused by the loss in the wave guide region as can be inferred from the electroluminescence spectra. The QW emission in this case is shorter than that of a properly designed structure so that it overlaps partially with the absorption edge in the passive region. The emission shorter than ~8200 Å suffered from a drastic loss. The laser is forced to oscillate at a longer wavelength. With the material quality attainable at this time, we expect that the threshold current can be reduced further by adopting an optimal design. Nevertheless, this result shows for the first time that LALE is an attractive technique in the realization of interesting device concept in optoelectronic integration.

7.3 Pseudo Auto Alignment Employing a LALE Doped Layer

We have shown in Chapter Three that GaAs can be doped during LALE to high conductivity by using DEZn as the dopant. An immediate application of this result is the use of such highly doped layer as the finishing layer of a laser structure to provide good Ohmic contact between the metal electrode and the semiconductor. This is also motivated by the difficult encountered during the fabrication of laser devices incorporating QW grown by LALE where the QW region is not precisely located. Precise alignment will be even harder when we are to address individual device of width of about ~10 μm or narrower.

The whole single QW GRIN-SCH laser structure is grown in a single run with four temperature steps. The first three steps are the same as described above but the QW is grown by LALE using TEGa. The final

selective area doping growth is also performed at 330 °C with the simultaneous injection of TEGa and DEZn. The 200 ML top LALE layer provides a visible marker for precise location of the QW region underneath. The laser diodes fabricated from this structure show normal current-voltage (I-V) and emission power-injection current (L-I) characteristics. Threshold current density as low as 544 A/cm^2 is obtained on a device of cavity length 570 μm. this experiment demonstrate the versatility of LALE for in situ processing.

7.4 GaAs/AlAs Bragg Mirrors by LALE

In recent years, multilayered periodic structures of two semiconductors of different refractive indexes have found important applications in photonic devices as high reflecting mirrors. The basic idea is well known to the optics community and stems from the theory of propagation of light wave in periodically stratified dielectric media. The building block of such periodic structure consists of a pair of layers of different refractive indexes n_H and n_L and layer thicknesses t_H and t_L, where the H (high) and L (low) denote the relative value of the refractive indexes. When the optical thicknesses of the layers in the periodic structure are such that $n_H t_H = n_L t_L = \lambda_0/4$, the structure exhibits high reflectivity of which the magnitude increases quickly with the number of high-low pairs. In analogous to the reconstructive reflection of X-rays by periodic crystal lattice, these optical devices are termed Bragg reflectors (mirrors). A basic requirement for producing a Bragg reflector of high peak reflectivity is the precise realization of the required quarter wavelength optical thickness

from layer to layer throughout the entire structure. This has been a great challenge to the growth techniques as MBE and MOCVD. By virtue of the self limiting growth, ALE and related growth are expected to find an important role in this respect. With LALE, localized Bragg mirrors can be produced. Array of miniature Bragg reflectors have many interesting applications in parallel optical signal processing.

The experimental Bragg reflector consists of 8 pairs of GaAs/AlAs stacks on (100) oriented N^+ GaAs substrate. The nominal layer thicknesses are 668 Å for GaAs and 739 Å for AlAs. Since the conditions for ALE or LALE using TMAl is not well established, the AlAs layers are grown by conventional MOCVD at 750 °C. The GaAs layers are grown at 380 °C by

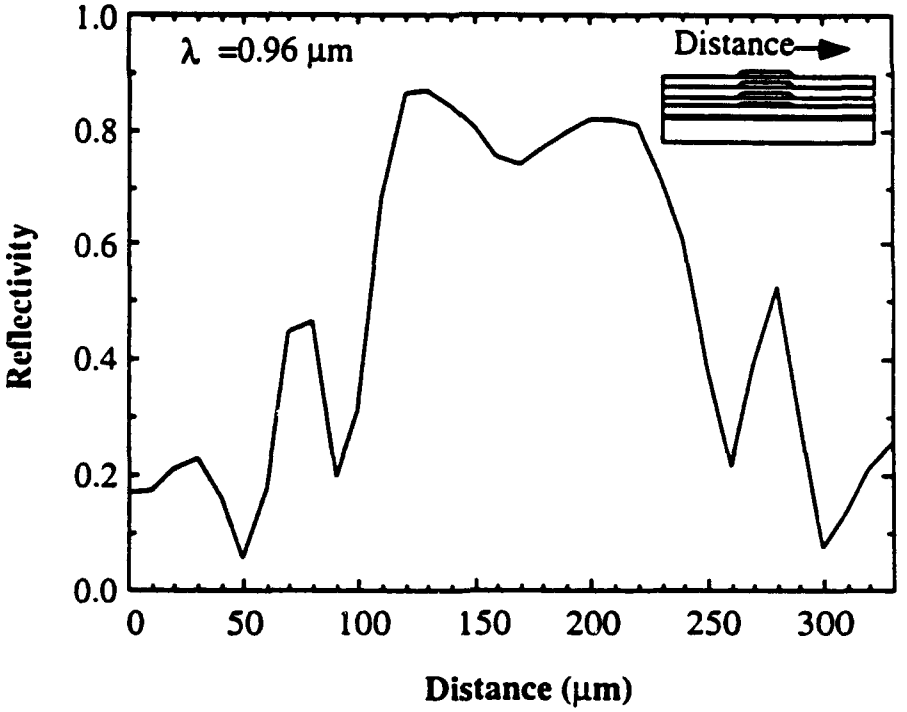

Fig.7.5 Reflectivity across a localized Bragg mirror consisting of 8-pairs of GaAs/AlAs.

LALE using TMGa and AsH_3. Shown in Fig.7.5 is the reflectivity across a localized Bragg mirror. The measurement is done with a focused Ti-sapphire laser tuned at $\lambda_0 = 0.96$ μm. The irregular saddle in the middle of the stripe is probably caused by slight deviation from monolayer per cycle in the later part of the structure as the stacks pile up. This deviation is expected to be much less significant when TEGa is used since the change in the local heat dissipation will have much less influence on LALE growth in this case. Nonetheless, this first demonstration of such device appears very encouraging.

7.4 Summary

In this chapter, we have presented our results on the application of LALE to optoelectronic devices fabrications. Among these, selective area deposition of isolated islands forms the basic structures for further implementations of optoelectronic integration. The successful fabrication and operation of broad area lasers testifies the device quality of the GaAs materials by LALE and the interfaces formed by hybridized MOCVD/LALE growth. The versatility of LALE for in situ processing is also exemplified by the use of LALE doped P^+ GaAs layer to provide a pseudo auto alignment marker as well as Ohmic contact. Finally, the application of LALE in the fabrication of miniature optical component (Brag mirrors) is also demonstrated. While all of these are the first demonstrations of the kind, we maintain that a multitude improvement is possible.

References for Chapter Seven

[1] S.P.DenBaars and P.D.Dapkus, "Atomic Layer Epitaxy of Compound Semiconductors with Metalorganic Precursors," J. Cryst. Growth, Vol.98, 195(1989).

[2] S.G.Hummel, C.A.Beyler, Y.Zou, P.Grodzinski, and P.D.Dapkus, "Use of Tertiarybutylarsine in the Fabrication of GaAs/AlGaAs Quantum Wells and Quantum Well Lasers," Appl. Phys. Lett. 57(7), 695 (1990).

[3] K.M.Dzurko, E.P.Menu, C.A.Beyler, J.S.Osinsk, and P.D.Dapkus, "Temperature Engineered Growth of Low Threshold Quantum Well Lasers by Metalorganic Chemical Vapor Deposition," Appl. Phys. Lett., Vol.54, 105(1989).

CHAPTER EIGHT

Final Remarks and Suggestions for Future Work

This work has been carried out during a time when selective area deposition of GaAs by LALE was achieved but the growth behavior was not well quantified, not to mention a deep understand of the mechanism. The characterization of the small area deposit was even left behind. The results of this work substantiate our knowledge of the selective area growth of GaAs by LALE using metalorganics. Great effort has been made in this work to characterize the material quality in terms of impurity incorporation and the PL efficiency which is a indication of both material purity and crystallinity. Because the success of this effort, the influence of the growth chemistry and growth parameters on the quality of the GaAs material can be studied. The conditions for achieving monolayer self limiting LALE growth with device quality material are established. The quality of the material grown by LALE is further tested by incorporating GaAs grown by LALE in part of the working device structure.

8.1 Important Conclusions from this Work

Gas phase decomposition of TMGa occurs appreciably above ~430 °C. This is one of the limiting factors for the usable substrate temperature for ALE and LALE growth carried out in atmospheric pressure. The existence of methyl radicals among the intermediate decomposition

products makes TMGa itself a source of carbon contamination, especially for low temperature growth. A possible route for carbon incorporation is through the dehydrogenation of alkylgallium species caused by the abstraction of H by the methyl radicals. The relative closeness of the activation energies for the successive breakage of the three Ga-C bonds in combination with a finite difference in the activation energies for decomposition at an As and a Ga site is the basic reason for the deviation from monolayer self limiting.

While the combinations of TMGa and AsH_3, TMGa and TBAs, and TEGa and AsH_3 can all yield self limiting LALE growth, the laser intensities required to achieve one ML/cycle growth, which is only determined by the property of the group III precursors, differ greatly. The threshold intensity in the case of TEGa is much lower than the case of TMGa. Because of the lower heating effect as a result of the low intensity, TEGa appears to be the choice of precursors in the applications where selective area deposition of better spatial resolution is of primary concern. In all the cases for different combination of precursors, overlap between the group III injection and the laser illumination is necessary. This gives the upper limit of the desorption time constants to be no greater than ~0.6s for TMGa and TEGa at their respective growth temperatures. Also true for both TMGa and TEGa is that the threshold energy flux for monolayer LALE growth is affected by the manner with which the photons are delivered. The process proceeds at a higher efficiency when the photons are delivered at a denser package for a shorter time, which is interpreted as the involvement multiphoton processes. The self liming with respect to TMGa

and TEGa fluxes is all observed. The different saturation behavior exhibited by TEGa in thermal ALE and LALE argues strongly in favor of photo enhancement in LALE. Even for the case of using TMGa where thermal effect is relatively more important, the contribution from thermal enhancement is estimated to be less than 0.2 ML/cycle for typical growth conditions.

The growth chemistry is shown to have great effect on carbon contamination and the optical quality of the GaAs grown by LALE. The replacement of AsH_3 by TBAs has resulted in reduced carbon incorporation with the background carrier concentration measured by C-V to be $p \sim 1 \times 10^{16}$ cm^{-3}. This carbon reduction is attributed to the lower decomposition temperature of TBAs and the abundance as well the survival of the methyl radical scavenging species AsH_x on the growth surface at low substrate temperature. This difference between TBAs and AsH_3 is expected to be less at higher temperature at which the lifetimes of the AsH_x species from TBAs or AsH_3 are all short. The use of TEGa also reduces carbon contamination with $p \leq 4 \times 10^{15}$ cm^{-3}. The reduction of carbon in this case is thought to be the consequence of a decomposition mechanism that gives Ga species free of carbon and stable hydrocarbon species which are not actively involved in carbon incorporation processes. The low substrate temperature required in LALE using TEGa may be the limiting factor for further improvement of the over all material quality judging from the lower PL efficiency from GaAs grown using TEGa and AH_3 than that using TMGa and TBAs. An ideal (somewhat fictitious) Ga precursor for LALE should then have a high thermal breakdown temperature (≥ 600 °C) and yet

still participate in photo enhancement processes with the production of Ga species free from carbon at reasonable quantum efficiency.

Intense room temperature PL response is observable from DH's with the central GaAs grown by LALE, indicating good material and interfaces. The PL efficiency of GaAs grown by LALE can be improved by the use of minimal exposure to the Ga sources and relatively long exposure to the group V precursors. GaAs of better quality can be obtained by growing at high end of the LALE intensity window and by the use of either long laser illumination or multiple laser pulses. These requirements narrow the ranges of parameters for obtaining material of reasonable quality.

The device quality of GaAs grown by LALE is demonstrated for the first time by the successful fabrication of laser diodes that incorporate the GaAs QW grown by LALE. Threshold current density as low as 515 A/cm^2 was obtained in the case of using TMGa and TBAs. The versatility of LALE for in situ processing is also exploited through the realization of laser devices containing sections of passive wave guides, the growth of laser structures with a Zn doped p^+ GaAs pseudo auto alignment marker, and the formation of localized Bragg reflectors with the GaAs layer grown by LALE.

8.2 Suggestions for Future Work

Although we have demonstrated the device application of LALE, it is not to say that this technique is now mature. Further development is

certainly necessary. A key issue that will determine the area of application of LALE is the experimentally achievable spatial resolution. Further experiments have to be performed on a upgraded system featuring vibration isolated platform with diffraction limited optics. The incorporation of an imaging system that produces the magnified image of the laser spot will be mandatory in such further study. This will also allow the in situ determination of the intensity distribution, reducing the empirical nature of the current LALE growth. Any work aimed at direct measurement of the temperature distribution under laser illumination will be certainly of great value in the understanding of the growth mechanism.

The study of ALE related mechanism has been traditionally carried out in either a dedicated system equipped with surface analysis tools or in a real growth system by *inferring from* the actual growth behavior. In the first approach, the experiment observation is usually the change in a probe beam (electrons or light). The origin for such change is subject to interpretation. The observation of the "saturation" of this change signifies only the attainment of a steady state for the surface processes and not necessarily monolayer material deposition. The details of how the steady state is obtained is also not distinguished. In the second approach, only the deposited material is measured. Growth mechanisms can be inferred from the data in the submonolayer regime. This could be a convincing approach, though extremely tedious, since the measured growth is less disputable. For example, suppose that we can obtain an accurate LALE growth rate as a function of photon flux per cycle for submonolayer growth. A logarithmic plot will have several possible characteristics depending on the growth

mechanism. For surface photochemical reactions, the plot is a straight line with the slope revealing the nature of the reaction, e.g. one for single photon processes, (in analogy to molecularity of a reaction). Non integer slope signifies a blend of single and multiple photon processes. Any deviation from a straight line reveals the involvement of thermal and photocatalytic effects. The thermal effect can be excluded using the approach described in Chapter Six. To date, a combination of the two approaches has been rare, if not absent. The correlation of surface science result and the direct growth observations will give more definite and satisfactory description of self limiting growth mechanism in LALE.

Alloy growth by LALE is another determinant factor for the success of this growth technique, which has not been explored to any extent. Our preliminary experiments on the growth of InxGa1-xAs by LALE using trimethylindium (TMIn) and TEGa in combination with AsH_3 has shown that direct (random) alloy (as opposed to "digital" alloy) growth is possible. The $Al_{0.3}Ga_{0.7}As/In_xGa_{1-x}As/Al_{0.3}Ga_{0.7}As$ structure with the $In_xGa_{1-x}As$ grown by LALE exhibits relatively strong PL response with the peak centered at λ~0.98 μm (1.265 ev). The LALE growth of $In_xGa_{1-x}As$ is performed at 320 °C with 0.5 s TMIn exposure followed by a 1.5 s TEGa exposure. The 0.1 s laser pulse is overlapping with the TEGa exposure. A problem found is that the bias temperature is too high for the low thermal stability of TMIn that the growth over the non illuminated area is also appreciable. A substrate temperature below 300 °C is thus recommended. In line with this , future work can also be carried out on the "digital" alloy growth, i.e. short period superlattices with or without post growth

annealing. There will certainly be full of new interesting phenomena and challenges.

BIBLIOGRAPHY

Adachi, S., "GaAs, AlAs, and $Al_xGa_{1-x}As$: Material Parameters for Use in Research and Device Applications," J. Appl. Phys., Vol.58(3), R1(1985).

Adachi, S., "Model Dielectric Constants of GaP, GaAs, GaSb, InP, InAs, and InSb," Phys. Rev. B35, 7454(1987).

Adachi, S., "Optical Properties of AlxGa1-xAs Alloy," Phys. Rev. B38(17), 345(1988).

Afromowitz, M. A., "Refractive Index of $Ga_{1-x}Al_xAs$," Solid State Comm. Vol.15, 59(1974).

Afromowitz, M. A., "Thermal Conductivity of $Ga_{1-x}Al_xAs$ Alloys," J. Appl. Phys., Vol.44(3), 1292(1973).

Allen, S. D., J.A.Goldstone, J.P.Stone, and R.Y.Jan, "Transient Nonlinear Laser Heating and Deposition: A Comparison of Theory and Experiment," J. Appl. Phys, Vol.59(5), 1653(1986).

Annapragada, A. V., S.Salim, and K.F.Jensen, Presented in the 1991 Spring Materials Research Society Meeting, April 17–May 1, Anaheim, California, U.S.A., Symposium D. Full paper in " Atomic Layer Growth and Processing ", Materials Research Society Symposium Proceedings Vol.222, Eds., T.F.Kuech, P.D.Dapkus, and Y.Aoyagi, p81.

Aoyagi, Y., A.Doi, and S.Iwai, and S.Namba, "Atomic-Layer Growth of GaAs by Modulated-Continuous-Wave Laser Metalorganic Vapor-Phase Epitaxy," J. Vac. Sci. Technol., B5(5), 1460(1987).

Aoyagi, Y., S.Masuda, and S.Namba, "Laser Enhanced Metalorganic Chemical Vapor Deposition Crystal Growth in GaAs," Appl. Phys. Lett., Vol.47(2), 95(1985).

Arens, G., H.Heinecke, N.Pütz, L.Lüth, and P.Balk, "On the Role of Hydrogen in the MOCVD of GaAs, "J. Cryst. Growth, Vol.76, 305(1986).

Aspnes, D. E., S.M.Kelso, R.A.Logan, R.Bhat, "Optical Properties of AlxGa1-xAs," J. Appl. Phys. Vol.60(2), 754(1986).

Ban, V. S. and S.L.Gilbert, J. Cryst. Growth, Vol.31, 284(1975).

Beagley, B., D.G.Schmidling, and I.A.Steer, "An Electron-Diffraction Study of the Molecular Structure of Trimethylgallium," J. Mol. Struct., Vol.21, 437(1974).

Bedair, S. M., J.K.Whisnant, N.H.Karam, M.A.Tischler, and T.Katsuyama, "Laser Selective Deposition of GaAs on Si," Appl. Phys. Lett. Vol.48(2), 174(1986).

Benson, S. W., in "Thermochemical Kinetics: Methods for Estimation of Thermochemical Data and Rate Parameters", 2nd Ed., J.Wiley (1976).

Butler, J. E., N.Bottka, R.S.Sillmon, and D.K.Gaskill, "In Situ, Real-Time Diagnostics of OMVPE Using IR-Diode Laser Spectroscopy," J. Cryst. Growth, Vol.77, 163(1986).

Carslaw, H. S. and J.C.Jaeger, in "Conduction of Heat in Solids," 2nd Edn., (Oxford, Clarendon Press, 1959).

Casey, H. C., Jr. and M.B.Panish, in "Heterostructure Lasers," Part A, (Academic Press, 1978), p31.

Chadwick, B. K., "Equilibrium Analysis of the MOCVD $Ga(CH_3)_3$-AsH_3-H_2 System," J. Cryst. Growth, Vol.96, 693(1989).

Chen, C. H., C.A.Larsen, and G.B.Stringfellow, "Use of Tertiarybutylarsine for GaAs Growth," Appl. Phys. Lett. 50(4), 218 (1987).

Chen, Q., J.S.Osinski, and P.D.Dapkus, "Quantum Well Lasers with Active Region Grown by Laser Assisted Atomic Layer Epitaxy," Appl. Phys. Lett. 57(14), 1437 (1990).

Cline, H. E. and T.R.Anthony, "Heat Treating and Melting Material with a Scanning Laser or Electron Beam," J. Appl. Phys., Vol.48(9), 3895(1977).

Clyne, M. A. A. and W.S.Nip, in "Reactive Intermediates in Gas Phase: Generation and Monitoring", D.W.Setser, Ed., Academic Press, (1979), p38.

Coates, G. E. and A.J.Downs, "The Vibrational Spectrum and Structure of Trimethylgallium," Spectrochim. Acta, Vol.20, 3353(1964).

Coates, G. E., J.H.S.Green, and K.Wade, "Organometallic Compounds: Vol.1, The Main Group Elements," (Methuen & CO, LTD), p204.

Colter, P. C., S.A.Hussien, A.Dip, M.U.Erdogan, W.M.Duncan, and S.M.Bedair, "Atomic Layer Epitaxy of Device Quality GaAs with 0.6 μm/h Growth Rate," Appl. Phys. Lett, Vol.59(12), 1440(1991).

Creighton, J. R. and B.A.Banse, in "Atomic Layer Growth and Processing," Eds., T.F.Kuech, P.D.Dapkus, and Y.Aoyagi, Mat. Res. Soc. Symp. Proc., Vol222, 15(1991).

Creighton, J. R., "Chemisorption and Decomposition of Trimethylgallium on GaAs (100)," Surface Sci., Vol.234, 287(1990).

Creighton, J. R., K.R.Lykke, V.A.Shamamian, and B.D.Kay, "Decomposition of Trimethylgallium on the Gallium-rich GaAs (100) Surface: Implications for Atomic Layer Epitaxy," Appl. Phys. Lett., Vol.57(3), 279(1990).

Curtis, B. J. and J.P.Dismukes, "Effect of Natural and Forced Convection in Vapor Phase Growth Systems," J. Cryst. Growth, Vol.17, 128(1972).

Dapkus, P. D., B.Y.Maa, Q.Chen, W.G.Jeong, and S.P.DenBaars, "Atmospheric Pressure Atomic Layer Epitaxy: Mechanisms and Applications," J. Cryst. Growth, Vol.107, 73(1991).

Davies, J. I., G.Fan, and J.O.Williams, "Metal-Organic Chemical Vapor Deposition (MOCVD) of Compound Semiconductors Part 1. – Optimization of Reactor Design for the Preparation of ZnSe," J. Chem. Soc., Faraday Trans. I, Vol.81, 2711(1985).

DenBaars, S. P. and P.D.Dapkus, "Atomic Layer Epitaxy of Compound Semiconductors with Metalorganic Precursors," J. Cryst. Growth, Vol.98, 195(1989).

DenBaars, S. P., B.Y.Maa, P.D.Dapkus, A.D.Danner, and H.C.Lee, "Homogeneous Thermal Decomposition Rates of Trimethylgallium and Arsine and Their Relevance to the Growth of GaAs by MOCVD," J. Cryst. Growth, Vol.77, 188(1986).

DenBaars, S. P., C.A.Beyler, A.Hariz, and P.D.Dapkus, "GaAs/AlGaAs Quantum Well Lasers with Active Region Grown by Atomic Layer Epitaxy," Appl. Phys. Lett., Vol.51(19), 1530(1987).

Doi, A., S.Iwai, T.Meguro, and S.Namba, "A Growth Analysis for Metalorganic Vapor Phase Epitaxy of GaAs," Jpn. J. Appl. Phys., Vol.27(5), 795(1988).

Doi, A., Y.Aoyagi, and S.Namba, "Stepwise Monolayer Growth of GaAs by Switched Laser Metalorganic Vapor Phase Epitaxy," Appl. Phys. Lett., Vol.49(13), 785(1986).

Donnelly, V. M., C.W.Tu, J.C.Beggy, V.R.McCrary, M.G.Lamont, T.D.Harris, F.A.Baiocchi, and R.C.Farrow, "Laser-Assisted Metalorganic Molecular Beam Epitaxy of GaAs," Appl. Phys. Lett., Vol.52(13), 1065(1988).

Donnelly, V. M., J.A.McCaulley, and R.J.Shul, in "Chemical Perspectives of Microelectronic Materials II," Eds., L.V.Interante, K.F.Jensen, L.H.Dubois, and M.E.Gross, Mat. Res. Soc. Symp. Proc., Vol.204, 15(1991).

Dzurko, K. M., E.P.Menu, C.A.Beyler, J.S.Osinsk, and P.D.Dapkus, "Temperature Engineered Growth of Low Threshold Quantum Well Lasers by Metalorganic Chemical Vapor Deposition," Appl. Phys. Lett., Vol.54, 105(1989).

Eltenton, G. E., "The Study of Reaction Intermediates by Means of a Mass Spectrometer," J. Chem. Phys. , Vol.15(7), 455(1947).

Epler, J. E. H.F.Chung, D.W.Treat, and T.L.Paoli, "AlGaAs Multiple-Wavelength Light-Emitting Bar Grown by Laser-Assisted Metalorganic Chemical Vapor Deposition," Appl. Phys. Lett., Vol.52(18), 1499(1988).

Eversteyn, F. C., P.J.W.Severin, C.H.J.v.d.Brekel, and H.L.Peek, "A Stagnant Layer Model for the Epitaxial Growth of Silicon from Silane in a Horizontal Reactor," J. Electrochem. Soc., Vol.117(7), 925(1970).

Giling, L. J. and J.Van de Ven, in "Advances in Crystal Growth," eds., P.M.Dryburgh, K.G.Barraclough, and B.Cockayne, (Prentice-Hall, Englewood Cliffs, NJ, 1987), p309.

Giling, L. J., "Gas Flow Patterns in Horizontal Epitaxial Reactor Cells Observed by Interference Holography," J. Electrochem. Soc., Vol.129(3), 634(1982).

Glockling, F. and R.G.Strafford, "Electron Impact Studies on Some Group III Metal Alkyls," J. Chem. Soc., (A), 1761(1971).

Goodings, C., N.J.Mason, P.J.Walker, and D.P.Jebb, "A New Inlet Design for Horizontal MOVPE Reactors," J. Cryst. Growth, Vol.91, 13(1989).

Haacke, G., S.P.Watkins, and H.Burkhard, "Metalorganic Chemical Vapor Deposition of High-Purity GaAs Using Tertiarybutylarsine," Appl. Phys. Lett., Vol.54(20), 2029(1989).

Hallais, J., Acta, Electronica, Vol.21, 129(1978).

Heinecke, H., E.Veuhoff, N.Putz, M.Heyen, and P.Balk, "Kinetics of GaAs Growth by Low Pressure MOCVD," J. Electron. Mat., Vol.13(5), 815(1984).

Hummel, S. G., C.A.Beyler, Y.Zou, P.Grodzinski, and P.D.Dapkus, "Use of Tertiarybutylarsine in the Fabrication of GaAs/AlGaAs Quantum Wells and Quantum Well Lasers," Appl. Phys. Lett. 57(7), 695 (1990).

Hunsperger, R. G., "Integrated Optics: Theory and Technology," 2nd ed., Springer-Verlag, 1985.

Hwang, G. J. and K.C.Cheng, J. Heat Transfer, Trans. ASME, Vol.95, 72(1973).

Ishii, H., H.Ohno, K.Matsuzaki, and H.Hasegawa, "Effect of Exposure to Group III Alkyls on Compound Semiconductor Surfaces Observed by X-ray Photoelectron Spectroscopy," J. Cryst. Growth, Vol.95, 132(1982).

Ito, S., T.Shinohara, and Y.Seki, "Properties of Epitaxial Gallium Arsenide from Trimethylgallium and Arsine," J. Electrochem. Soc., Vol.120(10), 1419(1973).

Itoh, H., M.Watanabe, S.Muka, and H.Yajima, "Ultraviolet Absorption Spectra of Metalorganic Molecules Diluted in Hydrogen Gas," J. Cryst. Growth, Vol.93, 165(1988).

Iwai, S., T.Meguro, A.Doi, Y.Aoyagi, and S.Namba, "Monolayer Growth and Direct Writing of GaAs by Pulsed Laser Metalorganic Vapor Phase Epitaxy," Thin Solid Films, Vol.163, 405(1988).

Jacko, M. G. and S.J.Price, "The Pyrolysis of Trimethyl Gallium," Can. J. Chem., Vol.41, 1560(1963).

Jeong, W. G., E.P.Menu, and P.D.Dapkus, "Steric Hindrance Effects in Atomic Layer Epitaxy of InAs," Appl. Phys.Lett., Vol.55(3), 244(1989).

Kanisawa, K., J.Osaka, S.Hirono, and N.Inoue, "Al-Ga Monolayer Lateral Growth Observed by Scanning Electron Microscopy," Appl. Phys. Lett., Vol.58(21), 2363(1991).

Kantrowitz, A. and J.Grey, "A High Intensity Source for the Molecular Beam. Part I. Theoretical," Rev. Sci. Instrum., Vol.22 (5), 328(1951).

Karam, N. H., H.Liu, I.Yoshida, and S.M.Bedair, "Direct Writing of GaAs Monolayer by Laser-Assisted Atomic Layer Epitaxy," Appl. Phys. Lett., Vol.52(14), 1144(1988).

Kimura, K., S.Horiguchi, K.Kamon, M.Mashita, M.Mihara, and M.Ishii, "Molecular Beam Epitaxy Growth of GaAs Using Triethylgallium and As_4," Jpn. J. Appl. Phys., Vol.26(3), 419(1987).

Klingman, K. J. and H.H.Lee, "Design of Epitaxial CVD Reactor I, Theoretical Relationships for Mass and Heat Transfer," J. Cryst. Growth, Vol.72, 670(185).

Kobrinsky, P. C. and P.D.Pacey, "The Reaction of Methyl Radicals with Molecular Hydrogen," Can. J. Chem., Vol.52, 3655(1974).

Koch, T. L., and U.Koren, "InP-Based Photonic Integrated Circuits," IEE Proceedings-J, Vol.138(2), 139(1991).

Kodama, K., M.Ozeki, K.Mochizuki, and N.Ohtsuka, "In Situ X-ray Photoelectron Spectroscopic Study of GaAs Grown by Atomic Layer Epitaxy," Appl. Phys. Lett., Vol.54, 656(1989).

Konagai, M., T.Yamada, T.Akatsuka, K.Saito, E.Tokumitsu, "Metallic p-Type GaAs and GaAlAs Grown by Metalorganic Molecular Beam Epitaxy," J. Cryst. Growth, Vol.98, 167(1989).

Koukitu, A., H.Nakai, A.Saegusa, T.Suzuki, O.Nomura, and H.Seki, "Solid Composition of $In_{1-x}Ga_xAs$ Grown by the Halogen Transport Atomic Layer Epitaxy," Jpn. J. Appl. Phys., Vol.27, L744(1988).

Kozuch, D. M., M.Stavolar, S.J.Pearton, C.R.Abernathy, and J.Lopata, "Hydrogen in Carbon-Doped GaAs Grown by Metalorganic Molecular Beam Epitaxy," Appl. Phys. Lett., Vol.57(24), 2561(1990).

Kuech, T. F. and E.Veuhoff, "Mechanism of Carbon Incorporation in MOCVD GaAs," J. Cryst. Growth , Vol.68, 148(1984)

Kuech, T. F., E.Veuhoff, T.S.Kuan, V.Deline, and R.Potemski, "The Influence of Growth Chemistry on the MOVPE Growth of GaAs and $Al_xGa_{1-x}As$ Layers and Heterostructures,' J. Cryst. Growth, Vol.77, 257(1986).

Larsen, C. A., N.I.Buchan, and G.B.Stringfellow, "Reaction Mechanisms in the Organometallic Vapor Phase Epitaxial Growth of GaAs," Appl. Phys. Lett., Vol.52 (6), 480(1988). This work is reviewed and a more complete compilation of the work of this group is presented in "Organometallic Vapor Phase Epitaxy" by G.B.Stringfellow (Academic Press, San Diego CA, 1989).

Larsen, C. A., N.I.Buchan, S.H.Li, and G.B.Stringfellow, "GaAs Growth Using Tertiarybutylarsine and Trimethylgallium," J. Cryst. Growth 93, 15 (1988).

Lee, P. W., T.R.Omstead, D.R.Mckenna, and K.F.Jensen, "In Situ Mass Spectroscopy and Thermogravimetric Studies of GaAs MOCVD Gas Phase and Surface Reactions," J. Cryst. Growth, Vol.85, 165(1987).

Lee, P. W., T.R.Omstead, D.R.Mckenna, and K.F.Jensen, "In situ Mass Spectroscopy Studies of the Decomposition of Organometallic Arsenic Compounds in the Presence of $Ga(CH_3)_3$ and $Ga(C_2H_5)_3$," J. Cryst. Growth, Vol.93, 134(1988).

Leys, M. R. and H.Veenvliet, "A Study of the Growth Mechanism of Epitaxial GaAs as Grown by the Technique of Metal Organic Vapor Phase Epitaxy," J. Cryst. Growth, Vol.55,145(1981)..

Lide, D. R., "Handbook of Chemistry and Physics," 71th edn., Ed. by, (CRC Press, 1990-1991), p6-71.

Liu, H., J.C.Roberts, J.Ramdani, and S.M.Bedair, "Laser Selective Area Epitaxy of GaAs Metal-Semiconductor-Field-Effect Transistor", Appl. Phys. Lett, Vol.58(15), 1659(1991).

Liu, H., J.C.Roberts, J.Ramdani, S.M.Bedair, J.Farari, J.P.Vilcot, and D.Decoster, "Fabrication of GaAs Photodiode Using Laser Selective Area Epitaxy," Appl. Phys. Lett., Vol.58(4), 388(1991).

Long, L. H., "Dissociation Energies of Metal-Carbon Bonds and the Excitation Energies of Metal Atoms in Combination," Pure Appl. Chem., Vol.2, 61(1961).

Lossing, F. P. and A.W.Tickner, "Free Radicals by Mass Spectrometry. I. The Measurement of Methyl Radical Concentrations," J. Chem. Phys., Vol.20(5), 907, (1952).

M.Tsuda, M., S.Oikawa, M.Morishita, and M.Mashita, "On the Reaction Mechanism of Pyrolysis of TMG and TEG in MOCVD Growth Reactors," Jpn. J. Appl. Phys., Vol.26(5), L564, (1987).

Maa, B. Y. and P.D.Dapkus, in "Atomic Layer Growth and Processing," Eds., T.F.Kuech, P.D.Dapkus, and Y.Aoyagi, Mat. Res. Soc. Symp. Proc., Vol222, 25(1991).

Maa, B. Y. and P.D.Dapkus, "Reaction Mechanisms of Tertiarybutylarsine on GaAs (001) Surface and Its Relevance to Atomic Layer Epitaxy and Chemical Beam Epitaxy," J. Electron. Mat. 20, 589 (1991).

Manasevit, H. M., "Single-Crystal Gallium Arsenide on Insulating Substrates," Appl. Phys. Lett., Vol.11, 156(1968) and H.M.Manasevit and W.I.Simpson, "The Use of Metal-Organics in the Preparation of semiconductor Materials: I. Epitaxial Gallium-V Compounds," J. Electrochem. Soc., Vol.116(12), 1725(1969).

Mashita, M., S.Horiguchi, M.Shimazu, K.Kamon, M.Mohara, and M.Ishii, "The Pyrolysis Temperature of Triethylgallium in the Presence of Arsine or Trimethylaluminum," J. Cryst. Growth, Vol.77, 194(1986).

Maycock, P. D., "Thermal Conductivity of Silicon, Germanium, III-V Compounds, and III-V Alloys," Solid State Electron. Vol.10, 161(1967).

McCrary V. R. and V.M.Donnelly, "The Ultraviolet Absorption Spectra of Selected Organometallic Compounds Used in the Chemical Vapor Deposition of Gallium Arsenide," J. Cryst. Growth, Vol. 84, 253(1987).

Mcdowell, C. A. and J.W.Warren, "The Ionization and Dissociation of Molecules by Electron Impact," Discuss. Faraday Soc., Vol.10, 53(1951).

Meguro, T. and Y.Aoyagi, in "Atomic Layer Growth and Processing," Mat. Res. Soc. Symp. Proc., Vo222, Eds., T.F.Kuech, P.D.Daphus, and Y.Aoyagi, (MRS, Pittsburgh, PA, 1991), p121.

Meguro, T., S.Iwai, Y.Aoyagi, K.Ozaki, Y.Yamamoto, T.Suzuki, Y.Okano, and A.Hirata, "Atomic Layer Epitaxy of AlAs and AlGaAs," J. Cryst. Growth, Vol.99, 540(1990).

Meguro, T., T.Suzuki, K.Ozaki, Y.Okano, A.Hirata, Y.Yamamoto, "Surface Process in Laser-Atomic Layer Epitaxy (Laser-ALE) of GaAs," J. Cryst. Crowth, Vol93, 190(1988).

Miyoshi, T., S.Iwai, Y.Iimura, Y.Aoyagi, and S.Namba, "Characterization of GaAs and AlGaAs Layers Grown by Laser Atomic Layer Epitaxy," Jpn. J. Appl. Phys, Vol.29(8), 1435(1990).

Mochizuki, K., M.Ozeki, K.Kodama, and N.Ohtsuka, "Carbon Incorporation in GaAs Layer Grown by Atomic Layer Epitaxy," J. Cryst. Growth, Vol.93, 557(1988).

Murphy, W. C., A.C.Beri, T.F.George, and J.Lin, "Analysis of Laser-Enhanced Adsorption/Desorption Processes on Semiconductor Surfaces Via Electronic Surface State Excitation," Mat. Res. Soc. Symp. Proc. Vol.17, (Elsevier Science Pub. Co., Inc., 1983), p273.

Nishinaga, T., T.Shitara, K.Mochizuki, and K.I.Cho, "Surface Diffusion and Related Phenomena in MBE Growth of III-V Compounds, "J. Cryst. Growth, Vol.99, 482(1990).

Nishinaga, T., T.Shitara, K.Mochizuki, and K.I.Cho, "Surface Diffusion and Related Phenomena in MBE Growth of III-V Compounds," J. Cryst. Growth, Vol.99, 482(1990).

Nishizawa J. and T.Kurabayashi, "On the Reaction Mechanism of GaAs MOCVD," J. Electrochem. Soc., Vol.132(3), 413(1983).

Nishizawa, J. and T.Kurabayashi, J. Electrochem. Soc., Vol.130, 413(1983).

Nishizawa, J., H.Abe, and T.Kurabayashi, "Doping in Molecular Layer Epitaxy," J. Electrochem. Soc., Vol.136(2), 478(1989).

Nishizawa, J., H.Abe, and T.Kurabayashi, "Molecular Layer Epitaxy," J. Electrochem. Soc., Vol.132(5), 1197(1985).

Nishizawa, J., T.Kurabayashi, H.Abe, and A.Nozoe, "Mechanism of Surface Reaction in GaAs Layer Growth," Surface Sci., Vol.185, 249(1987).

Nissim, Y. I., A.Lietoila, R.B.Gold, and J.F.Gibbons, "Temperature Distributions Produced n Semiconductors by Scanning Elliptical or Circular CW Laser Beam," J. Appl. Phys, Vol.51(1), 274(1980).

Norimatsu, S., and K.Iwashita, "10 Gbit/s Optical PSK Homodyne Transmission Experiment Using External Cavity DFB LDs," Electron. Lett., Vol.26(10), 648(1990).

Ohno, H., S.Ohtsuka, A.Ohuchi, T.Mutsubara, and H.Hasegawa, "Growth of GaAs, InAs, and GaAs/InAs Superlattice Structures at Low Substrate Temperature by MOVPE," J. Cryst. Growth, Vol93, 342(1988).

Omstead, T. R., P.M.Van Sickle, P.W.Lee, and K.F.Jensen, "Gas Phase and Surface Reactions in the MOCVD of GaAs from Trimethylgallium, Triethylgallium, and Tertiarybutylarsine," J. Cryst. Growth, Vol.93, 20(1988).

Ozeki, M., K.Kodama, Y.Sakuma, N.Ohtsuka, and T.Takanohashi, "GaAs/GaP Strained-Layer Superlattices Grown by Atomic Layer Epitaxy," J. Vac. Sci. Technol. B8(4), 741(1990).

Ozeki, M., K.Mochizuki, N.Ohtsuka, and K.Kodama, "Growth of GaAs and AlAs Thin Films by A New Atomic Layer Epitaxy Technique," Thin Solid Films, Vol.174, 63(1989).

Ozeki, M., K.Mochizuki, N.Ohtsuka, and K.Kodama, "New Approach to the Atomic Layer Epitaxy of GaAs Using a Fast Gas Stream," Appl. Phys. Lett., Vol.53(16), 1509(1988).

Ozeki, M., K.Nakai, K.Dazai, and O.Ryuzan, "Photoluminescence Study of Carbon Doped Gallium Arsenide," Jpn. J. Appl. Phys., Vol.13(7). 1121(1974).

Ozeki, M., N.Ohtsuka, Y.Sakuma, and K.Kodama, "Pulsed Jet Epitaxy of III-V Compounds," J. Cryst. Growth, Vol.107, 102(1991).

Pan, N., S.S.Bose, M.H.Kim, G.E.Stillman, F.Chambers, G.Devane, C.R.Ito, and M.Feng, Appl. Phys. Lett., Vol.51(), 596(1987).

Parker, H., A.R.Kuhthau, R.Zapata, and J.E.Scott,Jr., in "Rarefied Gas Dynamics," F.M.Devienne, Ed., Pergamon Press, (1958), p69.

Pertel, R., "Molecular Beam Sampling of Dynamic Systems", Int. J. Mass Spectr. Ion Phys., Vol.16, 39(1975).

Pilcher, G. and H.A.Skinner, in "Chemistry of the Metal-Carbon Bonds," Eds., F.R.Hartley and S.Patai, John Wiley & Sons Ltd., 1982, pp57.

Pratt, G. L. and D.Roger, "Homogeneous Isotope Exchange Reactions: Part 2.–CH_4/D_2," J. Chem., Soc., Faraday Trans. I, Vol.12, 2769(1976).

Pratt, G. L., in "Gas Kinetics", John.Wiley, (1969), p159.

Pütz, N., H.Heinecke, M.Hegen, and P.Balk, "A Comparative Study of $Ga(CH_3)_3$ and $Ga(C_2H_5)_3$ in the MOMBE of GaAs," J. Cryst. Growth, Vol.74, 292(1986).

Ready, J. F., "Effects of High Power Laser Radiation," (Academic Press, New York, 1971).

Reep, D. H. and S.K.Gandhi, "Deposition of GaAs Epitaxial Layers by Organometallic CVD: Temperature and Orientation Dependence," J. Electrochem. Soc., Vol.130(3), 675(1983).

Sakuma, Y., K.Kodama, and M.Ozeki, "Atomic Layer Epitaxy of GaP and Elucidation for Self-Limiting Mechanism," Appl. Phys. Lett., Vol.56(9), 827(1990).

Sakuma, Y., M.Ozeki, K.Kodama, and N.Ohtsuka, "Role of Interface Strain in Atomic Layer Epitaxy Growth Kinetics of $In_xGa_{1-x}As$," J. Cryst. Growth, Vol.114, 31(1991).

Sakuma, Y., M.Ozeki, N.Ohtsuka, and K.Kodama, "Comparative Study of Self-Limiting Growth of GaAs Using Different Ga-Alkyl Compounds: $(CH_3)_3Ga$, $C_2H_5(CH_3)_2Ga$, and $(C_2H_5)_3Ga$," J. Appl. Phys., Vol.68(11), 5660(1990).

Sasaki, M., Y.Kawakyu, and M.Mashita, "UV Absorption Spectra of Adlayers of Trimethylgallium and Arsine," Jpn. J. Appl. Phys. Vol.28(1), L131(1989).

Schlichting, H., in "Boundary Layer Theory," McGraw-Hill, New York, 6th edn, 1968.

Skouby, D. C. and K.F.Jensen, "Modeling of Pyrolytic Laser-Assisted Chemical Vapor Deposition: Mass Transfer and Kinetic Effects Influencing the Shape of the Deposit," J. Appl. Phys., Vol.63(1), 198(1988).

Steere, N. V., Ed., "CRC Handbook of Laboratory Safety," (Chemical Rubber Co., Cleveland, Ohio, 1967).

Stringfellow, G. B., "Non-Hydride Group V Source for OMVPE," J. Electron. Mat. 17(4), 327 (1988).

Sugiura, H., R.Iga, T.Yamada, and M.Yamaguchi, "Ar Ion Laser-Assisted Metalorganic Molecular Beam Epitaxy of GaAs," Appl. Phys. Lett., Vol.54(4), 335(1989).

Suntola, T. and J.Antson, U.S. Patent No. 4058430 (1977).

Suntola, T., A.Pakkala, and S.Lindfors, U.S. Patent No.4413022(1983).

Suzuki, H., K.Mori, M.Kawasaki, and H.Sato, "Spatially and Time-Resolved Detection of Gallium Atoms Formed in the Laser Photochemical Vapor Deposition Process of Trimethylgallium by Laser-Induced Fluorescence: Decomposition in the Adsorbed State," J. Appl. Phys., Vol.64(1),371(1988).

Sze, S. M., in "Physics of Semiconductor Devices," 2nd. edn, (John Wiley & Sons, Inc., 1981), p33.

Takahashi, R., Y.Koga, and Kugawara, "Gas Flow Pattern and Mass Transfer Analysis in a Horizontal Flow Reactor for Chemical Vapor Deposition," J. Electrochem. Soc., Vol.119(10), 1406(1972).

Tirtowidjojo, M. and R.Pollard, "Equilibrium Gas Phase Species for MOCVD of $Al_xGa_{1-x}As$," J. Cryst. Growth, Vol.77, 200(1986).

Tirtowidjojo, M. and R.Pollard, "The Influence of Reactor Pressure on Rate-Limiting Factors and Reaction Pathways in MOVPE of GaAs," J. Cryst. Growth, Vol.98, 420(1989).

Tischler, M. A. and S.M.Bedair, "Self-Limiting Mechanism in the Atomic Layer Epitaxy of GaAs," Appl. Phys. Lett., Vol.48(24), 1961(1986).

Tokumitsu, E., Y.Kudou, M.Konagai, and K.Takahashi, Jpn. J. Appl. Phys., Vol.24, 1189(1985).

Toor, I. A. and H.H.Lee, "Design of Epitaxial CVD Reactors II, Design Considerations and Alternatives," J. Cryst. Growth, Vol.72, 679(1985).

Tsuda, M., S.Oikawa, M.Morishita, and M.Mashita, "On the Reaction Mechanism of Pyrolysis of TMG and TEG in MOCVD Growth Reactors," Jpn. J. Appl. Phys., Vol.26(5), L564, (1987).

Tuck, D. G., in "Comprehensive Organometallic Chemistry," Vol.1, Eds., G.W.Wilkinson, F.G.A.Stone, and E.W.Abel, (Pergamon Press, 1982), pp693.

Usui, A. and A.Sunakawa, "GaAs Atomic Layer Epitaxy by Hydride VPE," Jpn. J. Appl. Phys., Vol.25, L212(1986).

Warren, J. W., "Measurement of Appearance Potentials of Ions Produced by Electron Impact Using a Mass Spectrometer," Nature, Vol.165, 810(1950).

Weast, R. C., Ed., In "Handbook of Chemistry and Physics", 68TH. CRC (1987-1988), E-84.

Wemple, S. H. and M.Didomenico, Jr.,"Behavior of Electronic Dielectric Constant in Covalent and Ionic Materials," Phys. Rev. B3, 1338(1971).

Williams, J. O., R.Hoare, N.Hunt, and J.Parrott in "Mechanisms of Reactions of Organometallic Compounds with Surfaces," Eds., D.J.Cole-Hamilton and J.O.Williams, NATO ASI Series B: Physics, Vol.198, (Plenum Press, 1989), p131.

Wolkenstein, T. and I.V.Karpenko, "On the Theory of Photoadsorptive Effect on Semiconductors," J. Appl. Phys. Vol.33, 460(1962).

Yamada, T., R.Iga, and H.Sugiura, "GaAs Corrugation Pattern with Submicron Pitch Grown by Ar Ion Laser-Assisted Metalorganic Molecular Beam Epitaxy," Appl. Phys. Lett., Vol.59(8), 958(1991).

Yoshida, M., H.Watanabe, and A.Uesugi, "Mass Spectrometric Study of $Ga(CH_3)_3$ and $Ga(C_2H_5)_3$ Decomposition Reaction in H_2 and N_2," J. Electrochem. Soc., Vol.132(3), 677(1985).

Yu, M. L., N.I.Buchan, R.Souda, and T.F.Kuech, in "Atomic Layer Growth and Processing," Eds., T.F.Kuech, P.D.Dapkus, and Y.Aoyagi, Mat. Res. Soc. Symp. Proc., Vol222, 3(1991).

Yu, M. L., U.Memmert, N.I.Buchan, and T.F.Kuech, in "Chemical Perspectives of Microelectronic Materials II," Eds., L.V.Interante, K.F.Jensen, L.H.Dubois, and M.E.Gross, Mat. Res. Soc. Symp. Proc., Vol.204, 37(1991).